

Copyright is owned by the Author of the thesis. Permission is given for a copy to be downloaded by an individual for the purpose of research and private study only. The thesis may not be reproduced elsewhere without the permission of the Author.

A study on the thermally induced gelation of quinoa protein isolate (QPI) dispersions

A Thesis Presented in Partial Fulfilment of the Requirements for the Degree of Master of Food Technology

Massey University, Auckland, New Zealand

Shubham Bhagwantrao Patole

2022

Abstract

Plant proteins is an alternate option for animal proteins. In the last decade, the market trend towards plant-based protein is significantly accelerated. To meet market demand, plant-based protein ingredients must compete with or outperform traditional animal protein sources in terms of techno-functional properties. Plant proteins typically have extremely different molecular, chemical, and physical properties than animal proteins. Due to this the main challenge is to stimulate the desirable appearance, texture, mouthfeel, and functionality of the products manufactured from plant proteins as compared with animal proteins. We choose quinoa as they can reduce the risk of several diseases such as anti-depressants, anti-inflammatory, and anti-cancer. High amount of flavonoids such as quercetin and kaempferol, and antioxidants are present in quinoa seeds. However, understanding the underlying characteristics of plant proteins and how they might be built into structures similar to those found in animal products is therefore crucial. So, to understand the gelation property of quinoa plant protein, this study aims to investigate the physicochemical and rheological behaviour of quinoa protein with different NaCl and CaCl₂ concentration, different polysaccharides concentration and to compare the heat-induced gelation behaviour between quinoa protein isolate and whey protein isolate.

The rheological properties and microstructural changes in the quinoa protein were monitored when addition of salt (NaCl and CaCl₂), polysaccharide, and comparison of plant protein and dairy protein at various pH and protein concentrations were performed. The changes in the storage modulus and microstructure of the suspension and gels were examined. This research evaluated the effect of addition of NaCl (0 mM to 200 mM) and CaCl₂ (20 mM and 50 mM) at various concentrations; addition of guar gum, locust bean gum, and xanthan gum at 0.05 %, 0.1 % and 0.2 % concentrations; and to assess and compare the gelation behaviour of the quinoa protein isolate, and whey protein isolate at pH 7, pH 5 and pH 3 with different protein concentration.

Addition of NaCl and CaCl₂ illustrated sol-gel transition using small and large deformation rheology, although all protein gels displayed weak gel characteristics. It was discovered that with addition of NaCl from 0 mM to 200 mM, gelation temperature decreased from 73 °C to 40 °C and complex modulus (G^*) increased from ~67 Pa to ~125 Pa. As the NaCl concentration

increased, heterogenous and larger aggregates of the gel microstructure developed. But for gel microstructure without salt addition, homogenous structure existed. In the case of CaCl_2 (20 mM and 50 mM), rheology showed weak gel rigidity. And from CLSM images, larger aggregates with big voids were observed in the case of 50 mM CaCl_2 , probably exhibiting phase separation. From SAXS and SANS, a particle size of $\sim 32 \text{ \AA}$ and $\sim 57 \text{ \AA}$, was observed for QPI gels containing 0 to 200 mM NaCl, respectively.

Polysaccharide addition at low concentration can increase the viscoelastic property of thermally induced QPI gels. For each polysaccharide (guar gum, locust bean gum, xanthan gum), as concentration increased (0.05 % to 0.2 %), gelation temperature decreased from 64 °C to 50 °C approximately for guar gum, and 46 °C to 31 °C for locust bean gum. Addition of xanthan gum revealed the maximum storage modulus (G'), as compared with other polysaccharides. In comparison with guar gum and locust bean gum, xanthan gum did not confirm gelation temperature due to high viscosity of the suspension at all the concentrations. Complex modulus (G^*) (1 Hz) increased as the concentration of each polysaccharide increased from 664 Pa to 1797 Pa for Xanthan gum. The CLSM microstructure was also in correlation with the rheological characterisation. The highest water holding capacity was also seen for highest xanthan gum concentration (0.2 %).

The protein concentration (3 wt% to 10 wt%) and various pH (pH 3, pH 5 and pH 7) affects the gelation behaviour and microstructural characteristics of quinoa protein and whey proteins. At all the pH values, whey protein shows high viscoelasticity as compared with quinoa protein. Highest viscoelasticity for QPI is achieved at pH 5. Hydrophobic bonds and electrostatic interactions are responsible for the gelation of quinoa protein isolate. The highest viscoelasticity for WPI is determined at pH 7. The thiol disulphide interchange reactions are responsible for the gelation behaviour of whey protein isolate. The increase in protein concentration for QPI and WPI gel formation increased. The gelation temperature decreased as the protein concentration increased (3 wt% to 10 wt%) for QPI and WPI at all the pH values (pH 3, pH 5 and pH 7).

Acknowledgements

I want to offer my heartfelt gratitude to my supervisor, Dr Zhi Yang, for allowing me to work on this project and for his unwavering support, motivation, direction, and valuable guidance during my master's programme. Dr. Zhi Yang's door was always open anytime I needed assistance, and he guided me in the appropriate approach to execute my research. He has provided me with excellent support and encouragement in the areas of study topic selection, data collecting and analysis, thesis writing, and even grammatical errors correction. Without his abundant knowledge and patience, I could not have completed my project.

I'd like to thank all the faculty and staff at Massey University Auckland's School of Food and Advanced Technology for their support and kind assistance during the course of my research, especially Negah Nikanjam and Noorzahan Begum for their assistance and support in all things related to laboratory use. I would also like to thank the people from Palmerston North campus who helped me in obtaining sample images from confocal laser scanning microscopy. I am also grateful to the people from ANSTO's Australian Centre for Neutron Scattering (ACNS) and National Deuterium Facility, Australia, who provided me to obtain sample images from small angle neutron scattering and ultra-small angle neutron scattering.

I would also like to thank my family and friends for giving me motivation, support, and encouragement to get through all the pandemic situation and tough times. Last but not the least, I would like to acknowledge everyone who has contributed to the completion of this thesis.

Table of Contents

Abstract	1
Acknowledgements	ii
List of Abbreviations	vii
List of Figures	ix
List of tables	xii
1. Introduction	1
1.1. Overview of the research.....	1
1.2. Thesis objective.....	2
1.3. Thesis structure	3
2. Literature Review	5
2.1. General introduction of quinoa seeds.....	5
2.2. Chemical compositions of quinoa seeds	7
2.2.1. Proteins	7
2.2.2. Carbohydrates	9
2.2.3. Lipids	9
2.2.4. Vitamins and minerals	10
2.3. Extraction of proteins from quinoa seeds.....	11
2.3.1. Wet extraction.....	12
2.3.2. Dry fractionations	14
2.4. Physicochemical properties and techno-functional properties of QPI.....	17
2.4.1. Gelation property	17
2.4.2. Emulsion capacity and stability	18
2.4.3. Solubility of quinoa protein isolates	18
2.4.4. Foaming capacity and stability	18
2.5. Food applications of quinoa proteins	19
2.6. Food Polysaccharides	22
2.6.1. Non-ionic food polysaccharides	24
2.6.1.1. Guar gum (GG).....	24
2.6.1.2. Locust bean gum (LBG)	24
2.6.2. Ionic polysaccharides	25
2.6.2.1. Xanthan gum.....	25
2.6.3. Protein-polysaccharide interactions	26
2.7. Whey proteins	30
2.7.1. Whey protein denaturation and gelation	33
2.7.2. Application of Whey protein in the food industry	34

2.8.	Food Protein Gels.....	38
2.8.1.	Heat-induced gelation of food proteins.....	38
2.8.2.	Cold-set gelation of food proteins.....	42
2.8.3.	Factors affecting the gelation of food proteins	43
2.8.3.1.	Effect of temperature	43
2.8.3.2.	Effect of protein concentration	43
2.8.3.3.	Effect of ionic strength	43
2.8.3.4.	Effect of pH	44
2.8.4.	Non-covalent and covalent interactions participating the protein gel formation 44	
2.8.4.1.	Hydrogen bonds.....	44
2.8.4.2.	Disulfide bonds.....	45
2.8.4.3.	Hydrophobic interactions	45
2.8.4.4.	Electrostatic interactions.....	46
2.8.4.5.	Van Der Waals interactions	46
2.9.	Physicochemical and microstructural characterizations of protein gels	46
2.9.1.	Rheology	47
2.9.1.1.	Oscillation rheology	47
2.9.2.	Types of measurements in the oscillation rheology.....	49
2.9.2.1.	Temperature sweep.....	49
2.9.2.2.	Time sweep.....	50
2.9.2.3.	Frequency sweep	50
2.9.2.4.	Stress/ strain sweep.....	50
2.9.3.	Confocal laser scanning microscopy (CLSM).....	50
2.9.4.	Small-angle X-ray scattering and Small angle neutron scattering (SAXS, SANS) 51	
3.	Effect of NaCl and CaCl₂ concentration on the rheological and structural characteristics of thermally-induced quinoa protein gels	53
3.1.	Abstract	53
3.2.	Introduction	53
3.3.	Materials and Methods	55
3.3.1.	Materials	55
3.3.2.	Preparation of quinoa protein isolate (QPI).....	55
3.3.3.	Sodium dodecyl sulfate polyacrylamide gel electrophoresis (SDS-PAGE)	56
3.3.4.	Rheological measurements	57
3.3.5.	Confocal laser scanning microscopy	57

3.3.6.	Solubility determination.....	58
3.3.7.	Ultra-small angle neutron scattering (USANS)	58
3.3.8.	Small-angle neutron scattering (SANS).....	59
3.3.9.	Small-angle X-ray scattering (SAXS)	60
3.3.10.	SANS and SAXS data analysis.....	60
3.3.11.	Statistical analyses	60
3.4.	Results and Discussions	61
3.4.1.	SDS-PAGE	61
3.4.2.	Viscoelastic properties during gelation.....	62
3.4.3.	Viscoelastic properties after gelation.....	63
3.4.4.	Confocal laser scanning microscopy (CLSM) observations.....	66
3.4.5.	Solubility.....	67
3.4.6.	Microstructures of the QPI before and after heating probed by USANS	68
3.4.7.	Nanostructures of the QPI before and after heating probed by SAXS and SANS 72	
3.5.	Conclusions	76
4.	Impact of incorporations of various polysaccharides on rheological and microstructural characteristics of heat-induced quinoa protein isolate gels	77
4.1.	Abstract	77
4.2.	Introduction	77
4.3.	Materials and Methods	80
4.3.1.	Materials	80
4.3.2.	Preparation of quinoa protein isolate (QPI).....	80
4.3.3.	Sample preparations.....	81
4.3.4.	Confocal Laser Scanning Microscopy (CLSM)	81
4.3.5.	Rheological characterisations	82
4.3.6.	Water holding capacity (WHC)	82
4.3.7.	Statistical analysis.....	82
4.4.	Results and Discussion.....	83
4.4.1.	Microstructural characteristics revealed by CLSM	83
4.4.2.	Effect of polysaccharides incorporation on the rheological properties during gelation	86
4.4.3.	Effect of polysaccharides incorporation on the rheological properties after gelation	89
4.4.4.	Impact of polysaccharides addition on the WHC	92
4.5.	Conclusions	93
5.	Impact of pH and protein concentrations on the thermal gelation behaviour of quinoa protein isolates and whey protein isolates dispersions.....	95

5.1.	Abstract	95
5.2.	Introduction	95
5.3.	Materials and method	97
5.3.1.	Materials	97
5.3.2.	Preparation of quinoa protein isolate (QPI)	97
5.3.3.	Sample preparations	97
5.3.4.	Rheological measurements	98
5.3.5.	Confocal laser scanning microscopy (CLSM)	98
5.3.6.	Statistical analysis	98
5.4.	Result and discussion	99
5.4.1.	Thermally induced gelation of QPI and WPI at pH 3, pH 5, and pH 7	99
5.4.2.	Thermally induced gelation of QPI, and WPI after gelation at pH 7, pH 5 and pH 3. 104	
5.4.3.	Microstructural characteristics of QPI and WPI gels as revealed by CLSM... 108	
5.5.	Conclusion and future work	112
6.	Conclusions and future work recommendation.....	113
6.1.	Conclusions	113
6.2.	Future work recommendation	114
7.	References.....	116
8.	Appendices	152

List of Abbreviations

BGN-PI	Bambara groundnut protein isolate
BSA	Bovine serum albumin
Carr	Carrageenan
CLSM	Confocal laser scanning microscopy
CPI	Canola protein isolate
DQSM	Defatted quinoa seed meal
GA	Gum arabic
GDL	Glucono- δ - lactone
GG	Guar gum
G'	Storage modulus
G''	Loss modulus
G^*	Complex modulus
HMP	High methoxyl pectin
Ig	Immunoglobulin
LBG	Locust bean gum
LMP	Low methoxyl pectin
MC	Micellar casein
MTGase	Microbial transglutaminase
MUFA	Mono-unsaturated fatty acid
PPI	Pea protein isolate
PUFA	Poly-unsaturated fatty acid
QPC	Quinoa protein concentrate
QPI	Quinoa protein isolate

SANS	Small angle neutron scattering
SAXS	Small angle x-ray scattering
SEM	Scanning electron microscopy
SPI	Soy protein isolate
TEM	Transmission electron microscopy
WPC	Whey protein concentrate
WPI	Whey protein isolate
XG	Xanthan gum
ι - carrageenan	iota- carrageenan
k - carrageenan	kappa- carrageenan
λ - carrageenan	lambda carrageenan

List of Figures

Fig 2.1: Different colours and clusters of quinoa plant located from south to west of Lake Titicaca in the Omasuyos region (Del Castillo et al., 2008; Garcia et al., 2015)	6
Fig 2.2: A basic process of wet protein extraction (Schutyser & van der Goot, 2011).....	12
Fig 2.3: The basic process of dry fractionation (Schutyser et al., 2015).....	14
Fig 2.4: Types of food polysaccharides	22
Fig 2.5: Chemical formula of the locust bean gum (Mortensen et al., 2017).....	25
Fig 2.6: Complex formations in protein-polysaccharide systems (Warnakulasuriya & Nickerson, 2018).....	27
Fig 2.7: Structure of α -lactalbumin (Bernstein et al., 1977).....	31
Fig 2.8: Structure of β -lactoglobulin (Kinsella & Morr, 1984).	31
Fig 2.9: A flowchart for production of whey protein isolate (WPI) and whey protein concentrate (WPC) (Bansal & Bhandari, 2016).....	32
Fig 2.10: A schematic illustration of protein gel networks, a. fine-stranded gel network b. coarse gel network (Hermansson, 1994).....	38
Fig 2.11: A schematic diagram of heat-induced gelation of globular proteins. T° represents the temperature and T_D represents the denaturation temperature of proteins (Totosaus et al., 2002).	39
Fig 2.12: Heat-induced gelation of a soy protein isolate solution (Nicolai & Chassenieux, 2019).	40
Fig 2.13: The two-step procedure of cold-set gelation. Firstly, a solution of the native protein is heated at a pH far away from pI so that protein aggregates are formed. Secondly, the addition of acid will reduce the pH and gelation is induced at an ambient temperature (Alting, 2003).	42
Fig 2.14: Oscillation stress and strain waves for (a) elastic and viscous materials; and (b) viscoelastic material (Kulkarni & Shaw, 2015).....	48
Fig 2.15: The schematic diagram of components of SAXS instruments (Nyman & Fullmer, 2015).	52
Fig 3.1: SDS-PAGE of quinoa protein under reducing conditions: Lane 1-molecular weight marker; Lane 2-quinoa protein isolate.	61

Fig 3.2: The evolution of G' (solid symbols) and G'' (open symbols) for QPI solutions at 10 wt% in D_2O during temperature induced gelation with increasing concentration of NaCl (A) and $CaCl_2$ (B). (NaCl: 0 mM (■), 20 mM (●), 50 mM (▲), 100 mM (◆), 200 mM (▼); $CaCl_2$: 20 mM (◀), 50 mM (▶)); (C) Complex modulus G^* at 1 Hz and gelation temperature T_{gel} of the QPI gels as a function of salt (NaCl and $CaCl_2$) concentration. Different letters (black) below the lines indicate significant differences in T_{gel} . Different letters (blue) above columns indicate significant differences in G^* . All the samples in the experiments were at pH 7 63

Fig 3.3: The G' and G'' as a function of frequency (A, C) and strain amplitude (B, D) for QPI solutions at 10 wt% in D_2O with various concentrations of salt addition measured at 25 °C. Symbols are the same as in the Fig. 1; (E) breaking stress of the QPI gels as a function of salt (NaCl and $CaCl_2$) concentration. Different letters above columns indicate significant differences in breaking stress..... 65

Fig 3.4: Confocal laser scanning microscopy images of QPI gels ($c=10$ wt%) that formed by heating at 85 °C for 30 min in the presence of salt (NaCl and $CaCl_2$) at various concentrations. 67

Fig 3.5: USANS profiles ($3 \times 10^{-5} < Q (\text{\AA}^{-1}) < 2 \times 10^{-3}$) of QPI samples (10 wt% in D_2O) with 0 mM (A), 20 mM (B), 100 mM (C) and 200 mM (D) of NaCl addition before and after heat treatment. USANS profiles of QPI gels that formed in the presence of various NaCl (E) and $CaCl_2$ (F) concentrations. Solid black lines are the unified fits using equation (1). The power-law scattering found in different Q regions are also indicated with the corresponding power-law exponent. (G) USANS profile of QPI gels containing 20 mM $CaCl_2$ and the unified fit to the experimental data are solid black lines and individual levels are illustrated as orange and blue dashed lines for levels 1 and 2, respectively. The USANS data are not desmeared..... 71

Fig 3.6: SAXS (A) and SANS (B) profiles of QPI gels that formed in the presence of various concentrations of NaCl and $CaCl_2$. The power-law scattering found in different Q regions are also indicated with a power-law exponent. (C) and (D) are the Kratky plots of SAXS and SANS profiles of QPI gels. Symbols are the same as in A and B. (E) and (F) are SAXS (E) and SANS (F) profiles of QPI gels containing 0 and 200 mM NaCl. Solid black lines are the correlation length model fits using equation (2). In (E) and (F), scattering curves were arbitrary vertically shifted to avoid overlap..... 75

Fig 4.1: Confocal laser scanning micrographs of 10 wt% QPI dispersions and gels in the absence and presence of guar gum, locust bean gum, and xanthan gum at 0.05 wt%, 0.1 wt%, and 0.2 wt%. The gels were formed by heating at 85 °C for 30 min.....85

Fig 4.2: The evolution of G' (solid symbols) and G'' (open symbols) for 10 wt% QPI dispersions during heat-induced gelation in the absence and presence of guar gum (A), locust bean gum (B), and xanthan gum (C). Gums concentrations: 0 wt% (■), 0.05wt% (●), 0.1wt% (▲), and 0.2wt% (▼).....88

Fig 4.3: The gelation temperature T_{gel} of the QPI gels containing guar gum and locust bean gum at 0 wt%, 0.05 wt%, 0.1 wt%, and 0.2 wt%. Different letters above columns indicate significant differences.89

Fig 4.4: The dependence of frequency (A, B, C) and strain amplitude (D, E, F) on G' (solid symbols) and G'' (open symbols) for QPI dispersions at 10 wt% with various concentrations of polysaccharides incorporation measured at 25 °C. Gums concentrations: 0 wt% (■), 0.05wt% (●), 0.1wt% (▲), and 0.2wt% (▼).91

Fig 4.5: Complex modulus G^* (1 Hz) (A), breaking stress (B), and water holding capacity (C) of the QPI gels containing guar gum, locust bean gum, and xanthan gum at 0 wt%, 0.05 wt%, 0.1 wt%, and 0.2 wt%. Different letters above columns indicate a significant difference.92

Fig 5.1: The evolution of G' (solid symbols) and G'' (open symbols) for QPI (A- pH 7; B- pH 5; C- pH 3) and WPI (E- pH 7; F- pH 5; G- pH 3) dispersion during heat-induced gelation in presence of NaCl (100 mM). D- T_{gel} of QPI; H- T_{gel} of WPI. QPI concentrations: 10 wt% (■), 7 wt% (●), 5 wt% (▲), 3 wt% (▼); WPI concentrations: 10 wt% (■), 7 wt% (●), 5 wt% (▲), 3 wt% (▼). Means that do not share a letter are significantly different..... 103

Fig 5.2: G' (solid symbols) and G'' (open symbols) as a function of frequency for QPI (A- pH 7; B- pH 5; C- pH 3) and WPI (E- pH 7; F- pH 5; G- pH 3) gels after heat-induced gelation in the presence of NaCl (100 mM). D- Complex modulus (G^* (1Hz)) of QPI and H- Complex Modulus (G^* (1Hz)) of WPI as a function of protein concentrations. QPI concentrations: 10 wt% (■), 7 wt% (●), 5 wt% (▲), 3 wt% (▼); WPI concentrations: 10 wt% (■), 7 wt% (●), 5 wt% (▲), 3 wt% (▼)..... 106

Fig 5.3: The dependence of G' (solid symbols) and G'' (open symbols) on strain amplitude for QPI (A- pH 7; B- pH 5; C- pH 3) and WPI (E- pH 7; F- pH 5; G- pH 3) dispersion during heat-induced gelation in the presence of NaCl (100 mM). D- Breaking Stress of QPI and H- Breaking Stress of WPI as a function of protein concentrations. QPI concentrations: 10 wt%

(■), 7 wt% (●), 5 wt% (▲), 3 wt% (▼); WPI concentrations: 10 wt% (■), 7 wt% (●), 5 wt% (▲), 3 wt% (▼).....	107
Fig 5.4: CLSM images of QPI, and WPI at pH 7, pH 5 and pH 3 before heat treatment (100x magnification).....	110
Fig 5.5: CLSM images of QPI, and WPI at pH 7, pH 5 and pH 3 after heat treatment (100x magnification).....	111

List of tables

Table 2.1: Different ecotypes of quinoa (González et al., 2015; Tapia, 2012).....	6
Table 2.2: Chemical compositions of quinoa seeds (g/100g) on a dry matter basis	7
Table 2.3: Amino acid composition of quinoa, wheat, and casein (milk protein) (g/100g dry matter).....	8
Table 2.4: Sugar contents in quinoa flour (Ogungbenle, 2003)	9
Table 2.5: Vitamin contents in quinoa (Kozioł, 1992; Ranhotra et al., 1993; Ruales et al., 2002) and wheat (Khan, 2016; Kozioł, 1992). (Data present in mg/100 g based on dry matter).....	10
Table 2.6: Minerals in quinoa, wheat, and barley. (Data present is in mg/100 g based on the dry matter) (Jancurová et al., 2009; Kozioł, 1992).....	11
Table 2.7: Summary of methods used for quinoa protein extractions with the protein yield and purity. QPC- Quinoa protein concentrate, QPI- Quinoa protein isolate.	15
Table 2.8: Application of quinoa in the food industry.....	20
Table 2.9: Characteristics of commonly used polysaccharides in the food industry.....	23
Table 2.10: Rheological studies of plant protein-polysaccharide systems	28
Table 2.11: Properties of acid whey protein (Anon, 2007; Mulvihill & Donovan, 1987)	32
Table 2.12: Denaturation temperatures of whey protein components (Jenness et al., 1988) ..	34
Table 2.13: Application of whey proteins in the food industry (Bansal & Bhandari, 2016; Kilara & Vaghela, 2018; Mulvihill & Ennis, 2003)	34
Table 2.14: Gelation application of whey protein isolate in food products.....	36
Table 2.15: Previous studies on thermally induced gelation of quinoa protein isolates or quinoa flour.....	41

Table 2.16: Parameters that are frequently used in the oscillation rheology (Tabilo-Munizaga & Barbosa-Cánovas, 2005; Tunick, 2011)	49
Table 3.1: Solubility (%) of the QPI in the presence of various concentrations of NaCl and CaCl ₂ at pH 7.	68
Table 3.2: USANS model fit structural parameters of QPI gels that formed in the presence of various concentrations of NaCl and CaCl ₂	74

1. Introduction

1.1. Overview of the research

In the past, there was a myth that animal proteins are essential for human growth. They contained higher amino acid score, higher digestibility, and had greater water solubility for the required nutrition of human body (Baladrán-Quintana et al., 2019). In recent years, many people have been shifting into consuming plant protein-based product. It has been challenging for the food industries to manufacture products which have high nutritional property that animal proteins have. There are 20 essential amino acids in proteins, among which 9 are not built by the human body and should be given by diet (Lopez & Mohiuddin, 2021). In food systems, protein has functionalities such as emulsifying, gelation, and texturizing (Weder & Belitz, 2003).

Beneficial health claims such as reduction in type II diabetes, obesity, cardiovascular diseases and low-density lipoprotein cholesterol can be achieved by consumption of plant proteins (Guasch-Ferré et al., 2019). So the changes in consumers' dietary lifestyles and the market trend of plant-based protein is expected to grow in near future due to strong factors of sustainability and less environmental impact associated with production of plant-based protein compared with animal protein (Felix et al., 2021). Plant foods, on the other hand, are high in fibre, carbohydrates, oligosaccharides, and polyunsaturated fatty acids as compared to animal-based proteins (Sá et al., 2020a). In addition to numerous health benefits, plant proteins can also help with cheese design by acting as a structural agent (Ouyang et al., 2021); plant proteins can also act as emulsifying agent to prepare plant-based beverages (Qamar et al., 2020). Because of poor techno-functionalities, digestibility, and bioactivities, as well as the presence of anti-nutritional chemicals with severe off-taste, some plant-derived proteins have limited applicability in food product compositions (Akharume et al., 2021; Venkateswara Rao et al., 2021). However, great research efforts have been established in the fields of breeding, genetic engineering, isolation, extraction, processing, manufacturing, and product development to overcome these techno-functionalities of plant proteins (Tan et al., 2021).

Due to this growing trend of shifting from animal based products to plant based products and usage of plant proteins for health benefits many researchers have worked on various plant-based protein such as quinoa protein (Abugoch, 2009; Abugoch et al., 2009; Abugoch et al.,

2008; Bhargava et al., 2006; Comai et al., 2011), amaranth protein (Avanza et al., 2005; Barba de la Rosa et al., 1992; López et al., 2018), soy protein (Drake et al., 2000; Hou et al., 2015; Hu et al., 2017; Hu et al., 2013; Joo et al., 2011; Jose et al., 2016; Li et al., 2009), pea protein (Chen et al., 2021; Klost et al., 2020; Kornet et al., 2021; Mession et al., 2015; Sun & Arntfield, 2010; Sun & Arntfield, 2011; Sun & Arntfield, 2012; Wong et al., 2013), rapeseed protein (Ainis et al., 2018; Campbell et al., 2016; Dong et al., 2011; Fleddermann et al., 2013; He et al., 2014; Wanasundara et al., 2016; Wang et al., 2020), and flaxseed protein (Gutiérrez et al., 2010; Kaushik et al., 2015; Rabetafika et al., 2011; Rubilar et al., 2010). One of the most extensively used plant-based protein in food industry is soy protein. Soy protein has good gelling property and emulsifying property, as well as high water holding capacity, which makes it the most usable non-animal protein for production of meat substitutes and in replacement of other animal protein (Yang, 2017). Similar properties such as gelation, and emulsification are also shown by quinoa hence, to gain and investigate more information, this research is being carried out.

In recent developments, researchers have found out the importance and benefits of quinoa on health, such as minimizing gastrointestinal diseases and cardiovascular diseases (Alrosan et al., 2022; Repo-Carrasco et al., 2003). Due to high nutritional protein quality and quantity, quinoa is one of the promising plants from which protein can be extracted and applied in the food industry for various innovative food products. Quinoa also contain all 9 essential amino acids (Navruz-Varli & Sanlier, 2016). More detailed information regarding quinoa is given in section 2.1. Furthermore, among many protein functionalities, the gelation property is regarded as one of the most critical ones (Ma et al., 2022). In general, gelation of protein is induced by unfolding and subsequent aggregation of the proteins (Zheng et al., 2022).

1.2.Thesis objective

The objectives of this project were

- To extract the quinoa protein isolate (QPI) and optimize the extraction conditions to obtain the QPI with a higher protein content (~90%)
- To investigate rheological properties of heat induced quinoa protein isolate gels in the presence of NaCl and CaCl₂ at different concentrations
- To characterise the rheological properties and microstructural characteristics of heat induced QPI gels in the presence of different polysaccharides at different concentrations

- To compare the rheological properties of heat induced QPI and whey protein isolate (WPI) gels at different concentrations and different pH

1.3.Thesis structure

Chapter 2 reviews the general introduction of quinoa, its history, and its nutritional composition in detail. It also reviews different extraction methods of quinoa proteins from quinoa seeds and summarizes potential applications of QPI in the food industry. The interactions between the plant protein and polysaccharides and their importance in determination of rheological properties and microstructural characteristics of food are also reviewed. The application of protein-polysaccharide interactions in the food industry is reviewed. Comparison of dairy protein and plant protein investigated by other authors are also assessed. Experimental methods commonly used for characterisation of food gels such as rheology, confocal laser scanning microscopy (CLSM), small-angle neutron scattering (SANS) and small-angle x-ray scattering (SAXS) were also introduced.

Chapter 3 explores the effect of NaCl (0 to 200 mM) and CaCl₂ (20 and 50 mM) on the gelation of quinoa protein isolate (10 wt%). It also reviews the sol-gel transition during heating, holding and cooling periods on rheology. The microstructural characteristics of the QPI solution and gels were probed by USANS, SAXS, SANS, CLSM.

Chapter 4 aimed to investigate the properties of heat induced gels (85°C for 30 min) of quinoa protein isolate in the presence and absence of various polysaccharides including guar gum (GG), locust bean gum (LBG), and xanthan gum (XG) at pH 7. The samples with three gum concentrations (0.05, 0.1, and 0.2 wt%) at a fixed QPI concentration (10 wt%) and a fixed ionic strength (50 mM NaCl) were studied in terms of their gelation behaviour, small and large deformation rheological properties, water holding capabilities and microstructural characteristics.

Chapter 5 compares heat induced gelation behaviour of QPI and WPI at different concentrations (3, 5, 7 and 10 wt%) and pH (3, 5, and 7). Mechanical properties of resultant gels were characterised by rheology, while the microstructural characteristics were examined by CLSM.

Chapter 6 discusses the major findings from the study. The results of this project are summarised, and major outcomes discussed and concluded. It also consists of recommendations for future work.

2. Literature Review

2.1. General introduction of quinoa seeds

Quinoa (*Chenopodium quinoa* Willd.), an indigenous grain of South America's Andean highlands, is an outstanding substitute crop grown in many parts of the World (González et al., 2015). Quinoa was firstly harvested in the Andes around 5,000–7,000 years ago and has since been developed in a variety of geographical regions ranging from Chile's northwest region to Bolivia's Altiplano. Quinoa has been used by tribal people for decades in Colombia, Ecuador, Peru, Bolivia, Chile, and Argentina's northwest, according to several chronicles and archaeological surveys (Sauer, 1950). Around 3,000 years ago, quinoa was used in the north of Chile as staple food (Núñez, 1974). Quinoa can thrive in a wide range of soil conditions. Depending on the variety, quinoa can mature in 4-7 months and can be cultivated at high altitudes, unlike maize (Carmen, 1984; Repo-Carrasco-Valencia & Serna, 2011).

Quinoa was a staple food during Pre-Columbian times (González et al., 2015; Murphy & Matanguihan, 2015). In the Inca Empire, quinoa was one of the first crops, according to Inca Garcilaso de la Vega, as he wrote in his book called *Comentarios Reales de los Inca* (De La Vega, 2006). Quinoa was scorned as "food for Indians" during the Spanish invasion of South America in the sixteenth century, and conquerors devastated quinoa fields, systematically restricting its "non-Christian" cultivation and use (González et al., 2015). Under the grip of Spanish rule, the Incan communities were prohibited to cultivate it and were required to plant corn instead. Andean communities preserved quinoa crops after the Spanish acquisition (Tapia, 2012).

Quinoa grains are grown and sold within New Zealand. Kiwi Quinoa, The New Zealand Quinoa Co., and Canterbury Quinoa are the three major quinoa growers and sellers in New Zealand. Kiwi Quinoa is a small company which is owned by a Kiwi couple and grows quinoa in the east of Taihape. The owner stated that the climate in Moawhango, Taihape is similar to the Andes, South America, and they harvested 70 tonnes of quinoa from just 30 hectares of land in 2018 (Stowell, 2019). The crops grown by Kiwi Quinoa were 700 m above the sea level, however in South America crops are grown 3000 m above the sea level. The New Zealand Quinoa Co. is in Hāwera, New Zealand (Galloway, 2017), and produces white quinoa rather than red and black quinoa.

Quinoa is a pseudo-cereal since it does not belong to the Gramineae family, but it contains seeds that can be ground into flour and used as a cereal (Murphy & Matanguihan, 2015; Repo-Carrasco-Valencia & Serna, 2011). It is a yearly dicotyledonous plant that grows to be ~0.5-2.0 m tall, with large panicles of ~1.8-2.2 mm. Depending on varieties, quinoa seeds have different colours including pale yellow, white, red, brown, and black. (Rojas et al., 2015) (Fig. 2.1). Different quinoa ecotypes and their characteristics are listed in Table 2.1.

Fig 2.1: Different colours and clusters of quinoa plant located from south to west of Lake Titicaca in the Omasuyos region (Del Castillo et al., 2008; Garcia et al., 2015)

Table 2.1: Different ecotypes of quinoa (González et al., 2015; Tapia, 2012)

Ecotypes of quinoa	Characteristics
Valley quinoa	With plant height of 150-200 cm or more, it is a late-ripening variety
Altiplano quinoa	Germinating around Titicaca Lake in Bolivia and Peru, it can tolerate heavy frost
Salar quinoa	Growing on the Bolivian Altiplano plains of Uyuni and Coipasa, it can withstand salty soils with high pH values
Sea level quinoa	The smallest ecotypes of quinoa (100 cm) found especially in the southern part of Chile having bitter-tasting grains and fewer stems attached.

2.2. Chemical compositions of quinoa seeds

The proximate analysis of quinoa seeds (protein, fat, ash, carbohydrate, and crude fibre) is presented in Table 2.2. Due to a high nutritional value of quinoa, the United Nations named 2013 as the ‘International Year of Quinoa’, to attract attention from worldwide for promotion and utilization of quinoa (Burlingame et al., 2012; Nowak et al., 2016). Having a balanced amino acid profile, quinoa is believed to be a complete food and is also named as a ‘mother grain’ in South America (Abugoch, 2009; Wu, 2015). Detailed compositions and their nutritional values of quinoa seeds including proteins, carbohydrates, lipids, vitamins, and minerals are discussed below.

Table 2.2: Chemical compositions of quinoa seeds (g/100g) on a dry matter basis

Protein	Fat	Ash	Carbohydrate	Crude fibre	Quinoa variety	References
16.5	6.3	3.8	69	3.8	Ecuadorian variety	(Kozioł, 1992)
16.7	5.5	3.2	74.7	10.5	Surumi variety	(Wright et al., 2002)
15.6	7.4	3.0	69.7	2.9	Red quinoa	(Bruin, 1964b)
12.5	8.5	3.7	60	1.92	ND*	(Dini et al., 1992)

*ND- not determined

2.2.1. Proteins

Protein is essentially required for the growth of the human body. According to Ando et al. (2002) and Wu (2015), the quinoa protein is mainly found in the embryo, perisperm and bran of quinoa seed, accounting for 57 %, 39 % and 4 % respectively (dry matter basis). Proteins are mainly divided into four categories, namely, albumin, globulin, prolamin and glutelin (Higgins, 1984). In quinoa, the most abundant proteins are globulins and albumins. Chenopodium is the main 11S globulin protein in quinoa (Mäkinen et al., 2016) accounting for ~37 % of the total protein with a molecular weight of ~60 kDa (Abugoch James, 2009). The 2S albumin accounts for 35 % of the total protein with a smaller molecular weight of ~8-9 kDa (Abugoch et al., 2008). Prolamin accounts for 0.5-7.0 % of the total proteins in quinoa

(Abugoch et al., 2008; Dakhili et al., 2019). Due to a low content of prolamin, quinoa seeds can be considered as gluten-free (Thanapornpoonpong et al., 2008). In terms of the amino acids profile, quinoa proteins are rich in methionine, histidine and lysine as compared with soy protein and wheat. Amino acids present in quinoa are higher in alanine, aspartic acid and arginine as compared with that of wheat and casein protein (Table 2.3).

Table 2.3: Amino acid composition of quinoa, wheat, and casein (milk protein) (g/100g dry matter).

Amino acid	Wheat	Casein	Quinoa
Alanine ⁿ	3.6	2.7	4.2
Aspartic acid ⁿ	5.1	6.3	8
Arginine ⁿ	4.7	3.7	7.7
Glycine ⁿ	4.2	1.6	4.9
Glutamic acid ⁿ	31.7	19.0	13.2
Histidine ^e	2.3	2.7	2.9
Leucine ^e	6.8	8.4	5.9
Isoleucine ^e	3.6	4.9	3.6
Lysine ^e	2.7	7.1	5.4
Methionine+ cysteine ^e	4.2	2.64	3.6
Phenylalanine+ tyrosine ^e	7.8	10.0	6.1
Proline ⁿ	10.2	-	5.5
Serine ⁿ	4.6	4.6	4.0
Tryptophan ^e	1.3	1.4	1.2
Threonine ^e	2.9	3.7	3.0
Valine ^e	4.4	6	4.2
Reference	(USDA, 2015)	(Wang et al., 1999)	(Elsohaimy et al., 2015; USDA, 2015)

*n: non-essential amino acid and e: essential amino acid

2.2.2. Carbohydrates

Carbohydrate is one of the major components accounting for ~67- 74 % (dry matter basis) of quinoa seeds. Starch is present in the perisperm constituting around 55 % - 60 % of the seed (Jancurová et al., 2009; Vega-Gálvez et al., 2010; Wu, 2015). There are two biomacromolecules present in starch granules: amylose and amylopectin. In comparison with corn, wheat, and potato, quinoa has a lower amylose content (3 % -20 %) (Damodaran et al., 2007; Lindeboom et al., 2005; Murphy & Matanguihan, 2015). In addition, quinoa starch can act as a thickener in frozen foods because it is freeze/thaw stable (Watanabe et al., 2007). The swelling power of quinoa starch is ~8.54 g water/ 100g dry starch at 95 °C which makes it ideal for making noodle-like products (Ahamed et al., 1996; Khan, 2016). Crude fibre is also present in quinoa accounting for ~2.5- 3.9 % (total dry matter) (Pathan & Siddiqui, 2022). Other than crude fibre, simple sugars are also present in quinoa (2 % total dry matter) (Table 2.4). Quinoa has a high maltose content of ~101mg/100 g dry quinoa flour, indicating that it might be utilised in malted beverages and bread (Wu, 2015). Pentosans are also present in a small amount (2.9- 3.6 % of total dry matter) (Jancurová et al., 2009).

Table 2.4: Sugar contents in quinoa flour (Ogungbenle, 2003)

Sugar	Content (mg/100 g dry quinoa flour)
Glucose	19
Fructose	19.6
D-Ribose	72
D-Galactose	61
Maltose	101
D-xylose	120

2.2.3. Lipids

According to Wu (2015) and Ogungbenle (2003), about 5 % -7 % (dry weight basis) of oil is present in quinoa seeds. Type II diabetes, cardiovascular diseases and obesity can be caused by excessive intake of saturated fatty acids. This issue can be alleviated by increasing

consumptions of unsaturated fatty acids, which are available in quinoa seeds (Hunnicuttt et al., 1994; Sacks et al., 2014; Sacks & Katan, 2002). Monounsaturated fatty acid (MUFA), such as oleic acid, accounts for 24.8 g/100 g of total oil extracted from quinoa flour. Polyunsaturated fatty acids (PUFA), i.e., linoleic and linolenic, account for 52.3 and 3.9 g/100 g in quinoa flour, respectively (Ruales & Nair, 1992). Of all lipids present in quinoa, ~87 % are unsaturated lipids and ~11 % are saturated lipids (Jancurová et al., 2009).

2.2.4. Vitamins and minerals

Vitamins play a significant role in maintaining human health. Vitamin deficiency can lead to hypovitaminosis. Vitamins can be divided into two groups, fat-soluble Vitamins, and water-soluble Vitamins (Anklam, 2005). According to Vega-Gálvez et al. (2010), ascorbic acid, α -tocopherol, thiamine, riboflavin and niacin are the main vitamins discovered in quinoa. Comparison of Vitamins in quinoa with that of wheat is shown in Table 2.5 and it is evident that the content of β carotene, α -tocopherol and ascorbic acid is higher in quinoa. A higher level of tocopherol reduces the risk of cardiovascular diseases and cancer because it protects the human body from free radical oxidation (Trumbo, 2005). Calcium, magnesium, ferrous, and copper, are all abundant in quinoa with contents of 1487, 2496, 132, and 51 (mg/100 g dry basis), respectively (Bruin, 1964a; Koziół, 1992; Repo-Carrasco et al., 2003). According to Konishi et al. (2004), the embryo also contains phosphorus, potassium, and magnesium, which contribute to the production of phytic acid and phytate in phytin globoids. Calcium, potassium, magnesium are higher in quinoa than wheat and barley (Jancurová et al., 2009). Comparison of minerals in quinoa with that of wheat and barley is presented in Table 2.6 and it is evident that contents of copper, ferrous, potassium, calcium, magnesium, and zinc are higher in quinoa.

Table 2.5: Vitamin contents in quinoa (Koziół, 1992; Ranhotra et al., 1993; Ruales et al., 2002) and wheat (Khan, 2016; Koziół, 1992). (Data present in mg/100 g based on dry matter).

Vitamins	Wheat	Quinoa
Vitamin A (β carotene)	0.02	0.39
Vitamin E (α -tocopherol)	1.0-1.15	5.37
Vitamin C (Ascorbic acid)	0	4.0
Vitamin B3 (Niacin)	1.06-3.6	1.06-1.52

Vitamin B2 (Riboflavin)	0.12-0.39	0.30-0.39
Vitamin B1 (Thiamine)	0.48-0.55	0.29-0.38

Table 2.6: Minerals in quinoa, wheat, and barley. (Data present is in mg/100 g based on the dry matter) (Jancurová et al., 2009; Kozioł, 1992).

Minerals	Barley	Wheat	Quinoa
Calcium	430	503	1487
Magnesium	1291	1694	2496
Potassium	5028	5783	9267
Phosphorous	3873	4677	3837
Ferrous	32	38	132
Copper	3	7	51
Zinc	35	47	44

2.3.Extraction of proteins from quinoa seeds

Defatted protein-rich bran and defatted whole seed flour are major materials that can be used for quinoa protein extractions (Scanlin & Lewis, 2017). According to previous studies, wet extraction and dry extraction are two most commonly used methods for protein extractions from quinoa seeds.

2.3.1. Wet extraction

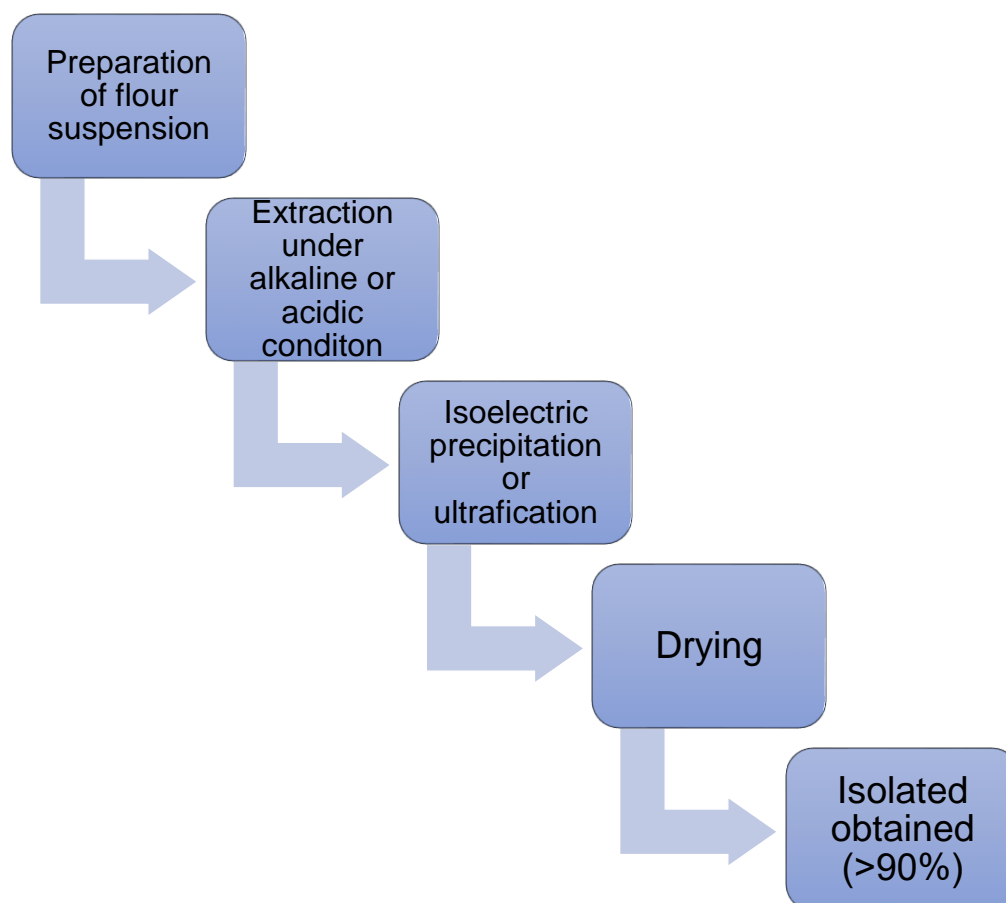


Fig 2.2: A basic process of wet protein extraction (Schutyser & van der Goot, 2011)

The wet extraction is typically used to obtain protein rich fractions. Major steps of the wet extraction are shown in Fig. 2.2. Firstly, the size of the primary material is reduced and subsequently dispersed in alkaline solutions to allow solubilisation of proteins. Thereafter, the solubilised proteins are recovered by isoelectric precipitation and then dried to obtain protein powder (Opazo-Navarrete et al., 2018; Papalamprou et al., 2010).

Brinegar and Goundan (1993) used a coffee mill to grind the quinoa seeds and acetone was used to defat the flour, then they were dried at 37 °C. The defatted flour was dispersed in a Tris-HCl buffer at pH 8 containing 0.1-1 M NaCl. Centrifugation at 10000 g (5 °C) for 10 min was conducted and the protein content of the supernatant obtained was analyzed by the

Bradford method. The supernatant was then acidified using acetic acid (10 %) to pH 4. The proteins were resolubilized in the same buffer at pH 8 and the protein content was again determined by the Bradford method. This extraction method resulted in a 65 mg/g protein yield of defatted flour.

The similar method of protein isolation was used by Abugoch et al. (2008) but quinoa seeds were washed 4-5 times to remove saponin using cold water before protein extractions. The dried seeds were then milled to flour before defatting using 10 (w/v) % hexane for 24 hr. The flour was then dispersed at pH 9 (Q9) or pH 11 (Q11) to allow protein solubilization for 30 min before centrifugation at 4 °C (9000 g for 20 min). The supernatant obtained were adjusted to pH 5 and then again centrifuged for 20 min (9000 g, 4 °C). The precipitated protein was then resuspended in water at pH 7 and spray dried. These isolates were named Q9 and Q11 by the authors and the protein content is ~77.2- 83.5 % determined by the Bradford method.

According to Guerreo-Ochoa et al. (2015), quinoa seeds were pulverised in a hammer mill to produce particles ranging from 100 to 500 μm . After that, ground meal was defatted for 12 hours in hexane at a meal: solvent ratio of 1:4 (w/v) under magnetic stirring (300 rpm) for 12 h. The defatted quinoa seed meal (DQSM) was then oven-air-dried at 40 °C for 2 hr. The DQSM was stored at 4 °C in polythene bags until further uses. According to the experimental design, protein from DQSM was extracted using various combinations of independent variables such as pH, NaCl concentration (M), temperature (°C), solvent type (NaOH 2 N or Buffer Tris-HCl 0.2 M), particle size (μm), and solvent/meal ratio (v/w). In a glass vessel, protein extraction was carried out under alkaline conditions (8 to 11 pH). The solution was constantly stirred (200 rpm) throughout the duration of the experiment for the following parameters: pH (8 to 11), NaCl concentration (0 to 1 M), time (1 to 2 h), temperature (20 to 50 °C), particle size (100 to 500 μm), and solvent/meal ratio (10 to 30 mL/g). The solution was immediately centrifuged for 30 minutes at 4 °C at 4000 g. The supernatant was filtered using Whatman filter paper No. 1 to determine the soluble protein using the Lowry method (Lowry et al., 1951) and protein content was determined by Kjeldahl method. The result was successful using conditions of pH (11.0), time (150 min), ratio (19.6/1 v/w) and temperature 36.2 °C, using a particle size of 500 μm and 0.1 N NaOH to adjust the pH and the protein yield achieved was 76.3 %.

In another QPI extraction study performed by Ruiz, Xiao, et al. (2016), quinoa seeds were ground to flour using a Fritsch Mill Pulverisette at 7000 rpm and the flour was passed through

a 200 μm sieve. The flour was defatted for 24 hours in a soxhlet extractor using petroleum ether. Thereafter, the petroleum ether was removed by evaporation after defatting. The defatted flour was suspended in deionized water (10% w/w), and the pH was adjusted to 8- 11 using 2 M NaOH. To enhance protein solubilization, these solutions were stirred for 4 h at room temperature and kept at 4 $^{\circ}\text{C}$ for another 16 h. The suspensions were then centrifuged at 6000g for 30 min at 10 $^{\circ}\text{C}$. The pH of the supernatants was adjusted to 4.5 using 2 M HCl before centrifugation for 30 min at 13,000g and 10 $^{\circ}\text{C}$. The precipitated pellets were resuspended in deionized water. To remove any salts, the protein pellets were washed with water 3- 4 times, before being re-suspended in deionized water and neutralised with 2 M NaOH. The suspensions were frozen in liquid nitrogen and then freeze-dried for 72 h to obtain the protein isolate powder. Approximately 75 % of protein yield was obtained at pH 11 with protein purity of 82 %. And for pH 8 protein yield obtained was ~62 % with protein purity of 88 %.

There are some advantages of wet fractionation: protein isolates obtained typically has a higher protein content of ~70% -90% Higher protein yield was observed when the extraction pH was increased. However, higher pH extractions lead to partially protein denaturation, which is detrimental for their gelation properties (G. A. Ruiz et al., 2016). But wet fraction also has some disadvantages: the extraction process is energy and labour intensive and may have a negative impact on physicochemical properties and techno-functional properties of protein isolates (Abugoch et al., 2008; Callisaya et al., 2009).

2.3.2. Dry fractionations

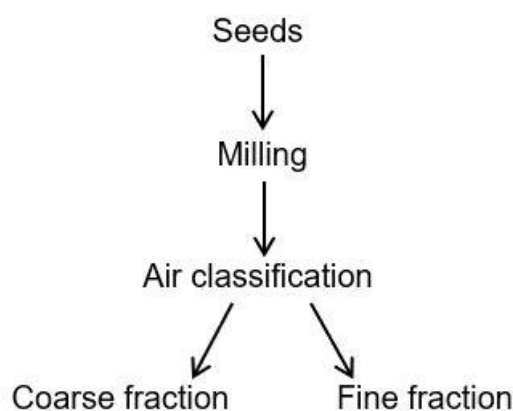


Fig 2.3: The basic process of dry fractionation (Schutyser et al., 2015)

The basic process of dry fractionation can be seen in Fig 2.3. Quinoa seeds were firstly pre-milled to separate the cotyledons from the seed using a laboratory scale mill using 1.25 mm and 2.0 mm screens. The rotor speed was 6000 rpm, and the feed rate was 20 g/min. The pre-milled quinoa seeds were then sieved by air jet sieving at 1500 Pa for 2.5 min with different sieves (0.800, 0.630, and 0.315 mm) (Opazo-Navarrete et al., 2018). After milling, air classification separates the smaller protein-rich fragments (approx. < 1.25 μm) from the larger starch granules (~2.5- 3.0 μm) (Schutyser et al., 2015). Rotor classifiers are commonly used for air classification of finely ground flours. The flour is distributed in a broad stream of air in this classifier. It then enters from the bottom and rises into a conical tank housing a spinning classification wheel with blades at the top. These blades provide a centrifugal-counterflow separation zone that separates small and big particles. The particle density has an effect on the separation behaviour as well. The size of the particles that end up in the fine fraction is determined by the drag forces caused by the air flow and the centrifugal forces created by the classifier wheel. Particles with a drag force greater than the centrifugal force may pass through the gaps in the wheel and enter the fine fraction (Pelgrom et al., 2013). Fractions (Quinoa protein concentrate) obtained using the dry fractionation method has a 47 % protein yield with a protein purity of 27.8 % (w/dw). Proteins can be kept in their native state by using the dry fraction method. However, it typically leads to a protein fraction with much lower protein content and purity compared to that obtained from the wet extraction process.

Table 2.7: Summary of methods used for quinoa protein extractions with the protein yield and purity. QPC- Quinoa protein concentrate, QPI- Quinoa protein isolate.

Method of protein extraction	Yield based on the dry matter of quinoa flour	Protein content	Protein extraction condition	Defatting solvent	Reference
-------------------------------------	--	------------------------	-------------------------------------	--------------------------	------------------

Wet Fractionation (QPI)	47 %		0.5 M NaCl/50 mM HCl pH 8	Cold acetone	(Brinegar & Goundan, 1993)
	77.2-83.5 %	-	pH 9 and pH 11	Hexane	(Abugoch et al., 2008)
	37-56 %	67-79 %	pH 7.5-10.5	Petroleum ether	(Callisaya et al., 2009)
	-	46-82 %	pH 8-12	Hexane	(Scanlin & Stone, 2009)
	76.3 %	-	pH 11	Hexane	(Guerreo-Ochoa et al., 2015)
	74.3 %	88-91 %	pH 8-11	Petroleum ether	(Ruiz, Xiao, et al., 2016)
	24-37 %	90-93 %	pH 8-11	Petroleum ether	(Ruiz, Opazo-Navarrete, et al., 2016)
Dry Fractionation (QPC)	47 %	28 %	Milling speed 6000 rpm and Sieving (1.5 to 2.0 μ m)	Petroleum ether	(Opazo-Navarrete et al., 2018)

Table 2.7 describes an overview of methods for quinoa protein extractions. The yield and purity of protein recovered by wet and dry fractionation methods are also compared. It can be seen that the wet extraction is the most commonly used method to obtain quinoa protein isolate with a high protein purity and protein yield. Further, the protein yield increases as the pH is increased. However, the dry fractionation method usually leads to protein extracts with a lower protein content because of different physical limitations such as powder fouling and starch degradation caused by mechanical forces. For example, smaller protein particles can adhere to the large starch particles during protein-starch separation, which has a detrimental effect on the yield and purity of the protein fraction (Dijkink et al., 2007).

2.4. Physicochemical properties and techno-functional properties of QPI

The QPI obtained from different extraction conditions show different techno-functional properties such as gelation, emulsification, solubility and foaming capability and stability. These techno-functionalities are critical for the QPI applications in food products and are described in the following sections.

2.4.1. Gelation property

Globular proteins can form gels with two different microstructures, which are fine and stranded or coarse networks depending on gelation conditions. While the fine stranded gel is transparent at pH values far from isoelectric point and at low ionic strength (Zhang et al., 2010), coarse gels are turbid when the ionic strength is increased and pH is close to the isoelectric point (Pathania et al., 2019). Denaturation of protein molecules by high hydrostatic pressure, heat treatment or pH adjustment can form a three-dimensional network induced by the protein aggregation (Kaspchak, Oliveira, et al., 2017). The easiest way to form a globular protein gel is to heat the globular protein above its denaturation temperatures (~70 °C-120 °C) (Tobitani & Ross-Murphy, 1997).

The effect of pH (3.5 and 7.0) and additions of CaCl₂ and MgCl₂ on the heat-set gelation of a quinoa protein isolate at 10% and 15% (w/w) concentrations was studied by Kaspchak, Oliveira, et al. (2017). The gels formed at pH 3.5 were viscoelastic and denser than those formed at pH 7.0, which were coarser and had syneresis. The addition of CaCl₂ and MgCl₂ enhanced the gel strength at pH 3.5, which could be attributed to the formation of fiber-like connections in the gel network. The divalent salts resulted in weaker gels with large agglomerates at pH 7.0, indicating that protein surface charges were screened and repulsions between proteins were dismissed. It was also found that the gelation temperature attained in this study (~64- 87 °C) was lower than the quinoa protein denaturation temperature (~98 °C).

Ruiz, Xiao, et al. (2016) studied the effect of extraction pH on the heat induced gelation of QPI. QPI were extracted at various pH values (pH 8 (E8), pH 9 (E9), pH 10 (E10), and pH 11 (E11)), which was then acid precipitated and freeze dried. The protein isolates E8 and E9 had a lower protein yield (~37 %) with a less extent of protein denaturation. Heating the 10% w/w protein isolate suspensions E8 and E9 resulted in extensive protein aggregation and formations of semi-solid gels with a dense microstructure. However, the quinoa isolate suspensions E10

and E11 aggregated less, did not form self-supporting gels, and exhibited loose particle interactions. It might be due to increased protein denaturation at E10 and E11 samples.

2.4.2. Emulsion capacity and stability

Emulsions are dispersions made up of two immiscible liquid phases that are mixed together with the aid of mechanical stress and surfactants (Kale & Deore, 2017). The maximum quantity of oil that can be incorporated in an aqueous solution containing a specific amount of the emulsifier without the phase inversion is defined as the emulsion capacity. Emulsions which can stay without any phase separation under a specific temperature and centrifugation force for a specific amount of time is defined as emulsion stability (McClements, 2004). The emulsion ability of quinoa protein isolate ranged from ~1.5 m²/g to 3.4 m²/g when protein concentration increased from 0.1 % to 3 %. With the increase in protein concentration emulsion ability increased. However, emulsion stability decreased from ~42 to 30 min as the concentration of quinoa protein isolate increased (0.1 to 3%) (Elsahaimy et al., 2015).

2.4.3. Solubility of quinoa protein isolates

Abugoch et al. (2008) studied the solubility of QPI that were obtained from alkaline extraction at pH 9 (Q9) and pH 11 (Q11). Protein isolated at pH 9 (Q9) showed a high solubility (~85 %) than that of Q11 (~41 %). Kaspchak, Oliveira, et al. (2017) found that the solubility of the QPI at acidic pH (below pH 6) is very low 0- 4 %, while at basic pHs i.e., (above pH 8) solubility is significantly increased to 77-97 %. This could be due to the solubility of QPI being minimum at the isoelectric point (pH ~4.5) as there are minimum electrostatic repulsions, which lead to protein association and precipitation.

2.4.4. Foaming capacity and stability

Foaming properties of QPI are greatly influenced by the protein hydrophobicity, interfacial layer qualities, and moisture retention capacity (Nadathur et al., 2016). Foaming capacity of quinoa is also dependent on the pH. At higher pH (above pH 7) the foaming capacity was ~80 % for 0.5 g QPI powder mixed into 50 mL distilled water and homogenized at 20,000 rpm for 2 min. The higher foaming capacity at a higher pH could be explained by the increased protein solubility due to increase in the net charge of protein in the aqueous dispersion (Shen et al., 2021). With the increase in the concentration of QPI from 0.1 to 3.0 % w/v , the foaming

capacity of quinoa protein increased from 58.3 to 78.6 % (homogenized at 16000 rpm for 1 min) (Elsouhaimy et al., 2015).

2.5. Food applications of quinoa proteins

Numerous studies have emphasised the importance of plant proteins for general good health and wellbeing, including weight control heart health and muscle maintenance (Akharume et al., 2021; Paul, 2009; Soenen & Westerterp-Plantenga, 2008). Owing to its excellent technical functionalities such as foaming capacity, quinoa proteins have been used in manufacturing of bread, beer, and biscuits (Deželak et al., 2014; Valcárcel-Yamani & Lannes, 2012). With excellent water/oil absorption, and gelation capabilities, quinoa can be used in the manufacturing of bakery products and sausages (Kinsella & Melachouris, 1976; Oshodi et al., 1997). Most of the applications of quinoa proteins are found in bakery and meat products as shown in Table 2.8.

Table 2.8: Application of quinoa in the food industry

Product	Quinoa fraction used	Replaced ingredient	Concentration applied	Used as	References
Pasta	Quinoa protein isolate	Semolina	0.8 g/ 100 g (total w/w basis)	Functional ingredient to increase the protein content, water absorption and volume expansion	(Gupta et al., 2021)
Cupcakes	Quinoa protein isolate	Wheat flour	20 %	Emulsifier, water absorption	(López-Alarcón et al., 2019)
Bologna	Fibre-rich fraction (quinoa starch)	Potato starch	NA	Emulsifier	(Fernández-López, Lucas-González, Roldán-Verdú, et al., 2020; Fernández-López, Lucas-González, Viuda-Martos, et al., 2020)

Pâté	Quinoa flour paste	Pork back fat	10 %	Fat replacer	(Pellegrini et al., 2018)
Goat nugget	Quinoa flour	Refined wheat flour	3 %	Functional ingredient	(Verma et al., 2019)
Cooked sausages	Quinoa flour	Refined wheat flour	5 %	Fat replacer	(Peña et al., 2015)
Beef meatball	Quinoa flour	Breadcrumbs	7.5 %	Functional ingredient to increase the protein content	(Bağdatli, 2018)
Beef burger	Quinoa flour	Breadcrumbs	10 %	Binder and extender replacer	(Özer & Secen, 2018)
Beef burger	Quinoa flour	Soybean flour	15 %	Binder and extender replacer	(Shokry, 2016)

2.6. Food Polysaccharides

Food proteins usually coexist with polysaccharides in many food products such as gels, salad dressings, jellies and pies to name a few (Nasrollahzadeh et al., 2021). Some polysaccharides commonly used in the food industry are shown in Fig 2.4. Incorporations of polysaccharides is one of the most efficient strategies to enhance the gel strength and water holding capability of protein gels (Monteiro & Lopes-da-Silva, 2017; Sónia R Monteiro et al., 2013; Patole et al., 2022). In the following section, the food polysaccharides used in this thesis including Guar gum, Locust Bean gum and Xanthan gum are introduced. Characteristics of commonly used polysaccharides in the food industry are listed in Table 2.9.

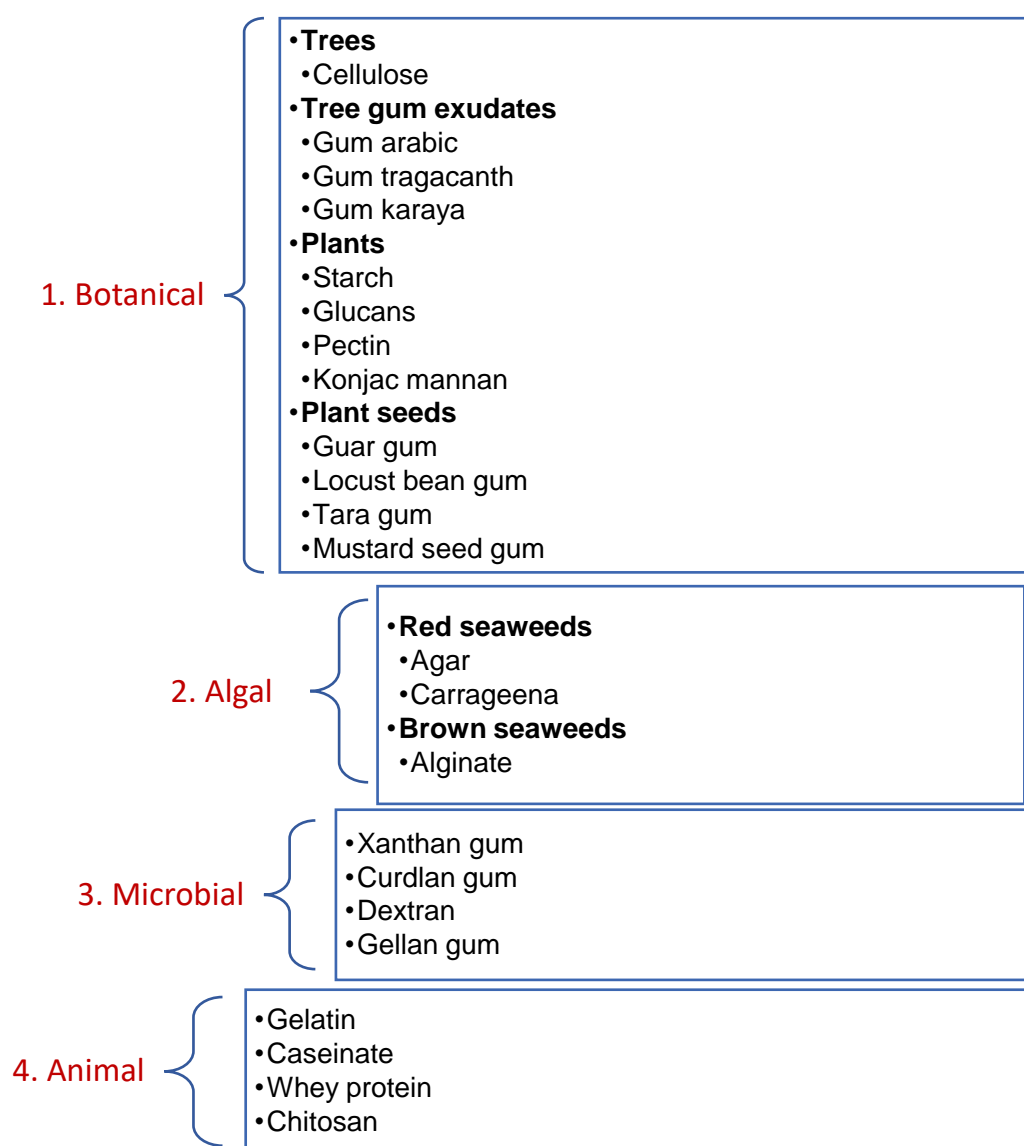


Fig 2.4: Types of food polysaccharides

Table 2.9: Characteristics of commonly used polysaccharides in the food industry

Name	Gelation characteristics	Gel strength, stability, and transparency	Gel syneresis	Reference
Agar	Thermo-reversible gelation upon cooling to 30– 40 °C and gels melt when heating above 76– 92 °C	High gel strength Highly heat stable Low transparency	High	(Sousa et al., 2021)
Alginates	Thermo-reversible gels induced by acid and multivalent cations	High strength High stability Low transparency	Medium	(Nordgård & Draget, 2021)
Carrageenan	κ -C can form gels in the presence of K^+ ι -C: can form gels in the presence of Ca^{2+} λ -C: no gelation with cations	κ -C: brittle but firm gels, inferior freeze-thaw stability ι -C: soft elastic gels, excellent freeze-thaw stability λ -C: no gelation	κ -C: high syneresis ι -C: no syneresis	(Tuvikene, 2021)
Guar gum	No self-gelation (25 °C to 90 °C)	-	-	(Mudgil et al., 2014)
Locust bean gum	No self-gelation Only with xanthan or κ -carrageenan can form gels	Stable and thermoreversible gels with xanthan Low transparency	No syneresis with the addition of xanthan or κ -carrageenan	(Barak & Mudgil, 2014)
Xanthan gum	No self-gelation but is highly viscous Gelation with LBG	High gel strength with combination with LBG.	Low syneresis	(Sworn, 2021;

Highly heat stable	Wüstenberg,
Highly	2015)
pseudoplastic	
Low gel	
transparency	

2.6.1. Non-ionic food polysaccharides

2.6.1.1. Guar gum (GG)

Guar gum is a non-ionic polysaccharide obtained from seeds of the drought-tolerant plant *Cyamopsis tetragonoloba*, a member of the Leguminosae family (George et al., 2019; Mudgil et al., 2014). Guar gum is a high molecular weight polysaccharide, which has a linear chain of (1→4) linked β-D-mannopyranosyl units with (1→6)-linked α-D-galactopyranosyl residues as side chains (Mudgil et al., 2014; Sharma et al., 2018). The galactose to mannose ratio of guar gum is 1:2. The higher hydrogen bonding and hydration property of guar gum are due to a higher degree of branching (Whistler, 1954). Guar gum is soluble in cold water rather than in hot water. At high temperatures, the viscosity of guar gum is reduced (Tripathy et al., 2008). Guar gum also produces high-viscosity solutions with pseudo-plasticity when the concentration is higher than 0.5 %. Guar gum is used in ice cream, dairy desserts, and bakery products as a binder and thickening agent. The main technical function of guar gum is to prevent syneresis and phase separation, and to control the texture of food products (Chudzikowski, 1971).

2.6.1.2. Locust bean gum (LBG)

Locust bean gum (LBG) has a galactose to mannose ratio of 5:3, and it is solubilized in hot water (~80 °C) (BeMiller & Whistler, 2012). Like guar gum, locust bean gum is also a non-ionic polysaccharide (Barak & Mudgil, 2014) and the chemical formula of LBG is shown in Fig 2.5. Ünal et al. (2003) reported that LBG reduced the syneresis and increased the water holding capacity of yoghurt. Locust bean gum can form a weak three-dimensional structure in warm water. The locust bean gum alone is not gelled but it can form gels in the presence of borate or saccharose (50 % by weight) (Voragen et al., 2003). Locust bean gum is an excellent thickener in beverages due to its high stability in a wide pH range (Gallagher et al., 2004).

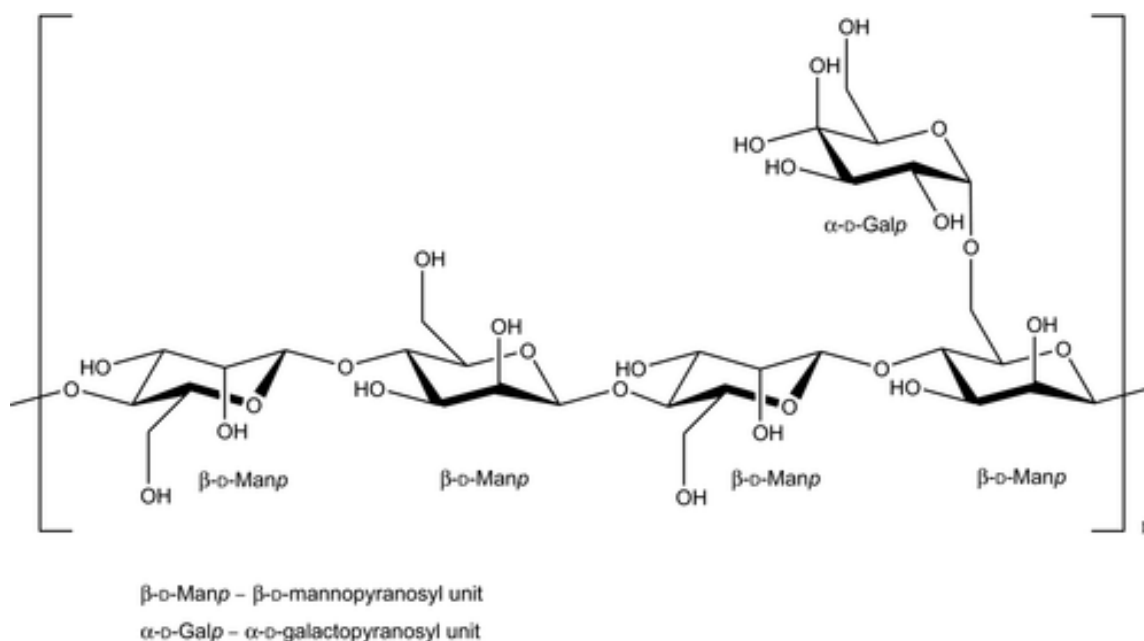


Fig 2.5: Chemical formula of the locust bean gum (Mortensen et al., 2017)

2.6.2. Ionic polysaccharides

2.6.2.1. Xanthan gum

Xanthan gum (XG) is an ionic polysaccharide obtained from an organism named *Xanthomonas campestris* (Jeanes et al., 1961). The main chain is made up of a 1,4-linked -D-glucose backbone with a charged trisaccharide side chain comprising a glucuronic acid residue between two mannose units at every alternate glucose residue's C(3) position. Xanthan gum changes from a disordered (random) structure to an ordered network in aqueous solutions when heated to ~70 °C (Bercea & Morariu, 2020). It also shows the pseudoplastic flow and it is stable at a broad range of temperature and pH (pH 1 to pH 13) (Kang & Pettitt, 1993). According to Habibi and Khosravi-Darani (2017), the addition of NaCl (more than 1-2% w/v) may slow down the hydration of xanthan gum in water. Monovalent salts such as sodium chloride can cause a decrease in viscosity of solution due to weakened intermolecular electrostatic interactions (Smith & Pace, 1982), however in the presence of divalent salts such as magnesium chloride or calcium chloride optimal rheological properties of gels were achieved (Milas & Rinaudo, 1986). Change in pH (pH 1 to pH 13) can cause xanthan gum to change the charge density, which affects the interactions with other food components like proteins (Agoub et al., 2007; Rinaudo & Moroni, 2009). Due to the pseudoplastic behaviour, xanthan gum provides good

mouthfeel and thickening properties, which can be used in many food products such as bakery, dairy products, syrups, soups and beverages (Kim et al., 2014; Mohammadi et al., 2014; Rosalam & England, 2006; Syafiq et al., 2014).

2.6.3. Protein-polysaccharide interactions

Protein-polysaccharide interactions are critical in the determination of rheological and textural properties of food products (Burgos-Díaz et al., 2016; Lytle et al., 2016; Pak et al., 2016; Semenova, 2017). Mixtures of polysaccharides and proteins are generally more efficient in improving gel strength than just using polysaccharide or protein alone in food formulations (Warnakulasuriya & Nickerson, 2018; Yang et al., 2021a; X. Yang et al., 2020). Several investigations have shown that interactions between polysaccharides and proteins might decrease colloidal stability, through the development of bridge or aggregation, or induce thermodynamic incompatibility (Doublier et al., 2000; Turgeon et al., 2007). There are two main reasons to studying protein-polysaccharide mixed systems. Firstly, each polymer shows different functionalities and physicochemical properties and may impart the different structures of gels. Secondly, mixed systems may have a synergetic effect on improving the mechanical strength and water holding capability of mixed food gels systems (Hou et al., 2015; Yang et al., 2021a). Table 2.10 briefly lists some of the protein- polysaccharide binary system.

The protein-polysaccharide interactions can induce phase separations due to two different separation mechanisms (De Kruif & Tuinier, 2001; Laneuville et al., 2000). Firstly, the segregative phase separation is caused by the same charges present on each polymer. These similar charges repel polymers, causing the segregative phase separation. On the other hand, the associative phase separation is caused by electrostatic attractions between opposing net charges leading to the thermodynamic incompatibility between biopolymers and leads to a biopolymer- and solvent-rich phase (Klassen et al., 2011). The phase separation caused by the mixed system results in the formation of soluble or insoluble complexes (Fig. 2.6). The phase separation is affected by several factors: 1) *pH*- due to its influence on the ionization of functional groups of biopolymers in solutions, pH has a substantial impact on the complex formation between polysaccharides and proteins (Kayitmazer, 2017; Schmitt et al., 1998). 2) *ionic strength*- the addition of salt (counterions) has a significant impact on protein-polysaccharide complexation due to two reasons; firstly, adding salts lead to charge screening hence it reduces the interaction between the polymer in the mixed system and secondly, when the concentration of the counterions increased, the release of counterions via ion exchange is

weakened and hence complex formation is suppressed (Ducel et al., 2005; Kizilay et al., 2011).

3) *mixing ratio of protein to polysaccharide*- the ideal mixing ratio corresponds to a complete charge neutralisation in the biopolymer mixture. The electrophoretic mobility of the biopolymer complexes is zero at the complete charge neutralisation ratio, indicating the maximum number of formed particles. The neutralisation of biopolymer mixture is insufficient at ratios below the optimal mixing ratio, thus the complexes may still be soluble (Chun et al., 2014).

Fig 2.6: Complex formations in protein-polysaccharide systems (Warnakulasuriya & Nickerson, 2018).

Table 2.10: Rheological studies of plant protein-polysaccharide systems

Protein-polysaccharide mixtures	Variables	Conclusions	References
Quinoa protein (QP), iota-carrageenan (iC)	Concentration (18, 30 and 42 g/L), GDL/QP mass ratio (0.33, 0.66, 1.00)	Gelation was induced by acidification (GDL) GDL/QP mass ratio affects the structure and size of aggregates formed and also affects the rate of acidification During the gel formation, Carr interacts with QP at a pH range of 3.4 – 3.9 due to electrostatic and hydrophobic interactions	(Montellano Duran et al., 2019)
Canola protein (CPI), high methoxyl pectin (HMP) and low methoxyl pectin (LMP).	pH (1.5 to 8.0), mixing ratio (1:1 to 30:1, CPI: pectin)	At pH 5.3 and 4.8 a maximum coacervation of CPI-HMP and CPI-LMP system occurred at a mixing ratio of 10:1. The mixtures showed a larger pseudoplastic behaviour compared with CPI alone	(Stone et al., 2015)
Caroba protein isolate (CPI), locust bean gum (LBG)	Concentration (2- 4 wt%), pH (2- 10)	G' and G'' increased as the protein concentration increased in the mixture. Phase separations were observed for LBG rich and CPI rich system The viscoelastic behaviour of the CPI-LBG mixed system is affected by pH	(Zárate-Ramírez et al., 2010)

Canola protein (CPI), kappa carrageenan (κ C)	Salts, urea, dithiothreitol	G' values increased in the CPI- κ C system in the following series with different salts- Chloride- Sulphate- Acetate > Thiocyanate ion (Cl^- - SO_4^{2-} - $\text{C}_2\text{H}_3\text{O}_2^-$ > SCN^-). Non-covalent interactions were involved in network formations	(Uruakpa & Arntfield, 2006)
Soybean flour , pectin	Different ratio (10/90, 25/75, 50/50, 75/25, 90/10), mixed concentration (Pectin and soy flour mixed together: 15.7/ 10.4 mg/mL; 7.4/ 10.4 mg/mL; 15.7/ 4.6 mg/mL and 7.4/ 4.6 mg/mL).	A high concentration of soy flour suspension and pectin stabilized the system. Soy flour suspension (13mg/ml) with pectin (16 mg/ml) showed a continuous network.	(Giancone et al., 2009)
Canola protein isolate (CPI), gum arabic (GA)	pH (1.5 to 7.0), biopolymer mixing ratio (1:1 to 8:1, CPI: GA)	CPI-GA mixed system showed elastic-like behaviour at pH 4.2 The mixed system also showed shear-thinning properties as the complex viscosity decreased with an increase in frequency	(Stone et al., 2014)

2.7. Whey proteins

Whey is defined as "the liquid substance obtained in cheesemaking by separating the coagulum from milk, cream, or skim milk" by the United States Code of Federal Regulations (21CFR184.1979) (Huffman & de Barros Ferreira, 2011). Casein proteins precipitate and whey proteins are generated during the coagulation of milk, which can be induced by the action of microorganisms, acids, or the use of enzymes (rennin or chymosin) (Kilara & Vaghela, 2018). Whey proteins can be obtained from two main streams: cheese manufacturing and casein production. Based on this, whey can be categorized into two types: acid whey and sweet whey. Acid whey is obtained from direct acidification of milk during casein production or during acid-coagulated cheese formation such as cottage cheese. The sweet whey is produced during the manufacturing of casein and cheese (i.e., cheddar cheese) by rennet coagulation of milk (Tunick, 2008). Acid whey has a pH range of 4.6-5.0 and sweet whey has a pH range of 6.0-6.5 (Bansal & Bhandari, 2016). The major proteins present in whey are β -lactoglobulin, α -lactalbumin, bovine serum albumin (BSA), immunoglobulin and proteose-peptone (Gangurde et al., 2011). The properties of these proteins are shown in Table 2.11. The structure of β -lactoglobulin and α -lactalbumin is different from each other which can be seen in Fig 2.7 and Fig 2.8, respectively.

At neutral pH, bovine β -lactoglobulin is a globular protein with a molar mass (M_w) of 18.3 kDa that exists mostly as a dimer (Schokker et al., 2000). β -lactoglobulin approximately accounts for 58 % of whey protein and contains one sulfhydryl group and two disulphide groups (Swaigood, 1982). Fox et al. (1998) indicated that whey proteins are completely denatured at 90 °C for 10 min. When the temperature is above 70 °C, β -lactoglobulin start to denature β -lactoglobulin dimers break into monomers at ~70 °C, and a thiol group and hydrophobic residues become exposed (Hoffmann & van Mil, 1997). The α -lactalbumin accounts for 13 % of total whey proteins. α -lactalbumin has four disulphide groups and no phosphate groups (Kilara & Vaghela, 2018). According to Havea et al. (1998) and Oldfield et al. (1998), β -lactoglobulin aggregates faster than α -lactalbumin under the heat treatment. Disulphide bond and hydrophobic interaction are responsible for aggregations of α -lactalbumin (Schokker et al., 2000). According to De Wit (1989), α -lactalbumin starts to denature at 64 °C. Bovine serum albumin (BSA) has one sulfhydryl group, 17 disulphide groups and no phosphate groups. BSA is similar to a blood serum molecule and it also has binding sites for hydrophobic molecules (Brown, 1977). Immunoglobulin (Ig) has four types: IgG₁, IgG₂, IgA, IgM, which accounts for

2 % of total milk protein (Swaisgood, 1982). Whey protein concentrates (WPC) and whey protein isolates (WPI) are produced via membrane separation techniques such as microfiltration or ultrafiltration. Ultrafiltration is a technique where whey proteins are passed through pore sizes of 0.001- 0.1 μm . A more detailed flow chart of manufacturing of WPC and WPI is shown in Fig 2.9.

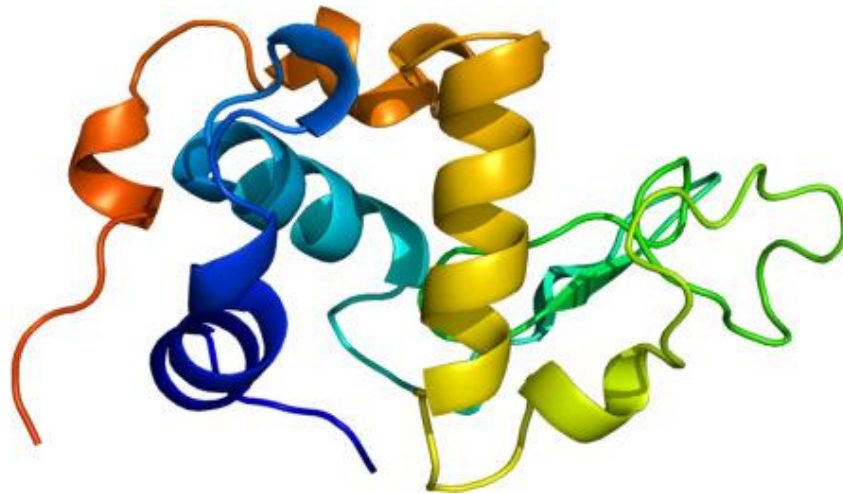


Fig 2.7: Structure of α -lactalbumin (Bernstein et al., 1977)

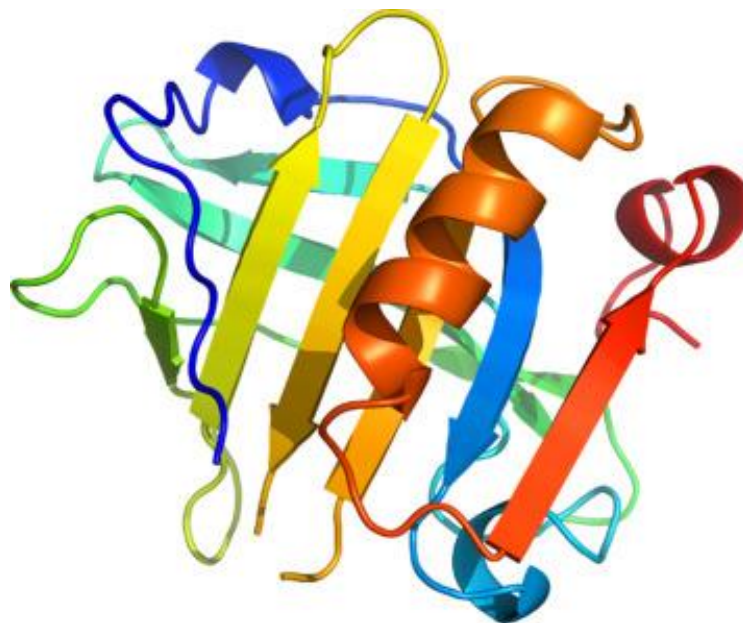


Fig 2.8: Structure of β -lactoglobulin (Kinsella & Morr, 1984).

Fig 2.9: A flowchart for production of whey protein isolate (WPI) and whey protein concentrate (WPC) (Bansal & Bhandari, 2016)

Table 2.11: Properties of acid whey protein (Anon, 2007; Mulvihill & Donovan, 1987)

Whey protein	Isoelectric point	Concentration in milk (g/kg)	Molecular weight (kDa)
β -lactoglobulin	5.13	3.3	18.36- 36.9
α -lactalbumin	4.2-4.5	1.2	14.147

Bovine serum albumin (BSA)	4.7-4.9	0.4	66.267- 69
Immunoglobulin	5.5-8.3	0.7	160
Proteose-peptone	5.1-6.0	0.8	4- 800

2.7.1. Whey protein denaturation and gelation

Whey protein is soluble in a wide range of pH and its solubility is dependent on temperature and the presence of ions (Kilara, 1984). For example, whey protein's solubility is increased at 40 °C in a pH range from 3.8 to 7.8 except for pH 4.5 (isoelectric point of WPI) (Pelegri & Gasparetto, 2005). When the WPI are dispersed in water, it leads to an increase in viscosity and thickening of the solution. The viscosity of whey protein solution starts to rise above 65 °C, and it rises much faster at temperatures exceeding 85 °C. It has been suggested that whey protein denatures between 65 °C and 85 °C and the denaturation further leads to aggregation and gelation (De Wit, 1989).

The reactive side-chain groups buried in the interior of the whey protein molecules are exposed and protein unfolds to the random configuration when the temperature is above the denaturation temperature of whey proteins. In addition, irreversible sulfhydryl-disulphide interchange reaction occurs during the heating, leading to the formation of disulphide linkages (Galani & Owusu Apenten, 1999). The aggregation and denaturation behaviour of whey proteins is complicated, as the whey protein is a mixture of different proteins, which exhibit different denaturation temperatures (Table 2.12). For example, bovine serum albumin (BSA) can aggregate faster and forms stiffer gels than that of β -lactoglobulin (Gezimati et al., 1996; Hines & Foegeding, 1993). Globular proteins have been extensively used as structuring and gelation agents in food industry (Nieto-Nieto et al., 2014). However, plant globular proteins such as QPI and dairy globular proteins like WPI may demonstrate different gelation behaviour in terms of gelation time and gel strength due to different physiochemical properties and microstructures (Tanger et al., 2021). In this thesis, the gelation behaviour of QPI will be compared to that of WPI in order to better understand the gelation behaviour differences between plant and dairy proteins.

Table 2.12: Denaturation temperatures of whey protein components (Jenness et al., 1988)

Whey protein components	Denaturation temperature
β -lactoglobulin	62°C
α -lactalbumin	78°C
Bovine serum albumin	64°C
Immunoglobulin	72°C

2.7.2. Application of Whey protein in the food industry

Whey protein isolate is one of the most immensely used dairy proteins in the food industry. WPI has found many applications in the food industry (Table 2.13). One of the most important functionalities of WPI is gelation, which is critical for many food applications as shown in Table 2.14.

Table 2.13: Application of whey proteins in the food industry (Bansal & Bhandari, 2016; Kilara & Vaghela, 2018; Mulvihill & Ennis, 2003)

Category	Application	Techno-Functionalities
Convenience foods	Gravy mixes, sauces, canned soups, dehydrated cream soups and sauces, salad dressings	Emulsifier, water holding capacity, freeze-thaw stability, egg yolk replacer, viscosity controller, stabilizer, flavour enhancer
Infant formula	Pre-term formula, term formula, follow-on formula	Nutritional benefits
Meat products	Luncheon meats, frankfurters	Fat binding, water holding capacity, gelation
Confectionary	Areated cany mixes, sponge cakes	Whipping properties, egg white replacement, foam stability, fat binding

Dairy products	Cream cheese, cream cheese spreads, cheese fillings and dips, yoghurt	Sensory properties, emulsifier, gelling, curd cohesiveness, nutritional benefits
Bakery products	Croissants, cakes, muffins, bread	Egg replacer, emulsifier, nutritional benefits
Beverages	Milk-based flavoured beverages	Colloidal stability, viscosity, nutritional benefits

Table 2.14: Gelation application of whey protein isolate in food products

Products	Whey ingredients used	Concentration of whey proteins	Conclusion	Reference
Set yoghurt	Unheated WPI, heat-treated WPI, heat-treated WPI + sodium tripolyphosphate (WPI-STPP), heat treated WPI + pectin	Heat-treated WPI-STPP- 50 g kg ⁻¹	<ol style="list-style-type: none"> Heat-treated WPI- STPP showed a complex, uniform, and denser microstructure. The use of heat-treated WPI-STPP also showed high protein quantity and hardness and viscosity as compared with commercial yoghurt 	(Cheng et al., 2017)
Camel milk yoghurt	Polymerized whey protein isolate (PWPI)	8 % w/v	<ol style="list-style-type: none"> PWPI was used in replacement of thickeners such as agar or starch PWIP also showed increased protein content, water holding capacity and viscosity compared with camel milk yoghurt without the addition of PWPI The addition of PWPI also showed a decrease in syneresis 	(Sakandar et al., 2014)
Oats-based symbiotic yoghurt	Pre-polymerized whey protein isolate (PWP)	PWP- 0.8 % w/w	<ol style="list-style-type: none"> The microstructure of the samples revealed an increased concentration of PWP led to a denser protein network 9 week of storage shelf-life study showed <i>L. casei</i> and <i>Bifidobacterium</i> remained at a therapeutic level 	(Walsh et al., 2010)

			3. Organoleptic test conducted by consumer showed fair acceptability of the product	
Protein fortified set yoghurt (Chinese Laosuan Nai)	Polymerized whey protein (PWP),	PWP- 0.4 % w/v	<ol style="list-style-type: none"> 1. PWP was used successfully as a co-thickening agent in all the yoghurt samples. 2. The average acceptability of all the samples was obtained from trained panellists 3. The addition of PWP with Whey protein concentrate (WPC), Non-fat dairy milk (NFDM) and Whole milk powder (WMP) revealed dense microstructure, higher viscosity and lower syneresis 	(Wang et al., 2015)
Symbiotic corn-based yoghurt	Polymerized whey protein	Polymerized whey protein- 0.3%	<ol style="list-style-type: none"> 1. The addition of polymerized whey protein and xanthan gum affected the structure of the yoghurt 2. The microstructure of the corn-based yoghurt revealed high viscosity and denser structure 	(Wang et al., 2017)
Beverage	Whey protein isolate (WPI)	WPI- 4 % w/w	<ol style="list-style-type: none"> 1. Heat set soluble complex of WPI showed decreased viscosity. 2. The heat-treated soluble complex also showed a smaller particle diameter than the non-heat-treated soluble complex of WPI 3. WPI and HMP can be used in beverages showing increased colloidal stability 	(Wagoner & Foegeding, 2017)

2.8. Food Protein Gels

From rheology, any viscoelastic networks showing higher storage modulus (G') than loss modulus (G'') can be defined as a gel (de Vries, 2004; Saha & Bhattacharya, 2010). Aguilera (1992) defined gels as materials that show mechanical rigidity and are neither a solid nor a liquid. Clark (1992) defines gels as the material comprising a continuous and distinct solid-like network that is formed from particles or polymers embedded in a solvent or medium. When the degree of crosslinking between polymers such as proteins exceeds a critical value, known as the gelation point, the 3 dimensional network was formed and gelation occurred, according to the Flory-Stockmayer model (Hettiarachchy & Ziegler, 1994; Smith, 1994). Food protein gels can be either cold set or heat induced. In general, there are two types of gel networks, fine-stranded and coarse network (Fig. 2.10). In the fine-stranded network gels, the protein are unfolded and attached to each other to form strings-like structure, whereas, coarse gels are formed by random aggregation of proteins (Hermansson, 1994).

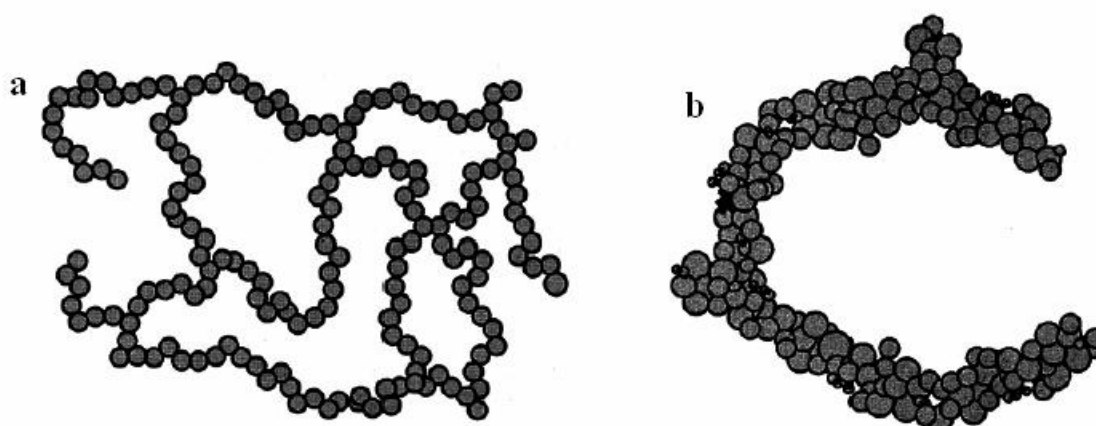


Fig 2.10: A schematic illustration of protein gel networks, a. fine-stranded gel network b. coarse gel network (Hermansson, 1994).

2.8.1. Heat-induced gelation of food proteins

In simple words, transforming a protein solution to a solid-like structure by denaturing proteins under the heat treatment is named as heat-induced gelation. Heat-induced protein gelation includes few steps. Firstly, when native globulins are heated above the denaturation temperature, small aggregates are formed. Secondly, the small aggregates are reassembled into dense, roughly spherical particles, which then stick together to form large aggregates. Finally,

these large aggregates permeate and form a three-dimensional crosslinking network (Nicolai & Chassenieux, 2019). A schematic representation of heat-induced gelation of globular proteins is shown in Fig. 2.11.

As protein solutions are heated, protein molecules start to denature, and aggregates are formed due to crosslinking. The protein aggregates are grown in sizes as the heating duration increases, eventually forming a gel (Erik van der & Foegeding, 2009; Mezzenga & Fischer, 2013). The cross-linking between proteins depends on the type of proteins and external conditions such as concentration of proteins, pH, and ionic strength. Moreover, aggregates must have a self-similar structure on substantial length scales to form a 3D network (Nicolai & Chassenieux, 2019). A schematic illustration of heat-induced gelation of soy protein isolates leading to the formation of self-similar and fractal-like aggregate is shown in Fig. 2.12. During the denaturation of proteins, intermolecular forces such as non-covalent bonds (e.g., hydrogen bonds and hydrophobic interactions) and disulphide bonds are formed between proteins to form cross-linking of protein structures (Fitzsimons et al., 2007). Table 2.15 summarizes previous studies on heat induced gelation of quinoa protein isolates.

Fig 2.11: A schematic diagram of heat-induced gelation of globular proteins. T° represents the temperature and T_D represents the denaturation temperature of proteins (Totosaus et al., 2002).

Fig 2.12: Heat-induced gelation of a soy protein isolate solution (Nicolai & Chassenieux, 2019).

Table 2.15: Previous studies on thermally induced gelation of quinoa protein isolates or quinoa flour.

Samples studied	Rheological measurements	Conclusions	Reference
QPI concentration- 10% (w/w), 15% (w/w) pH- 3.5, 7.0 Salt- CaCl ₂ , MgCl ₂ (0, 0.55 mol g ⁻¹)	Temperature sweep- 20 °C to 90 °C; cooled down from 90 °C to 20 °C at 2 °C/min at a constant frequency (1 Hz) and strain (1 %)	<ol style="list-style-type: none"> 1. Heat set gelation occurred at both pH values. 2. The gels formed at pH 3.5 were more viscoelastic and denser than those formed at neutral pH. 3. Addition of CaCl₂ and MgCl₂ increased the gelation at pH 3.5 but weaker gels were formed at pH 7. 	(Kaspchak, Oliveira, et al., 2017)
QPI concentration- 10% (w/w) Quinoa protein suspensions- E8, E9, E10, E11 (proteins were extracted at pH 8, pH 9, pH 10, pH 11, respectively)	Temperature sweep- 20 °C to 90 °C (heating rate 1 °C/min); holding at 90 °C for 5 min; before cooling to 20 °C at 3 °C/min; at a strain of 1 % and frequency of 0.1 Hz	<ol style="list-style-type: none"> 1. E8 and E9 samples showed higher gel strength with a dense microstructure. 2. E10 and E11 did not formed self-supporting gels and had loose particle arrangements. 	(Ruiz, Xiao, et al., 2016)
Quinoa flour (QF) concentration- 300 g/kg, 250 g/kg, 200 g/kg, 150 g/kg at 90 °C (Condition 1). Temperature of 60 °C, 70 °C, 80 °C and 90 °C at 300 g/kg (Condition 2).	Temperature was increased to 25 °C to 60 °C, 70 °C, 80 °C and 90 °C, respectively, holding at the target temperature for 30 min before cooling to 25 °C.	<ol style="list-style-type: none"> 1. For the 1st condition- Increase in QF concentration increased the G' values. 2. For the 2nd condition-the G' values of QPI gelled at 70 °C, 80 °C and 90 °C were similar (~ 17000 Pa), G' is significantly lower (~1150 Pa) when gelled at but at 60 °C 	(Felix et al., 2021)

2.8.2. Cold-set gelation of food proteins

The cold-set gelation process typically involves few steps. Firstly, the protein solution is heated above the protein denaturation temperature but below the gelation temperature so that small protein aggregates are formed without gelation. Secondly, to induce the gelation, the addition of either salt (e.g., CaCl_2 or NaCl), enzymes (e.g., transglutaminase), or lowering pH by bacterial cultures, or acids like glucono- δ -lactone (GDL) could further cross-link aggregates to form a gel network at an ambient temperature (Alting, 2003). The addition of small amounts of salts induced the formation of a fine-stranded transparent gel due to reduced distinct distance between crosslinked strands (Nicolai, 2019). However, the addition of a high concentration of salts resulted in the formation of turbid and particulate gels (Barbut, 1995; Barbut & Foegeding, 1993; McClements & Keogh, 1995). Fig. 2.13 illustrates the two steps involved in the cold gelation of globular proteins. For example, WPI can form cold set gels by firstly heating below its gelation temperature ($68.5\text{ }^\circ\text{C}$) to form small aggregates. The addition of glucono- δ -lactone (GDL) to the WPI solution induced a progressive decrease in pH to the isoelectric point ($\sim\text{pH } 5$), and the gel network is formed (Alting et al., 2003).

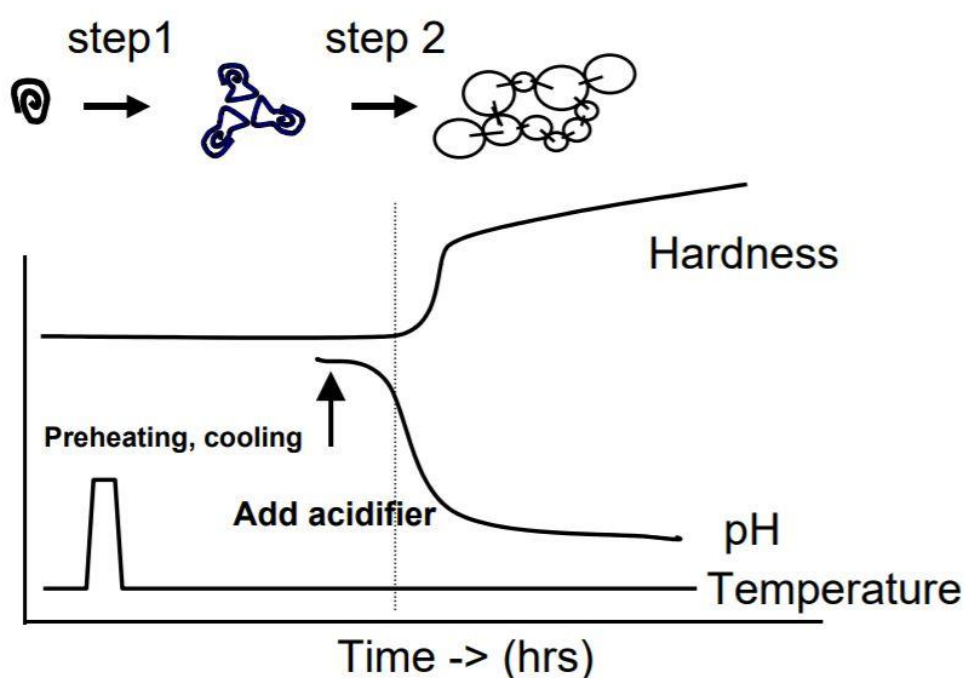


Fig 2.13: The two-step procedure of cold-set gelation. Firstly, a solution of the native protein is heated at a pH far away from pI so that protein aggregates are formed. Secondly, the addition of acid will reduce the pH and gelation is induced at an ambient temperature (Alting, 2003).

2.8.3. Factors affecting the gelation of food proteins

2.8.3.1. Effect of temperature

Temperature plays an important role in the formation of plant protein gels. When soy protein isolate (SPI) solution is heated above 50 °C, proteins unfold, resulting in irreversible protein accumulation via hydrogen and disulphide bonds, as well as hydrophobic interactions (Chen et al., 2016). For most of plant proteins, the gelation temperature is varied from 70 °C to 120 °C as different proteins have different denaturation temperatures (Kaspchak, Oliveira, et al., 2017; Tarone et al., 2013). Kaspchak, Oliveira, et al. (2017) reported that quinoa protein gelation occurred in the temperature range from 64.6 °C to 87.3 °C. For example, Chen et al. (2017) studied the effect of temperature and reported that increase in temperature during gelation decreases the gelation time, soy protein isolate solution (90 g/L) was heated from 65 °C to 85 °C containing 0.1 M NaCl. It was found that at 85 °C, the G' value of SPI solution was two times higher than the G' value at 65 °C. Moreover, at a higher temperature (85 °C), SPI gel was formed within less than 10 min, while at a lower temperature (65 °C) longer time (>100 min) is required for the gelation.

2.8.3.2. Effect of protein concentration

With the increase in protein concentrations, the gel strength increases. Chen et al. (2016) reported that with the increase in protein concentration of soy globulin from 0.3 g/L to 90 g/L, storage modulus (G') increases upto ~1000 Pa (90 g/L). The storage modulus for 0.3 g/L was not determined as it showed weak gel. G' was increased three times when the concentration of SPI was increased from 50 g/L to 90 g/L (90 °C, 0.05 M NaCl) and the gelation time was decreased from 20 min to 3 min (Chen et al., 2017). Savadkoohi and Farahnaky (2012) reported that as the concentration of the tomato seed protein isolate increased from 1% (w/w) to 10% (w/w) the G' increased from ~1500 Pa to ~2300 Pa.

2.8.3.3. Effect of ionic strength

The ionic strength has an effect on proteins solubility and its hydration property (Montero & Borderías, 1988), ultimately affecting the microstructure of the gel network (Totosaus et al.,

2002). The addition of monovalent ions (NaCl) to globular protein such as whey protein or soy protein forms fine stranded gel networks when the concentration of ions is below 100 mM (Totosaus et al., 2002). But adding small concentrations (20 mM to 50 mM) of divalent salts has a significant impact on gel formations (Foegeding et al., 1995). For example, the addition of Ca^{2+} promotes soy protein aggregation by screening electrostatic interaction between charged protein molecules (Li et al., 2009). Due to the exchange of $\text{H}^+/\text{Ca}^{2+}$ electrostatic repulsion is reduced between soy protein and Ca^{2+} leading to the formation of a three-dimensional network (Canabady-Rochelle et al., 2009). Addition of 7.5 mM Ca^{2+} in soy protein increased G' to ~ 2000 Pa when compared to 0 mM Ca^{2+} with G' showing ~ 1100 Pa when heated from 25 °C to 85 °C (Wang et al., 2018).

2.8.3.4. Effect of pH

pH plays a significant role in the formation of gels. Fibrillar gel networks (soy protein, pea protein and whey protein) are formed when the pH is acidic ($< \text{pH } 4$) (Kavanagh et al., 2000; Munialo, Martin, et al., 2014). Kaspchak, Oliveira, et al. (2017) reported that QPI (15 w/w%) formed a stronger gel at pH 3.5 when heated from 70 °C to 90 °C than at pH 7.0 in the presence of divalent salts such as MgCl_2 . The G' value of more than 10^5 Pa was observed at pH 3.5, whereas G' value was just below 10^3 Pa at pH 7.0. The solubility of QPI at acidic pH is low since there are no repulsive charges which leads to protein association and precipitation resulting in higher G' at pH 3.5. Renkema et al. (2002) also found higher G' (~ 15000 Pa) for 12 wt% soy protein isolate at pH 3.8 when compared with pH 7.6 ($G' = \sim 2500$ Pa) (95 °C, 0.2 M NaCl).

2.8.4. Non-covalent and covalent interactions participating the protein gel formation

2.8.4.1. Hydrogen bonds

The short-range attractive interactions between polar groups are classified as hydrogen bonds. When a hydrogen atom links to a strongly electronegative atom involving nitrogen, oxygen, fluorine, or sulphur, it forms a hydrogen bond (Schmitt et al., 1998; Semenova & Dickinson, 2010). Hydrogen bonds are also responsible for protein folding and unfolding (Semenova & Dickinson, 2010). Hydrogen bonds are critical in the formation of proteins' secondary and tertiary structures since they cause significant coordination of the molecules (intermolecular or intramolecular) involved (Bryant & McClements, 1998). Furthermore, hydrogen bonds are

weakened at a higher temperature but strengthened during cooling, contributing to the formation of protein gel network structures (Phillips et al., 2013; Semenova & Dickinson, 2010).

2.8.4.2. Disulfide bonds

Disulfide bonds stabilize the folded structure of the protein (Damodaran, 1996). Disulfide bonds are formed between the thiol groups of cysteine residues by process of oxidative folding. It links two segments of the protein chain and may form hydrophobic core of the folded protein resulting into stabilizing the secondary and tertiary structures (Bulaj, 2005). Disulfide bonds act as a defense mechanism against denaturation and proteolytic degradation (Mansfeld et al., 1997).

The formation of a single disulfide bond in a protein is a two-step, reversible process that involves two thiol/disulfide exchange reactions (Bulaj, 2005; Creighton, 1997). In the first step, a nucleophilic protein thiolate attacks a low molecular weight disulfide forming mixed disulfide species. In the next step, another nucleophilic attack from a second protein thiolate breaks the mixed disulfide. Hence, a protein disulfide bond is formed when a low-molecular-weight thiol is substituted by a cysteine thiolate. Disulfide bonds in protein gelation can facilitate the extension of polypeptide chains, improve molecular entanglements within the network structure and prevent relative thermal motions of the polypeptides, thereby stabilizing the protein gel network structure (Phillips et al., 2013).

2.8.4.3. Hydrophobic interactions

Non-polar side chains of amino acids are hydrophobic and play important role in the formation of hydrophobic interactions (Matthews, 2001). When side chains with non-polar amino acids are dispersed in aqueous solutions, hydrophobic interactions are developed to enable the protein to fold into a three-dimensional structure (Bamdad et al., 2012).

The hydrophobic groups are embedded inside of globular proteins, whereas the hydrophilic groups are mainly located on the surface. Due to the structural unfolding and exposure of hydrophobic groups during the heating treatment, hydrophobic interactions between non-polar segments of surrounding polypeptides are strengthened as the temperature rises, which facilitates the formation of the protein gel networks (McClements et al., 2009; Phillips et al., 2013).

2.8.4.4. Electrostatic interactions

Charged amino acid side groups are commonly present in proteins, enabling electrostatic interactions. Molecules with the same charge repel each other and opposite charges attract together. The attractive force can form and stabilize the gel network (Sheinerman et al., 2000). The ionic strength and pH influence the charges of protein molecules. Change in pH of protein solution changes the charges of proteins. Protein molecules are positively or negatively charged when the pH is below or above the isoelectric point. But once the protein solution reaches its isoelectric point, the net charge of the protein is zero (Wang et al., 2009). An increase in temperature induced a decrease in electrostatic interactions (Shimada & Cheftel, 1988). The folding and unfolding of protein molecules are regulated by electrostatic interactions which dictate the arrangement of the gel network and its properties (Semenova & Dickinson, 2010).

2.8.4.5. Van Der Waals interactions

Van der Waals interactions occur between adjoining non-bonded and uncharged atoms, generating forces between permanent dipoles and/or induced dipoles (Phillips et al., 2013; Semenova & Dickinson, 2010). The attractive interactions are converted into substantial repulsion at very short-range separations (2-3 nm). There is almost no influence in gel formation with these interactions even if they are present in atom or molecule (Semenova & Dickinson, 2010). Van der Waals interactions might serve as attractive forces supporting aggregation to create a gel when polymer molecules are large enough like colloidal particle (0.1 nm to 1 μ m) (Bryant & McClements, 1998).

2.9. Physicochemical and microstructural characterizations of protein gels

Mechanical properties and microstructural characteristics are two important aspects of protein gels. In this thesis, gelation kinetics of QPI dispersions and mechanical properties of QPI gels were probed by small and large deformation oscillatory rheological measurements. The microstructural characteristics of QPI gels were characterised by confocal laser scanning microscopy and small-angle neutron scattering (SANS) and small-angle X-ray scattering (SAXS) techniques.

2.9.1. Rheology

Rheology is the study of the deformation behaviour of materials under applied forces (Robertson et al., 2009; Windhab, 1995). For example, all the liquids or dispersions are composed of molecules or particles. When molecules and particles are set in motion, they are forced to glide along each another. Internal friction causes flow resistance in the fluids which is measured by rheology (Mezger, 2020).

2.9.1.1. Oscillation rheology

Small amplitude deformation oscillation (SAOS) rheology is a non-destructive method i.e., distorting the material structure with a small sinusoidal stress wave and measuring the resultant strain wave (Gunasekaran & Ak, 2000). The nature of materials can be determined from the phase shift between applied stress and responded strain or vice versa. When the phase difference between a stress wave and a strain wave is 0° then the material is purely elastic. On the other hand, if the phase difference is 90° then the material is purely viscous (Fig. 2.15a). If the phase difference between the strain and stress waves is between 0° and 90° then the material is viscoelastic (Fig. 2.15b). Many food gels such as yoghurt and tofu can be considered as viscoelastic materials. Table 2.16 refers to the parameters that are frequently used in the oscillation rheology.

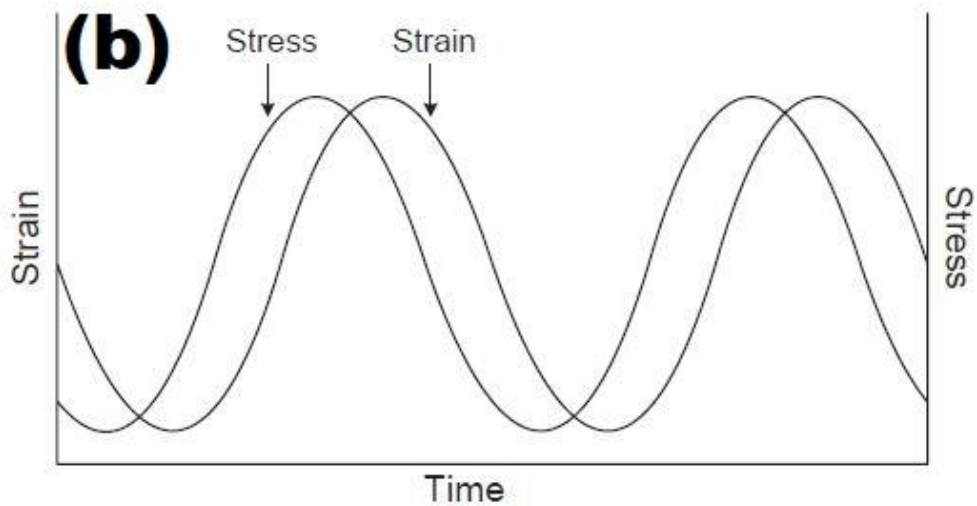
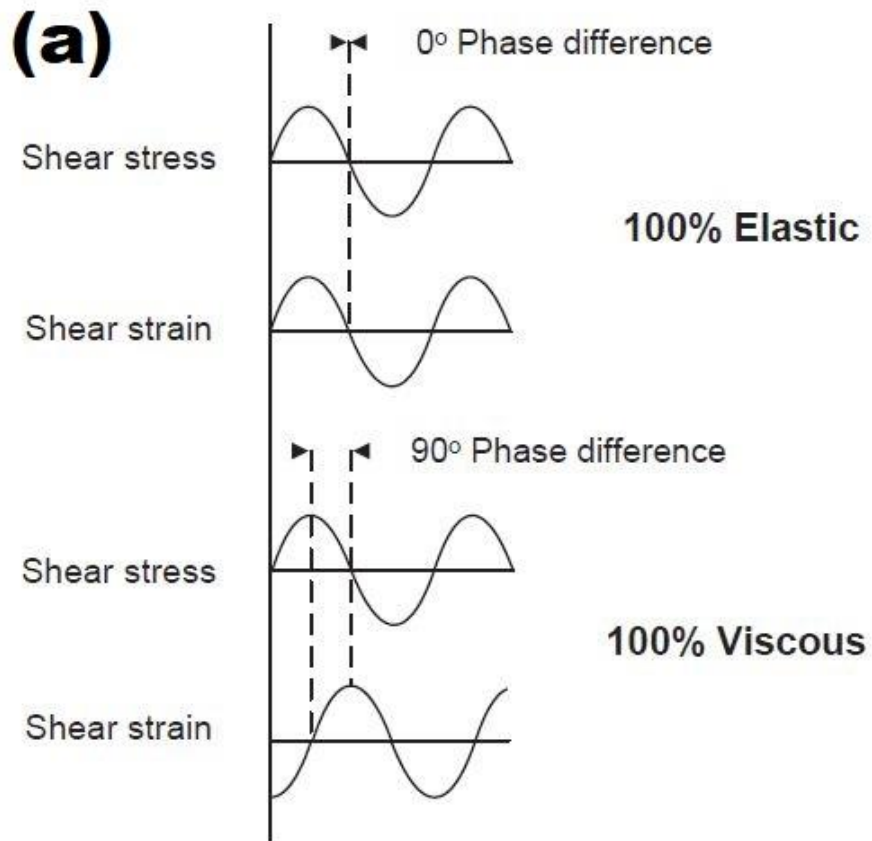


Fig 2.14: Oscillation stress and strain waves for (a) elastic and viscous materials; and (b) viscoelastic material (Kulkarni & Shaw, 2015).

Table 2.16: Parameters that are frequently used in the oscillation rheology (Tabilo-Munizaga & Barbosa-Cánovas, 2005; Tunick, 2011)

		Abbreviations	Description
1	Elastic modulus (storage modulus)	G'	Storage modulus is a measure of the deformation energy stored in the sample. G' represents the elastic behaviour of the sample
2	Viscous modulus (loss modulus)	G''	Loss modulus is a measure of the energy dissipated in the sample. G'' represents the viscous behaviour of the sample
3	Complex modulus	G^*	G^* is a measurement of the sample's overall resistance to deformation.
4	The loss tangent or $\tan \delta$	$\tan \delta$ $\tan \delta = G''/G'$	The loss tangent is the ratio of loss modulus (G'') to storage modulus (G'). The viscoelastic behaviour of a material can be defined with the $\tan \delta$. If $\tan \delta$ is more than 1, it shows a viscous behaviour. If $\tan \delta$ is less than 1, it shows an elastic behaviour.

2.9.2. Types of measurements in the oscillation rheology

2.9.2.1. Temperature sweep

Sinusoidal strain is applied at a constant frequency during temperature sweep as temperature increases and decreases. Temperature sweep can provide several critical parameters including melting point, glass transition temperature, and rubbery plateau modulus (Kulkarni & Shaw, 2015).

Temperature sweep can also determine the time of onset of gelation. The gelation point of the material can be defined at $G'=G''$.

2.9.2.2. Time sweep

Oscillatory time sweeps at a fixed strain and frequency provide information on how the structure evolves during the gelation without disturbing the material (Bui et al., 2012).

2.9.2.3. Frequency sweep

Frequency sweep determines the viscoelasticity of materials. Frequency sweeps are measured at a constant temperature and oscillation amplitude. If the material shows solid-like elastic behaviour, the G' is higher than G'' at a wide range of frequency (Franck, 2004).

2.9.2.4. Stress/ strain sweep

Stress or strain sweep characterizes the rigidity and integrity of the materials internal structure under large deformations. As the stress or strain amplitude is increased, the material's internal structure is destroyed, and breaking stress or breaking strain can be obtained (Ross- Murphy, 1995).

2.9.3. Confocal laser scanning microscopy (CLSM)

In CLSM, confocal means that the image is taken from the focal plane only and laser scanning means images are taken only where the laser is illuminated as compared with full illumination of sample in conventional widefield microscopy (Canette & Briandet, 2014). The laser projects different wavelengths onto an object, and the detector identifies the three-dimensional distribution of several food constituents such as lipids, proteins, and polysaccharides in a sample (Pawley, 2006).

CLSM uses multicolor fluorescence staining and labelling to visualize the various components of nano encapsulated food ingredient (Vandenbossche et al., 1991). Fewer steps are required to prepare samples for viewing in CLSM as compared with TEM and SEM (Ferrando & Spiess, 2000). Addition of dye and mixing it before loading onto the glass slide for CLSM analysis is

the only step to prepare samples. Magnification of the CLSM can be adjusted electronically (Dürrenberger et al., 2001). Samples can be visualized vertically (x, z and y, z) and horizontally (x, y) (Auty, 2013; Ferrando & Spiess, 2000). CLSM also has the ability to image physiological changes and processes such as aggregation, phase separation, coagulation, etc without disturbing the samples (Sharif et al., 2020), whereas scanning electron microscopy (SEM) has the limitation of studying the surface of nanoparticles and microparticles (Goldstein et al., 2017). Transmission electron microscopy (TEM) is able to image the internal structure of microparticles and nanoparticles however it requires extensive sample preparations including fixation, drying, staining, and sectioning (Pechtold et al., 2001).

However, there are some limitations of CLSM. CLSM's major restriction is the lack of suitable lasers with efficient fluorophore excitations. High-intensity laser illumination might be destructive to the sample. CLSM has limited image resolution upto 100 μm as compared with TEM (< 50 picometer) and SEM (0.5 to 4 μm) (Sharif et al., 2020).

2.9.4. Small-angle X-ray scattering and Small angle neutron scattering (SAXS, SANS)

Small-angle neutron scattering is a robust technique to probe microstructures of the soft materials, gels, emulsions, and even the precipitates of the steel. The structures can be probed in a range of 1 nm to 100 nm (Hollamby, 2013). In SANS measurements, neutrons are utilized to probe structural and dynamic features of materials by monitoring their direction and energy change after interacting with a sample (Lopez-Rubio & Gilbert, 2009). The measurement of scattered intensity as a function of scattering angles is known as elastic neutron scattering. SANS, reflectometers, and diffractometers are devices that use elastic neutron scattering. SANS used low-Q range ($Q < 0.5 \text{ \AA}^{-1}$) (Price & Skold, 1986). SAXS is a technique to measuring the intensity of X-rays scattered by a sample as a function of scattering angles ranging from 0.1° to 5° . Similar to SANS, SAXS measurement can provide microstructural information at a length scale ranging from 1 nm to 100 nm (Li et al., 2016). SAXS and SANS can provide structural information of the materials including particle shape, pore size distribution, and fractal dimension (Bale & Schmidt, 1984). Fig 2.16 shows the schematic diagram of components of SAXS instrument. A monochromatic X-ray irradiates a sample and scatters within a small angle region ($2\theta \leq 5^\circ$), a detector downstream detects the scattering intensity, and a beamstop with photodiode in front and near the detector stops and detects the transmitted beam intensity. Both the transmitted intensity and scattering intensity are proportional to

incident beam intensity (Xie et al., 2018). M. Zhao et al. (2020) characterized the microstructure of native and heat-treated rice glutelin (5 mg/mL, pH- 12, heated to 60, 80 and 100 °C for 30 min and 60 min) using SAXS. They found out that scattering curves of all the samples exhibit similar shape, and all the curves were sharply decreased in the range of q-value of 0.008- 0.1 Å⁻¹. The fractal dimension (d_f) of the glutelin particle after heat treatment decreased to 1.50. This confirms that heat treated glutelin particles have smaller size and density than native protein. The author also reported typical bell shape for all the samples using Kratky plots with a q value in the range of 0.008 – 0.07 Å⁻¹ which confirms the spherical morphology of glutelin particles.

The the main advantage of the SAXS and SANS measurement is that the structure of samples can be probed in their native (such as full hydration) states. Both techniques can apply to solutions and gels without undergoing extensive sample preparations such as drying and staining (Chu & Hsiao, 2001; Li et al., 2016). SAXS and SANS can also measure turbid samples such as acidified dairy gels, which cannot be done using traditional light scattering techniques (Wang et al., 2019).

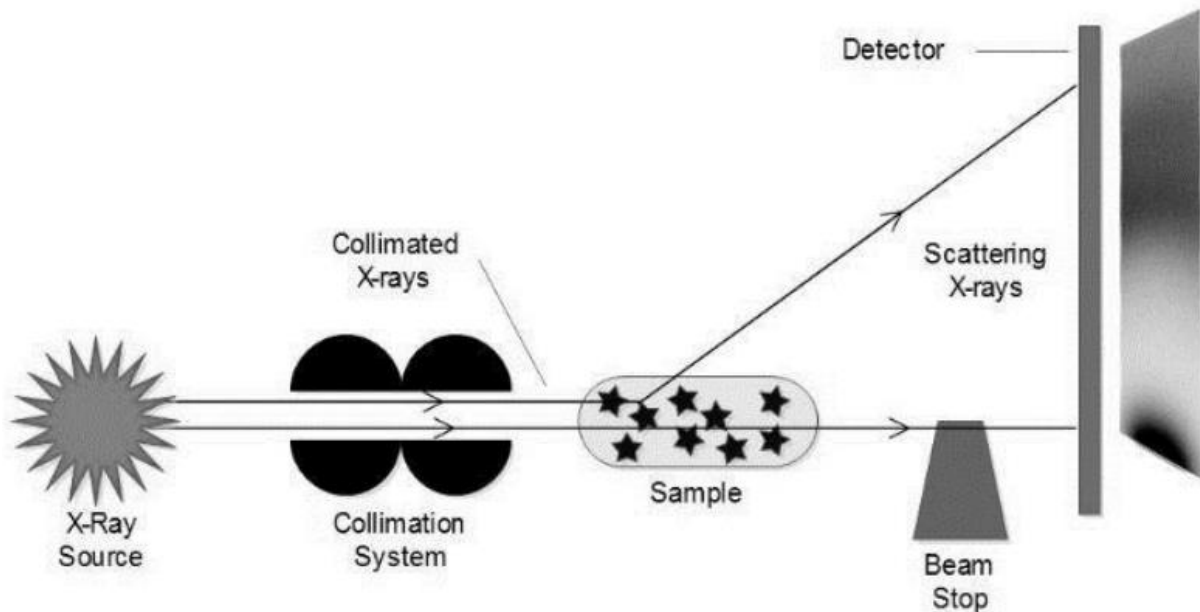


Fig 2.15: The schematic diagram of components of SAXS instruments (Nyman & Fullmer, 2015).

3. Effect of NaCl and CaCl₂ concentration on the rheological and structural characteristics of thermally-induced quinoa protein gels

3.1. Abstract

The effect of ionic strength on the heat-induced gelation of quinoa protein isolates (QPI) at pH 7 was investigated. The gelation behaviour and gel strength were characterised by oscillatory rheology. The microstructural characteristics of QPI solutions and gels were probed by ultra-small angle neutron scattering (USANS), small-angle X-ray and neutron scattering (SAXS, SANS), and confocal laser scanning microscopy (CLSM). This suite of techniques provided structural details covering a wide range of length scales from tens of micron to nanometre. It was found that the gelation temperature decreased from 73 °C to 40 °C and the G^* (1 Hz) increased from ~67 Pa to ~1285 Pa with increasing concentration of NaCl from 0 to 200 mM. A particle size of ~32 Å and ~57 Å was identified within the QPI gel containing 0-200 mM NaCl from SAXS and SANS, respectively and whose size decreased upon addition of CaCl₂. For all QPI samples, heat treatment promoted protein aggregation on the micron scale, while a larger structural unit (R_g ~ 170 nm) was kept intact as revealed by USANS. A similar mass fractal structure ($d_f=2$) was observed in the QPI gels containing 0-200 mM NaCl, while CaCl₂ addition caused the formation of large protein agglomerates (R_g ~2.5-4.0 μm) with a more compact and denser structural organisation ($d_f=2.5$) inside the protein blobs. CLSM showed that the QPI gels containing CaCl₂ are prone to phase separation. Overall, this finding shows the thermal gelation behaviour of QPI can be modulated by the ion type and concentration, which is similarly observed in other globular protein systems. These results provide useful information for the design and preparation of quinoa gels for food applications.

3.2. Introduction

To accommodate the rapid growth in population and alleviate greenhouse gas emission, one strategy is to significantly increase the availability of plant-based food alternatives and decrease the consumption of animal-based food. Important efforts have been recently devoted to fabricating meat-analogues and dairy-alternatives using plant proteins (Bohrer, 2019). Quinoa (*Chenopodium quinoa*) originates from South America and is one of the emerging protein sources having a well-balanced amino acid profile (McClements et al., 2019). Quinoa has a protein content from 12 to 23 % depending on variety (Abugoch et al., 2008; Dakhili et

al., 2019) it is mainly composed of two protein fractions-11S globulin (50-60 kDa) and 2S albumin (8-9 kDa), which account for around 37 % and 35 % of the total proteins in quinoa (Kaspchak, de Oliveira, et al., 2017; Ruiz, Xiao, et al., 2016).

Amongst the various techno-functionalities of proteins, gelation is regarded as one of the most critical attributes as it is central to various applications in the food and pharmaceutical industries (Foegeding et al., 1995; Gosal & Ross-Murphy, 2000). For example, gel formation is critical for producing yoghurt, meat substitutes and tofu-like products (Dakhili et al., 2019; Mäkinen et al., 2016). Protein gels consist of three-dimensional networks of interconnected and partially aggregated polypeptides, with water entrapped inside the network. The mechanical properties and structural characteristics of proteins gels not only depend on the polypeptides' nature, but also on the gelation conditions (Silva et al., 2019; Yang et al., 2017). There are generally two gelation routes: heat-induced gelation and cold gelation (Maltais et al., 2008). Temperature, pH, ion type and concentration affect the thermal-induced gelation and dictate the structure and properties of the final gel.

Thermal-induced aggregation and gelation are typical characteristics in various globulin proteins such as β -lactoglobulin (Foegeding et al., 1995; Ikeda et al., 1999; Nguyen et al., 2017; Phan-Xuan et al., 2013; Xiao et al., 2020), soy globulin (Chen et al., 2017; Jose et al., 2016; H. Zhao et al., 2020), canola protein (Yang et al., 2014), and pea globular protein legumin (Klost & Drusch, 2019; Sun & Arntfield, 2012). Compared to these proteins, the thermal gelation behaviour of quinoa protein, particularly as influenced by ionic type and strength, have been far less studied (Kaspchak, de Oliveira, et al., 2017; Ruiz, Xiao, et al., 2016). Kaspchak, de Oliveira, et al. (2017) investigated the mechanical strength of the QPI gels at concentration, C=10 wt% after a thermal treatment (20 to 90 °C) in the presence of 0.055 mol/g CaCl₂ and MgCl₂. However, to the extent of our knowledge, the effect of adding monovalent salt such as NaCl on the thermal gelation of QPI has not yet been reported. As many food products are often prepared with NaCl addition, understanding how protein gels behave in the presence of NaCl is therefore critical.

Understanding the physicochemical properties, particularly the microstructures, of protein gels is extremely important to various applications as well as digestion (Singh et al., 2014). One such structural property is the fractal dimension of the aggregates which can be correlated to the rheological properties of the gel using scaling concepts (Eleya et al., 2004). While static light scattering is considered to be one of the most powerful technique to determine the fractal dimension of colloidal aggregates, experimental conditions such as sample turbidity and the length scale probed by light scattering are limiting parameters. Microscopy image analysis is

the most direct method for observing the gel's aggregate/network; however, it is challenged to obtain an image of a gel without imparting artefacts during sample preparation. Moreover, obtaining the quantitative structural information from microscopy analysis is typically challenging. In this regard, (ultra) small-angle X-ray and neutron scattering (SAXS, SANS, USANS) are excellent techniques to probe the multiscale structural features of protein gels in details over a wide length scale (Gilbert, 2019; Lopez-Rubio & Gilbert, 2009); however, most scattering studies have been focused on animal or dairy proteins (Ako et al., 2009; Hiroi et al., 2020; Kundu et al., 2013; Li et al., 2018; Pouzot et al., 2005; Wang et al., 2019), and studies on plant protein systems are scant (Pasquier et al., 2019).

In this study, the thermal-induced gelation of QPI in the presence of mono- and divalent salts (NaCl and CaCl₂) at various concentrations was investigated. The mechanical properties of the QPI gels were examined with small and large oscillatory deformation rheology. The nanostructure of the QPI before and after heat treatment was probed using SAXS and SANS. Because QPI gels contain large structure on the micron length scale, USANS and CLSM were also employed. We believe that this study is the first to employ USANS to probe the microstructures of plant protein in solutions and gels.

3.3. Materials and Methods

3.3.1. Materials

Quinoa seeds (*Chenopodium quinoa*) were grown locally in New Zealand and kindly provided by KiwiQuinoa. Deuterium oxide (D₂O), sodium chloride (NaCl), calcium chloride (CaCl₂), and sodium azide were of analytical grade and obtained from Sigma Aldrich (Auckland, New Zealand). D₂O (Sigma Aldrich, USA) was used in all sample preparations for physicochemical and microstructural characterisations.

3.3.2. Preparation of quinoa protein isolate (QPI)

The quinoa protein isolate (QPI) was extracted from defatted quinoa flour according to Kaspchak, de Oliveira, et al. (2017) with small modifications. Briefly, raw quinoa seeds were ground using a coffee grinder (Coffee and Spice Grinder, Breville, NZ) and passed through a 500 µm sieve (Endecotts, UK). The grounds were subsequently soaked in 0.5 M NaCl solution, containing 0.02 w/w% sodium azide, at a weight ratio of quinoa flour to NaCl solution of 1:10.

The pH of the mixture was then adjusted to 8 with 1 M NaOH under magnetic stirring. The suspension was kept stirring overnight at 20 °C to maximize the extraction of proteins, and the pH was regularly checked and adjusted to 8 if needed. The suspension was centrifuged at 10000×g at 20 °C (Sigma, 6-16KS with rotor 12356, Germany) for 15 min to obtain the supernatant. The fat layer on the surface of the supernatant was carefully removed by a wooden spatula. These steps were repeated at least twice until the supernatant presented low turbidity. The pH of the supernatant was subsequently adjusted to 4.5 using 1 M HCl to precipitate the protein. The mixture was centrifuged at 10000×g at 20 °C for 15 min to recover the protein in the pellet. Milli-Q water was added, and the mixture was vigorously mixed before centrifuging at the same conditions for three times to wash the protein pellet. The pellet was then resolubilised in Milli-Q water containing 0.02 w/w % sodium azide and neutralised to pH 7 with 1 M NaOH under stirring. The QPI solution was frozen at -20 °C for 48 h and lyophilised using a freeze dryer (Labconco, Model 7753034, USA) for 3-5 days and milled to powders with a pestle and mortar. The obtained QPI powder was stored in sealed plastic bottles avoiding sunlight at 20 °C in a desiccator for further use. The proximate analyses of QPI obtained was performed at the Nutrition Laboratory of Massey University (School of Food and Advanced Technology, Palmerston North, New Zealand). On a dry matter basis, the protein, fat, ash, and moisture contents of the QPI powder were 91.6 %, 4.9 %, 2.8 %, and 0.7 %, respectively.

3.3.3. Sodium dodecyl sulfate polyacrylamide gel electrophoresis (SDS-PAGE)

25 µL of 0.4% QPI solution was mixed with 7.5 µL of Laemmli sample buffer (4 ×, Bio-Rad, USA) and 0.8 µL of β-mercaptoethanol at room temperature before running the gel. Thereafter, the sample was boiled for 10 min and 10 µL of the sample was loaded on a commercial Mini-protein TGX precast gel (Bio-Rad, USA) consisting of 4 % stacking gel and 15 % resolving gel. The electrophoresis was carried out using a PowerPac Basic (Bio-Rad, USA) at a constant 150 V in a running buffer prepared by the dilution of 10× Tris/Glycine/SDS running buffer (Bio-Rad, USA). The gel was carefully removed from the electrophoresis tank and stained with Coomassie Brilliant Blue R-250 staining solution (Bio-Rad, USA) for 4 h before destaining with 10% isopropanol/glacial acetic acid solution overnight. A protein molecular weight marker (Precision Plus Protein Dual Xtra Standards (Catalog #161-0377), Bio-Rad, USA) was run on the same electrophoresis gel to identify the protein bands of the QPI sample.

3.3.4. Rheological measurements

A rotational TA DHR-3 stress-controlled rheometer (TA instruments, USA) equipped with parallel plate geometry (diameter 40 mm, gap 1 mm) was employed to perform small and large deformation oscillatory rheological characterisation. A stock QPI solution (12.5 wt%) was prepared by suspending the QPI powder in D₂O under mild stirring at 20 °C for 24 h to enable protein hydration and solubilisation. The QPI solutions (10 wt%) with various ionic strength were then prepared by mixing the QPI stock solution, concentrated NaCl or CaCl₂ solution (1 M), and D₂O. The mixture was stirred using a magnetic stirrer at 20 °C for another 24 h and the pH was regularly checked and adjusted to 7 using 1 M HCl or 1M NaOH.

Aliquots of QPI solution were transferred onto the bottom plate with a plastic dropper. The sample was then carefully trimmed, and low viscosity mineral oil (M 5904, Sigma Aldrich, USA) was added around the edge of the sample to prevent evaporation. The rheological measurements were conducted in the following protocols: (1) A temperature sweep was carried out by heating the samples from 25 °C to 85 °C at 1 °C/min, holding at 85 °C for 30 min, and cooling down to 25 °C at 1 °C/min. During this step, the frequency and strain amplitude were maintained at 1 Hz and 1 %, respectively, to monitor the gel formation; (2) at the end of the temperature sweep, a frequency sweep measurement was performed at a constant strain 1 % while the frequency was varied from 0.01 to 100 Hz; (3) finally, a strain sweep was performed with temperature and frequency maintained at 25 °C and 1 Hz, and the strain varied from 0.1 % to 10000 %. All measurements were repeated at least twice.

3.3.5. Confocal laser scanning microscopy

QPI solutions at 10 w/w % were prepared similarly to those prepared for rheological measurements with a series of NaCl concentrations: 0 mM, 50 mM, 100 mM, and 200 mM; and CaCl₂ concentrations at 20 mM and 50 mM. Several drops of 1 % Fast Green (Sigma Aldrich, USA) were vortex mixed with the prepared solutions for 10 seconds at 20 °C. 100 µL of each mixture was transferred into a slide with a cavity, covered with a coverslip and sealed with nail polish to prevent water evaporation (Wang et al., 2019). For gel samples, the slides were incubated in an oven (Thermofisher, USA) at 85 °C for 30 min. The QPI solutions with the corresponding gels were observed using a confocal laser scanning microscope (Leica TCS

SP5, Leica Microsystems) equipped with a 100 × oil immersion objective lens at a wavelength of 630 nm. Fast green was excited by a helium-neon laser at 633 nm and the emission was detected between 638 and 750 nm. Image J software (NIH, USA) was used to process all the images.

3.3.6. Solubility determination

Solubility of QPI in the presence of various concentrations of NaCl and CaCl₂ was determined according to the method described by Le Priol et al. (2019) with slight modifications. QPI dispersions (10 %) were prepared according to the section 3.2. The QPI dispersions were subsequently centrifuged at 1500 g for 15 min at 22 °C using an Eppendorf centrifuge (Eppendorf 5424, Germany). The supernatant was carefully pipetted and the soluble protein concentration in the supernatants was determined using a Bradford Protein Assay Kit (Bio-Rad, USA) with gamma-globulin as the standard. The absorbance of the protein solutions was determined with a UV-Vis spectrophotometer (1900, Shimadzu, Japan) at 595 nm. The solubility was calculated as the percentage of the initial total protein concentration before centrifugation.

3.3.7. Ultra-small angle neutron scattering (USANS)

USANS measurements were performed on the KOOKABURRA instrument located at ANSTO, Sydney, Australia (Rehm et al., 2013; Rehm et al., 2018). A neutron wavelength $\lambda=4.74 \text{ \AA}$ and a Cd aperture (diameter 29 mm) were used. The scattering intensity was recorded in the wave vector, Q -range of approximately 3×10^{-5} to $2 \times 10^{-3} \text{ \AA}^{-1}$, probing the structure in a size range of 200 nm to 10 μm . USANS data was reduced based on the previously described procedure (Kline, 2006), using python scripts in Gumtree (Xiong et al., 2017).

The solvent (100% D₂O) was selected to improve contrast and reduce the incoherent scattering. The sample preparation procedure is similar to that described in section 3.2. The samples ~ 1 mL were injected into demountable USANS samples cells (thickness 1 mm) with disposable syringes. For gel samples, the sample cells were incubated in an oven at 85 °C for 30 min to allow gel formation. USANS measurements were initiated after the sample re-equilibrated to room temperature (~25 °C). For protein solution samples, a six-sample position tumbler was used to prevent sample sedimentation during the USANS measurement. All the USANS measurements were conducted at room temperature and lasted up to 5 h.

The Unified Fit (UF) model was used to analyse the USANS data. The Guinier scattering representing particle size and the Porod (power-law) scattering indicating the presence of mass or surface fractals can be obtained from the UF model (Beaucage, 1995; Beaucage & Schaefer, 1994). The UF model is expressed as:

$$I(Q) = \sum_{i=1}^n G_i \exp\left(\frac{-Q^2 R_{gi}^2}{3}\right) + B_i \exp\left(\frac{-Q^2 R_{g(i+1)}^2}{3}\right) \left[\frac{(\operatorname{erf}\left(\frac{QR_{gi}}{\sqrt{6}}\right))^3}{q} \right]^{P_i} \quad (1)$$

where n is the number of structural levels observed, G is the exponential Guinier pre-factor, R_g is the radius of gyration. B and P are the pre-factor and the exponent of the power-law function, respectively. The fits were conducted in the SasView software (version 5.0.3, <http://www.sasview.org/>) and Irena SAS macro embedded in Igor Pro (Ilavsky & Jemian, 2009), which can take the smearing conditions for USANS into account by setting the slit setting the slit-height to 0.0584 \AA^{-1} (Yang et al., 2015).

3.3.8. Small-angle neutron scattering (SANS)

SANS experiments were performed on the QUOKKA instrument at ANSTO, Sydney, Australia, in a Q -range of 0.003 to 0.4 \AA^{-1} (Gilbert et al., 2006; Wood et al., 2018). The samples were prepared following the same procedure as described in section 3.5. To prevent sample sedimentation, similar to USANS, a multi-position tumbler was used. All SANS measurements were conducted at room temperature ($\sim 25 \text{ }^\circ\text{C}$) and lasted up to 3 h for each measurement. Instrumental configurations were: (i) source-to-sample distance (SSD) = sample-to-detector distance (SDD) = 20 m, (ii) SSD = SDD = 8 m and (iii) SSD = 4 m and SDD = 1.3 m with 500 mm detector offset, using a λ of 5 \AA with 10 % resolution; an additional focussing optics configuration (iv) with the same SSD and SDD as (i) which was used to access lower Q_{\min} with λ of 8.1 \AA with 10 % resolution. Sample aperture diameter of 12.5 mm was used for all configurations. Source aperture of 50 mm was used for (i), (ii) and (iii) and 30 mm for (iv). The data were reduced following a standard procedure (Kline, 2006) using the Igor Pro software (Wavemetrics, USA) with solvent background subtraction.

3.3.9. Small-angle X-ray scattering (SAXS)

The sample preparation procedure described in section 3.6 was followed for the SAXS measurements. For gel formation, the QPI solution was filled into capillary tubes (inner diameter 2 mm), followed by incubation at 85 °C for 30 min. To avoid evaporation, the capillary tubes were sealed with wax or epoxy-resin prior to incubation. A NanoSTAR SAXS instrument (Bruker, Mannheim, Germany) was used to collect the SAXS data in a Q range of 0.01 to 0.4 Å⁻¹. The samples were kept at room temperature (~25 °C) prior to SAXS measurements. The samples to detector distance was 72.15 cm. SAXS data collection time for all samples was 1 h to provide good statistics at high Q for enhanced background subtraction. For some weakly scattering samples, data were collected for two 1 h periods and the data averaged. Data were reduced with solvent background subtraction.

3.3.10. SANS and SAXS data analysis

A correlation length model (Hammouda et al., 2004) was used to fit the SANS and SAXS scattering profiles of the QPI gels with 0-200 mM NaCl addition. The equation is expressed below:

$$I(Q) = \frac{A}{Q^n} + \frac{C}{1 + (Q\xi)^m} \quad (2)$$

here the first term accounts for the power-law (Porod) scattering from protein aggregates (exponent= n) and the second Lorentzian term depicts the scattering from small protein particles or inhomogeneities with a correlation length (size) of ξ . Following the particle size feature, the scattering intensity follows a power-law decay with a power law exponent of m . A and C are scalars for the first and second term, respectively. The fits were conducted in the SasView software (version 5.0.3, <http://www.sasview.org/>).

3.3.11. Statistical analyses

All the experiments were conducted in either duplicate or triplicate and the results were represented as mean \pm standard deviation (SD). Mean comparisons were achieved by conducting analysis of variance (ANOVA) using the Least Significant Difference (LSD) test in the SPSS package 21.0 (Chicago, IL, USA). The significance level was set at $p < 0.05$.

3.4. Results and Discussions

3.4.1. SDS-PAGE

SDS-PAGE profiles of the QPI under reducing conditions are shown in Fig. 3.1. QPI mainly consists of globular and albumin proteins and shows a complex protein band profile. Similar protein bands were observed in recent electrophoresis studies on the QPI obtained by alkaline extraction methods (Kaspchak, de Oliveira, et al., 2017; Ruiz, Xiao, et al., 2016; Shen et al., 2021). The intense protein band around 50 kDa was attributed to the 11S globulin (Mäkinen et al., 2016; Shen et al., 2021) and other protein bands with molecular weight of ~22-25 kDa and ~30-38 kDa were assigned to the basic and acidic polypeptide subunits of the 11S globular chenopedin, which are linked by single disulfide bond (Abugoch et al., 2008; Kaspchak, de Oliveira, et al., 2017; Shen et al., 2021).

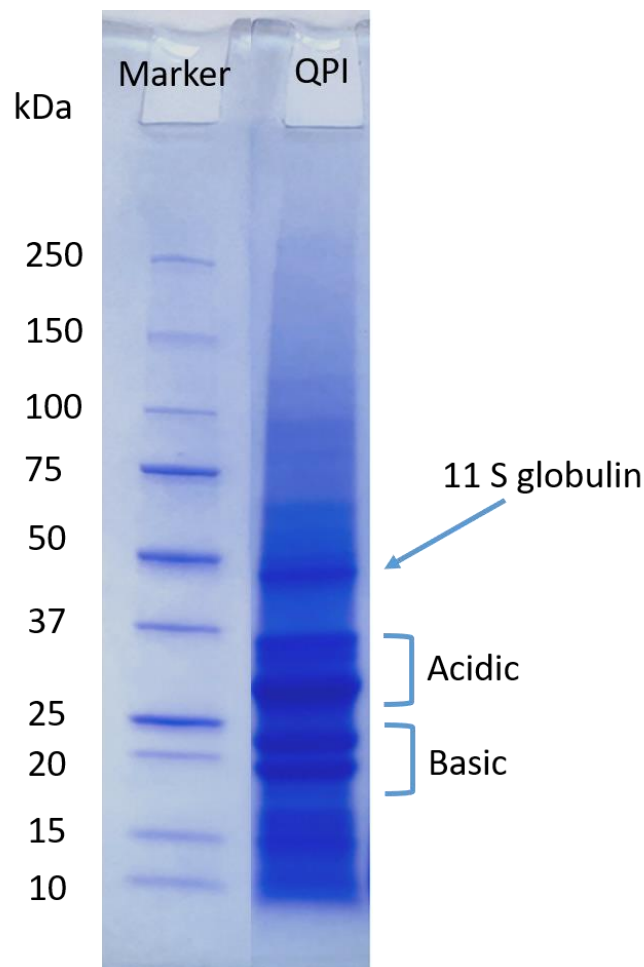


Fig 3.1: SDS-PAGE of quinoa protein under reducing conditions: Lane 1-molecular weight marker; Lane 2-quinoa protein isolate.

3.4.2. Viscoelastic properties during gelation

Viscoelastic properties of the QPI suspension in the presence of various concentrations of NaCl and CaCl₂ during thermal-induced gelation were monitored with small oscillatory deformation rheological measurement. Storage modulus G' , loss modulus G'' and temperature were recorded as a function of time as shown in Fig. 3.2 (A, B). For all the samples, G' and G'' increased at the stages of temperature ramp, temperature holding, and temperature decrease. During the temperature ramp, the onset of the G' and G'' increase occurred earlier and at lower temperature (Fig 3.2A. inset) for the samples containing higher concentrations of NaCl. The temperature at which the G' reached 1 Pa is defined as the gelation temperature T_{gel} (Lucey & Singh, 1997; Z. Yang et al., 2020); values for T_{gel} are plotted versus the NaCl concentration in Fig. 3.2C (RH axis). The gelation temperature decreased from ~ 73 °C to ~ 40 °C with increasing the concentration of NaCl from 0 to 200 mM. Soy protein and faba bean protein have shown a similar gelation behaviour (Chen et al., 2017; Langton et al., 2020) with soy protein displaying an earlier onset of gelation (Chen et al., 2017).

For the QPI containing CaCl₂, a small peak of G' and G'' was observed at ~ 20 min (~ 45 °C); which was also found in a recent gelation study of QPI in the presence of CaCl₂ (Kaspchak, de Oliveira, et al., 2017). As a result of this, the gelation temperature could not be identified accurately. The appearance of this peak could be due to the formation of a weak protein network at low temperature or the presence of structural inhomogeneities. A more detailed discussion from a structural point of view will be provided in section 3.4. For all QPI samples, the increase of G' and G'' is continuous but slower at the latter stage of temperature ramp and at the holding temperature of 85 °C. This implies that the protein molecules progressively denature, and the hydrophobic groups originally buried inside of the protein are increasingly exposed to form protein aggregates and network. During cooling, almost all QPI gels showed an increase in G' and G'' , which is probably attributed to the enhancement or formation of covalent and non-covalent bonds (H. Zhao et al., 2020). It has been suggested that hydrogen bonds are reinforced, and electrostatic repulsion is diminished at low temperature (Chen & Dickinson, 2000).

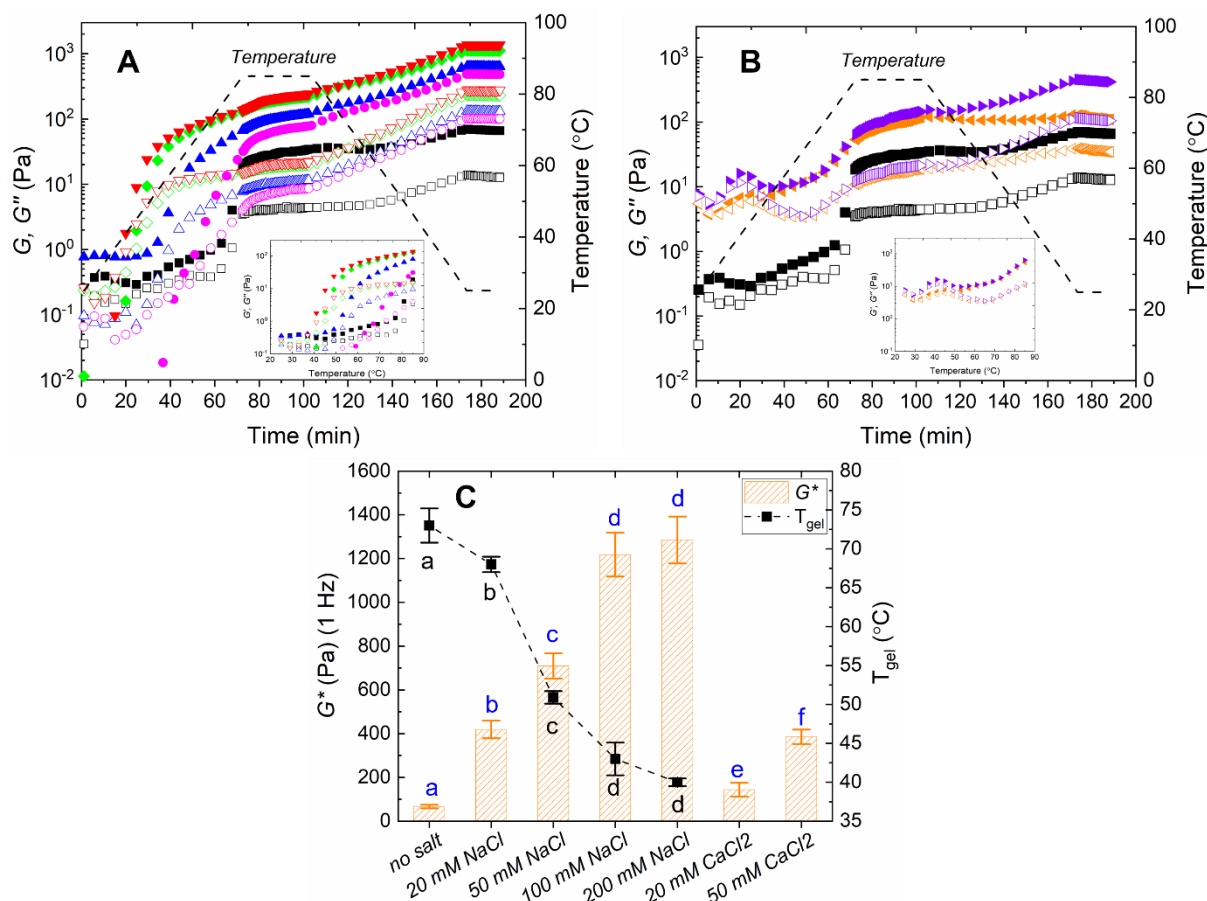


Fig 3.2: The evolution of G' (solid symbols) and G'' (open symbols) for QPI solutions at 10 wt% in D_2O during temperature induced gelation with increasing concentration of NaCl (A) and $CaCl_2$ (B). (NaCl: 0 mM (■), 20 mM (●), 50 mM (▲), 100 mM (◆), 200 mM (▼); $CaCl_2$: 20 mM (◀), 50 mM (▶)); (C) Complex modulus G^* at 1 Hz and gelation temperature T_{gel} of the QPI gels as a function of salt (NaCl and $CaCl_2$) concentration. Different letters (black) below the lines indicate significant differences in T_{gel} . Different letters (blue) above columns indicate significant differences in G^* . All the samples in the experiments were at pH 7

3.4.3. Viscoelastic properties after gelation

After cooling the samples were allowed to equilibrate at 25 °C for 15 min before conducting frequency and strain sweeps. The viscoelastic response of all the QPI samples as a function of frequency is shown in Fig. 3.3 (A, C). For all samples, G' and G'' are parallel to each other and only slightly increased with an increase in frequency. In addition, at all frequencies probed, the ratio of G' to G'' was no greater than 10. This implies the thermal-induced QPI gels are weak (Mitchell, 1980; Wang et al., 2019). Most thermally induced plant protein gels are weak gels,

as they are mainly formed by non-covalent bonds such as electrostatic attraction, hydrogen bonds, and hydrophobic interactions (Ruiz, Xiao, et al., 2016; Sun & Arntfield, 2012). To compare the gel strength among all samples, the complex moduli G^* (1 Hz) are plotted in Fig. 3.2C (LH axis). Increasing the concentration of either NaCl or CaCl₂ led to a greater gel strength. For instance, G^* (1 Hz) increased from ~67 Pa to ~1285 Pa when the concentration of NaCl was increased from 0 to 200 mM. Similar behaviour has been found in β -lactoglobulin and soybean protein gels (Chen et al., 2017; Ikeda et al., 1999).

Strain sweep measurements were conducted to study the large deformation behaviour of QPI gels. G' and G'' as a function of strain amplitude are reported in Fig. 3.3 (B, D). All gel samples showed a quantitatively similar behaviour. At very small strains, both G' and G'' were independent of the strain amplitude, demonstrating a linear viscoelastic behaviour. This also confirmed that the 1 % strain, selected for temperature and frequency sweeps experiments, was within the linear viscoelastic region (LVR). As the strain was increased, both G' and G'' decreased, implying a strain thinning characteristics. This is typical for a colloidal gel and was also found in soybean protein gels (Bi et al., 2013; H. Zhao et al., 2020) and hemp protein gels, e.g. (Dapčević-Hadnađev et al., 2018). As the strain amplitude further increased, a cross-over of G' and G'' occurred. The stress at which the cross-over occurred is considered to be the breaking stress. Fig. 3.3E shows that the breaking stress of QPI gels increased with increasing concentration of either NaCl or CaCl₂, in agreement with the small deformation rheology results.

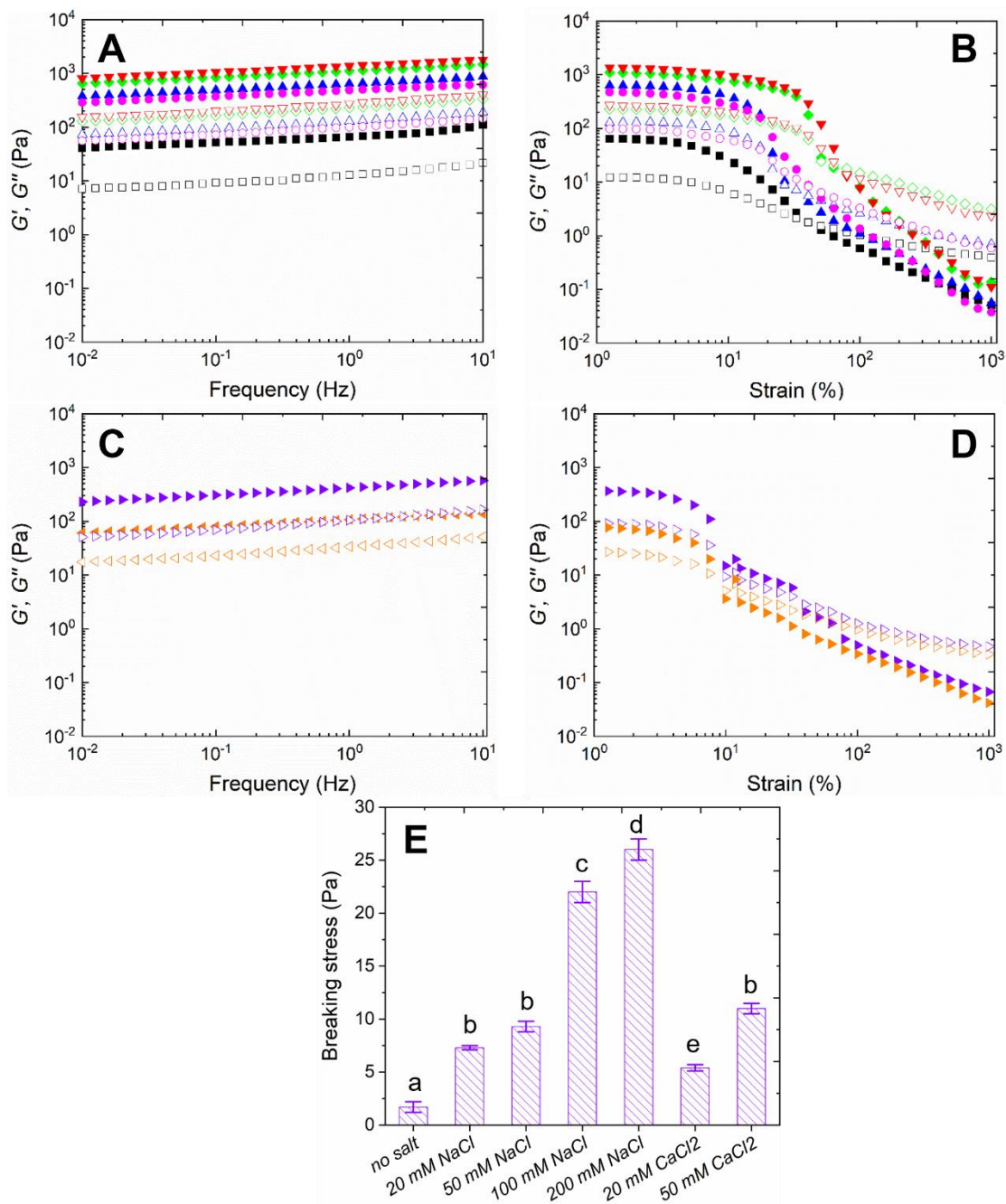


Fig 3.3: The G' and G'' as a function of frequency (A, C) and strain amplitude (B, D) for QPI solutions at 10 wt% in D₂O with various concentrations of salt addition measured at 25 °C. Symbols are the same as in the Fig. 1; (E) breaking stress of the QPI gels as a function of salt (NaCl and CaCl₂) concentration. Different letters above columns indicate significant differences in breaking stress.

3.4.4. Confocal laser scanning microscopy (CLSM) observations

The microstructure of the QPI before and after heat treatment observed by CLSM is demonstrated in Fig. 3.4. The proteins stained by Fast Green appeared as green, while the voids or pores in between the protein particles are shown in black. It can be observed that the microstructures of QPI solutions were homogeneous at lower NaCl ionic strength (0-50 mM) and smaller protein aggregates were observed in the QPI containing 100 and 200 mM NaCl. For QPI solution containing 20 and 50 mM CaCl₂, larger protein aggregates are seen and some heterogeneous interconnected protein network is formed. These CLSM observations further support the formation of weak QPI gel networks with CaCl₂ addition even at room temperature, which could contribute to the appearance of G' and G'' peaks at lower temperature (~35-40 °C) (Kaspchak, de Oliveira, et al., 2017). After heat treatment, the interconnected gel networks were observed in all the QPI samples. The QPI samples without salt addition have the finest and most homogeneous microstructure. As more NaCl was added, the gel microstructure appeared more heterogeneous and larger aggregates are formed. Similar observations have been made in β -lactoglobulin (Pouzot et al., 2004), soy protein isolate (Bi et al., 2013), faba bean proteins (Langton et al., 2020), and hemp protein isolate gels (Dapčević-Hadnađev et al., 2018) with increasing ionic strength. This was ascribed to the fact that electrostatic repulsion impaired by the surface charge of the proteins are dominated at no salt or low salt (e.g. 20 mM NaCl) conditions. With an increase in NaCl concentration, the charge screening effect of NaCl diminishes the electrostatic repulsions, thus the attractive interactions between protein molecules are promoted to become stronger gels (Ikeda et al., 1999). This results in protein aggregation, and when the protein concentration is sufficiently high, the interconnection of protein aggregates occurs and protein gels are formed (Bi et al., 2013; Clark et al., 2001; Wu et al., 2017). However, there were no significant structural variations between the QPI gels with 20-200 mM NaCl addition. It is possible that in a narrow range of the NaCl concentration the gel structure is self-similar on the length scale observed by CLSM (Pouzot et al., 2004). The QPI gels containing CaCl₂ showed a markedly different microstructure compared to the ones containing NaCl. Much larger and well-defined protein aggregates were observed and voids within the protein network became larger particularly in the sample containing 50 mM CaCl₂. The phase separation between protein aggregates and solution could be responsible for the weak gel rigidity as shown in the rheology results (Bi et al., 2013). Jeyarajah and Allen (1994) and Phan-Xuan et al. (2013) showed that adding divalent salt like CaCl₂ caused more

significant structural changes than when monovalent salt like NaCl was added into protein gels. It is because divalent salts are more effective in screening electrostatic repulsions (Remondetto & Subirade, 2003) and can cross-link the negatively charged portion of proteins through the so-called “salt-bridge” effect (Hongsprabhas & Barbut, 1997).

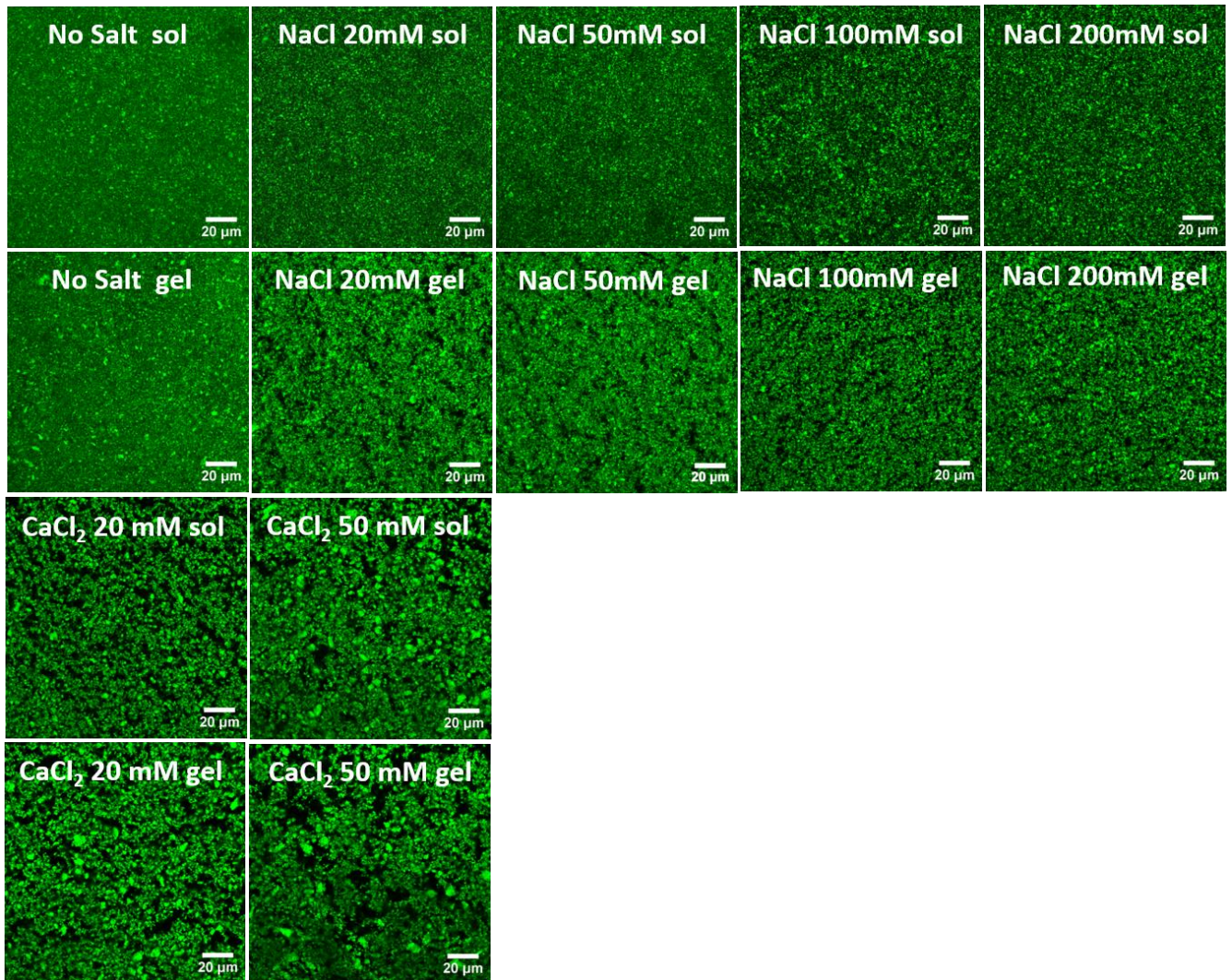


Fig 3.4: Confocal laser scanning microscopy images of QPI gels (c=10 wt%) that formed by heating at 85 °C for 30 min in the presence of salt (NaCl and CaCl₂) at various concentrations.

3.4.5. Solubility

Solubility (%) of the QPI in the presence of various concentrations of NaCl and CaCl₂ is shown in Table 3.1. An increase of NaCl from 0 to 200 mM induces a gradual decrease in the protein

solubility from ~72 % to ~40 %. Similar results were found in a previous study on barley protein, especially at higher salt concentrations (Yalçın & Çelik, 2007). A minimum protein solubility of ~5 and 4 % is observed upon the addition of 20 and 50 mM CaCl₂, respectively. This could be because NaCl and CaCl₂ screen the charges on the protein surface thus promoting the attraction between, and aggregation of, protein particles. This could also explain the earlier onset of QPI gelation in the presence of NaCl. The aggregation would facilitate the protein network formation and the promotion of the gel network strength as revealed by rheology. The divalent salt such as CaCl₂ is more effective in screening charges of proteins and can also induce the protein cross-linking through salt bridges, thereby inducing more prominent protein aggregation and lower protein solubility. These results are in agreement with the CLSM observations and rheological results.

Table 3.1: Solubility (%) of the QPI in the presence of various concentrations of NaCl and CaCl₂ at pH 7.

QPI Samples	Solubility (%)
No salt	72 ± 3% ^f
20 mM NaCl	58 ± 3% ^e
50 mM NaCl	53 ± 2% ^d
100 mM NaCl	48 ± 2% ^c
200 mM NaCl	40 ± 3% ^b
20 mM CaCl ₂	5 ± 1% ^a
50 mM CaCl ₂	4 ± 1% ^a

Results are the average of duplicates. Different superscript letters represent significant differences based on the SPSS LSD test ($P < 0.05$).

3.4.6. Microstructures of the QPI before and after heating probed by USANS

The USANS scattering patterns of the QPI containing various concentrations of NaCl and CaCl₂ before and after thermal treatment are shown in Fig. S1 and Fig. S2 (Refer to section 8 Appendices). For all the QPI samples, scattering patterns in the high- Q region almost overlap before and after heat treatment; however, an increase in the scattering intensity in the low- Q

region was observed in all gel samples. This implies that the heat treatment predominately promoted the interaction and aggregation between proteins while the smaller protein structural unit were not appreciably affected. A similar intensity increase in the low- Q region has been identified in various protein systems such as bovine serum albumin (BSA) (Chodankar et al., 2008) and ovalbumin (Hiroi et al., 2020; Hiroi et al., 2016) after heat treatment. It is also worth noting that the scattering intensity deviation between the solution and gel occurred at a lower Q with increasing NaCl concentration (cf. vertical lines in Fig. 3.5 left-hand side). The reason is that the greater ionic strength (e.g. 100 and 200 mM NaCl) can promote protein aggregation even in the solutions (“salting out” effect), as also observed in the corresponding CLSM micrographs (Fig. 3.4). Consequently, in those samples the scattering differences between the solution and gel were only identified in the low- Q region.

USANS scattering profiles of QPI in the presence of CaCl_2 before and after heat treatment are illustrated in Fig. S2. For QPI samples containing 20 mM and 50 mM CaCl_2 , heat treatment mainly caused an increase in the overall scattering intensity while the shape and features within the scattering curves were nearly unchanged. The scattering intensity before and after heat treatment is either superimposed or parallel with each other. This is different when compared to the QPI samples containing 0-200 mM NaCl, as the increase of the scattering intensity, $I(Q)$ occurred only in the low- Q region, while the mid- to high Q region remained nearly the same after heating. For example, for QPI containing 100 mM NaCl, the scattering intensity $I(Q=3.5\times 10^{-5} \text{ \AA}^{-1})$ increased from $8.3 \times 10^4 \text{ cm}^{-1}$ to $1.2 \times 10^5 \text{ cm}^{-1}$ after heating. This suggests the heat treatment did not significantly change the protein structure that had already been crosslinked by CaCl_2 at room temperature. In the following sections, we focus on the interpretation of scattering profiles of QPI gels.

The USANS profiles of all QPI gels containing NaCl are plotted in Fig. 3.5E to allow better comparison. The structural parameters obtained from fitting to the unified model are listed in Table 3.2. Interestingly, the scattering curves nearly superimposed for the QPI gels in the presence of 0-200 mM NaCl (Fig. 5E). In the Q range of $(3\times 10^{-5} < Q (\text{ \AA}^{-1}) < 10^{-3})$, the scattering intensity follows a power-law decay with a power-law exponent of ~ 2 , suggesting the presence of a self-similar mass fractal structure (Martin, 1986). This finding is in line with the CLSM observations, where the QPI gels containing 0-200 mM NaCl show similar spatial organisations of proteins to form a relatively homogeneous, wide spanning and self-similar fractal network (Fig. 3.4). In previous reports, similar mass fractal scattering ($d_f \sim 2$) was observed in the SAXS of heat induced β -lactoglobulin gels containing 100-200 mM NaCl (Ako et al., 2009). Despite QPI gels containing 0-200 mM NaCl showing large variations in their viscoelastic properties,

their microstructures are quite similar in the length scale probed by USANS (200 nm-10 μm). This implies that the length scale probed by USANS might not be directly relevant to differences in viscoelastic response in QPI gels containing different amount of NaCl (0-200 mM) (Costanzo et al., 2020). As viscoelasticity is a macroscopic and complex property probed by rheology, various length scales and structural inhomogeneities could contribute (Ikeda et al., 1999); the different rheological properties found in the QPI gels containing 0-200 mM NaCl may not be reflected in the length scale probed by USANS (Mehalebi et al., 2008).

The USANS scattering profiles of the QPI gels containing CaCl_2 and NaCl demonstrate qualitative differences. Instead of showing a single power-law scattering in the low to mid- Q region, another Guinier knee was observed in the QPI gels containing CaCl_2 (Fig. 3.5F). Using a two-level unified fit (Fig. 3.5G), R_g values of $\sim 2.7 \mu\text{m}$ and $4.0 \mu\text{m}$ were calculated in QPI gels containing 20 and 50 mM CaCl_2 , respectively (Table 3.2). Assuming those particles are spheres, the corresponding radii, R , of $3.5 \mu\text{m}$ and $5.2 \mu\text{m}$ can be calculated using $R = (5/3R_g^2)^{0.5}$ (Pedersen, 1997). This seems consistent with CLSM observations (Fig. 3.4), where micron-scale particles could be ascribed to large protein aggregates or blobs. Note that for QPI gel containing 50 mM CaCl_2 , the Guinier region is not fully resolved due to the limit in the lowest- Q achievable in the current USANS measurement. Therefore, the size obtained is likely to only represent a portion of large protein aggregates. Following the Guinier knee, the scattering in the mid- Q ($2 \times 10^{-4} < Q \text{ (}\text{\AA}^{-1}\text{)} < 10^{-3}$) region demonstrates a steeper power-law decay, with a greater exponent of 2.5 compared to 2 found in the control and NaCl gels (Fig. 3.5F). This implies that the small protein colloids ($R_g \sim 170 \text{ nm}$, see below) are organised into branched and mass fractal structures within the micron scale protein aggregates (Teixeira, 1988). Moreover, the arrangement of protein colloidal particles is more compact and denser in the CaCl_2 gels than that in control and NaCl gels (Schaefer et al., 1984). However, those large protein blobs tend to be phase separated as observed in Fig.4, which perhaps accounts for the weak gel strength.

Moving to a higher- Q , a Guinier knee that represents a characteristic particle size of $R_g \sim 170 \text{ nm}$ was observed in all QPI gel samples (Fig. 3.5E, 3.5F, and 3.5G). This particle feature could be ascribed to small structural units that constitute the network system as they were also found in the scattering curves of all the solution samples and did not show any prominent changes upon heating (Fig. S1 and Fig. S2, refer to section 8 Appendices) (Hiroi et al., 2020; Pasquier et al., 2019). In the high- Q range ($10^{-3} < Q \text{ (}\text{\AA}^{-1}\text{)} < 0.02$), the scattering follows a power-law

decay $I(Q) \sim Q^{-3.4}$, which implies that those small protein particles have relatively rough surfaces (Martin, 1986).

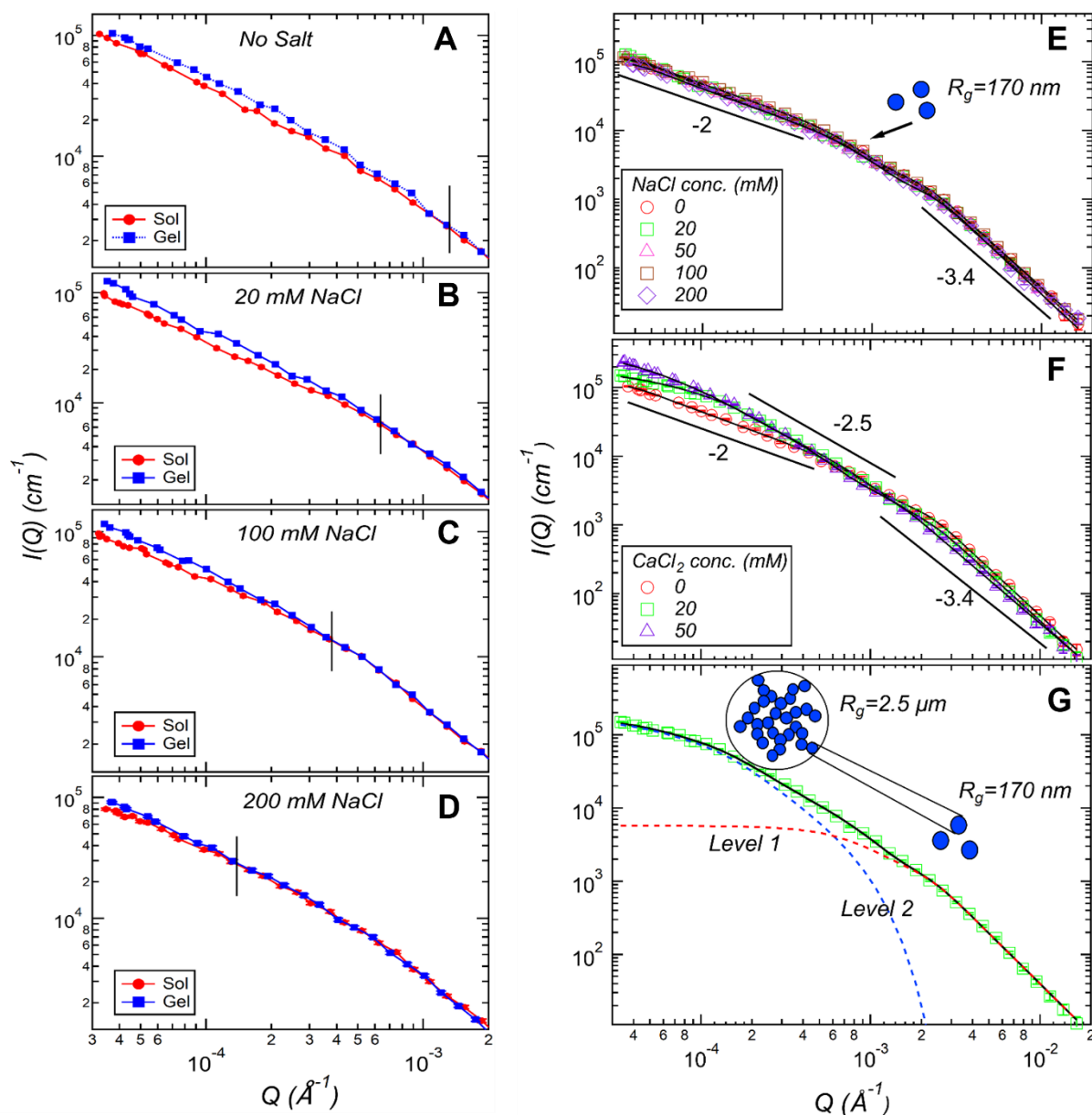


Fig 3.5: USANS profiles ($3 \times 10^{-5} < Q \text{ (\AA}^{-1}) < 2 \times 10^{-3}$) of QPI samples (10 wt% in D_2O) with 0 mM (A), 20 mM (B), 100 mM (C) and 200 mM (D) of NaCl addition before and after heat treatment. USANS profiles of QPI gels that formed in the presence of various NaCl (E) and $CaCl_2$ (F) concentrations. Solid black lines are the unified fits using equation (1). The power-law scattering found in different Q regions are also indicated with the corresponding power-law exponent. (G) USANS profile of QPI gels containing 20 mM $CaCl_2$ and the unified fit to the experimental data are solid black lines and individual levels are illustrated as orange and blue dashed lines for levels 1 and 2, respectively. The USANS data are not desmeared.

3.4.7. Nanostructures of the QPI before and after heating probed by SAXS and SANS

The nanostructure of the QPI solutions and gels in the presence of NaCl and CaCl₂ were further probed by SAXS and SANS (Fig. 3.6). For all the samples, the scattering curves before (not shown here) and after heating are nearly identical within experimental error. This agrees with the USANS results: after heating, the scattering intensity was nearly the same in the high- Q region and the intensity upturn was observed only in the low- Q region. This implies that during the thermal induced QPI gelation, protein aggregation and association only occurred on the micron scale while the nanoscale protein internal structure was not considerably altered. Similar observations have been found in a SANS study of canola protein gels formed by thermal treatment (Pasquier et al., 2019). Matching the high- Q scattering USANS pattern, the low scattering intensity in SANS and SAXS follows $I(Q) \sim Q^{-3.5}$, indicating the presence of rough surface fractals. In contrast to β -lactoglobulin, a Guinier plateau or a structure factor (correlation) peak in the low- Q region was not observed here, which might be attributed to the low solubility and aggregation of the QPI protein at pH 7 (Kaspchak, de Oliveira, et al., 2017; Ruiz, Xiao, et al., 2016).

The overall SAXS and SANS scattering intensity decreased progressively as the salt concentration increased (Fig. 3.6). The direct binding of salts to proteins may alter the X-ray and neutron contrast between the protein-salt complex and solvent (Phan-Xuan et al., 2013; Zittle et al., 1957). In addition, the H/D exchange between protonated protein molecules and deuterated solvent is also expected to occur, which may result in the increase of protein neutron scattering length density (SLD) (Banc et al., 2016). The increase of protein neutron SLD towards that of the solvent would cause the reduction of scattering contrast between proteins and solvents, thus reducing the neutron scattering intensity. Another reason could be the decrease of the number of scattering objects (small protein particles) as they are prone to aggregate to form larger protein structures particularly at higher salt concentrations (Fig. 3.4) (Ako et al., 2009). All those factors could contribute to the change of scattering intensity in different solvents. It is worth noting the presence of salt only induces very slight changes of both X-ray and neutron SLD of the solvent (Table S1, refer to section 8 Appendices), thus the change of protein particle/solvent contrast is negligible, which is not the reason to cause the decrease of scattering intensity.

To better present and examine the feature in the mid- Q region, Kratky plots of all the samples are shown in Fig. 3.6C and 3.6D. In both SAXS and SANS profiles of QPI gels containing 0-200 mM NaCl, a Guinier shoulder was observed in the mid- Q region ($0.02 < Q \text{ (}\text{\AA}^{-1}\text{)} < 0.08$), which suggests the existence of nanoscale protein particles or inhomogeneities. The correlation length model (equation (2)) was used to fit those scattering profiles. Exemplar fits of SAXS and SANS scattering profiles of QPI gels containing 0 and 200 mM NaCl are shown in Fig. 8E and 8F, respectively. Note that equation (2) has been previously used to reproduce the small angle scattering data of wheat gluten gels (Banc et al., 2016; Costanzo et al., 2020), canola protein gels (Pasquier et al., 2019), and gelatine gels (Yang et al., 2016). From the fits, the correlation length (ξ) or particle size of $\sim 32 \text{ \AA}$ (from SAXS) and $\sim 57 \text{ \AA}$ (from SANS) were obtained for all the QPI gels containing 0-200 mM NaCl. The different sizes obtained from SAXS and SANS could be due to the presence of inhomogeneity within the QPI gels or a more complex model being required to describe these systems (Banc et al., 2016). As the deuterated solvent (100% D_2O) was used in both SAXS and SANS measurements, the H/D exchange between the labile protons on protein molecules and D_2O occurred. This exchange might lead to the non-uniform deuterium labelling on protein molecules. For instance, the existence of denser regions within protein gels could hinder the D_2O solvent penetration and diffusion, thus the H/D exchange in these regions would be depressed and consequently form an effective hydrogen-rich zone (H-zone). This would ultimately result in the variation of X-ray and neutron contrast between protein gels and solvent and cause the mismatch of SANS and SAXS profiles. Similar observations have also been identified in a recent SAXS and SANS study of gluten gels (Banc et al., 2016). Future contrast-variation SANS studies of QPI protein gels in different deuterated solvents (e.g. varying $\text{H}_2\text{O}:\text{D}_2\text{O}$) could be helpful to better understand the mismatch between SAXS and SANS profiles.

Note that a faint scattering curvature located $Q \sim 0.1 \text{ \AA}^{-1}$ was also observed in all SAXS and SANS profiles, and this feature was not able to be reproduced well with a correlation length model. This can be observed in Fig 3.6E and 3.6F (black arrows) where the fit starts to deviate from the scattering data at $Q \sim 0.1 \text{ \AA}^{-1}$. This feature likely arises from the form factor (shape) of individual protein molecules or tiny protein particles/inhomogeneities (Pasquier et al., 2019). Further small angle scattering studies on the purified protein fractions of QPI are needed to understand and resolve its nanostructure unambiguously, given that the QPI are protein mixtures which are predominately composed of 11S globulins, 2S albumins, and other protein fractions with smaller molecular weight (Abugoch et al., 2008; Kaspchak, de Oliveira, et al., 2017; Ruiz, Xiao, et al., 2016).

Besides the change of scattering intensity, the shape of the scattering patterns was also considerably altered in the QPI gels containing 20 and 50 mM CaCl₂. As shown in Fig. 3.6C, the deviation from power-law scattering occurred at a higher- Q ($\sim 0.03 \text{ \AA}^{-1}$) in the QPI gels containing CaCl₂ compared to the ones containing 0-200 mM NaCl. In the SANS Kratky plot (Fig. 6D), CaCl₂ addition changed the scattering from a Guinier knee feature to power-law behaviour up to $Q \sim 0.03 \text{ \AA}^{-1}$. This could be due to the micro-phase separation and formation of larger aggregates at the expense of smaller protein particles in QPI gels when CaCl₂ is added. This finding is in agreement with a previous SAXS study of β -lactoglobulin gels in the presence of high NaCl concentrations (180-500 mM) or at a lower pH (5.4-5.8) closer to the isoelectric point (4.5) (Ako et al., 2009). In the SAXS profiles of QPI gel containing CaCl₂ (Fig. 3.6A), a small peak also appeared at $Q \sim 0.2 \text{ \AA}^{-1}$; this might be attributed to the formation of small protein inhomogeneities due to calcium binding or protein cross-linking.

Table 3.2: USANS model fit structural parameters of QPI gels that formed in the presence of various concentrations of NaCl and CaCl₂

Samples	Level-1 unified fit		Level-2 unified fit	
	Size R_g (nm)	Exponent P	Size R_g (nm)	Exponent P
QPI gel	170 (10)	3.4 (0.1)		2.0 (0.1)
QPI gel+20 mM NaCl	170 (10)	3.4 (0.1)		2.0 (0.1)
QPI gel+50 mM NaCl	175 (10)	3.4 (0.1)		2.0 (0.1)
QPI gel+100 mM NaCl	173 (10)	3.4 (0.1)		2.0 (0.1)
QPI gel+200 mM NaCl	170 (10)	3.4 (0.1)		2.0 (0.1)
QPI gel+20 mM CaCl ₂	175 (10)	3.5 (0.1)	2500 (150)	2.5 (0.1)
QPI gel+50 mM CaCl ₂	200 (10)	3.4 (0.1)	4000 (300)	2.5 (0.1)

Numbers in parentheses represent σ error bars (or 68.3% confidence levels)

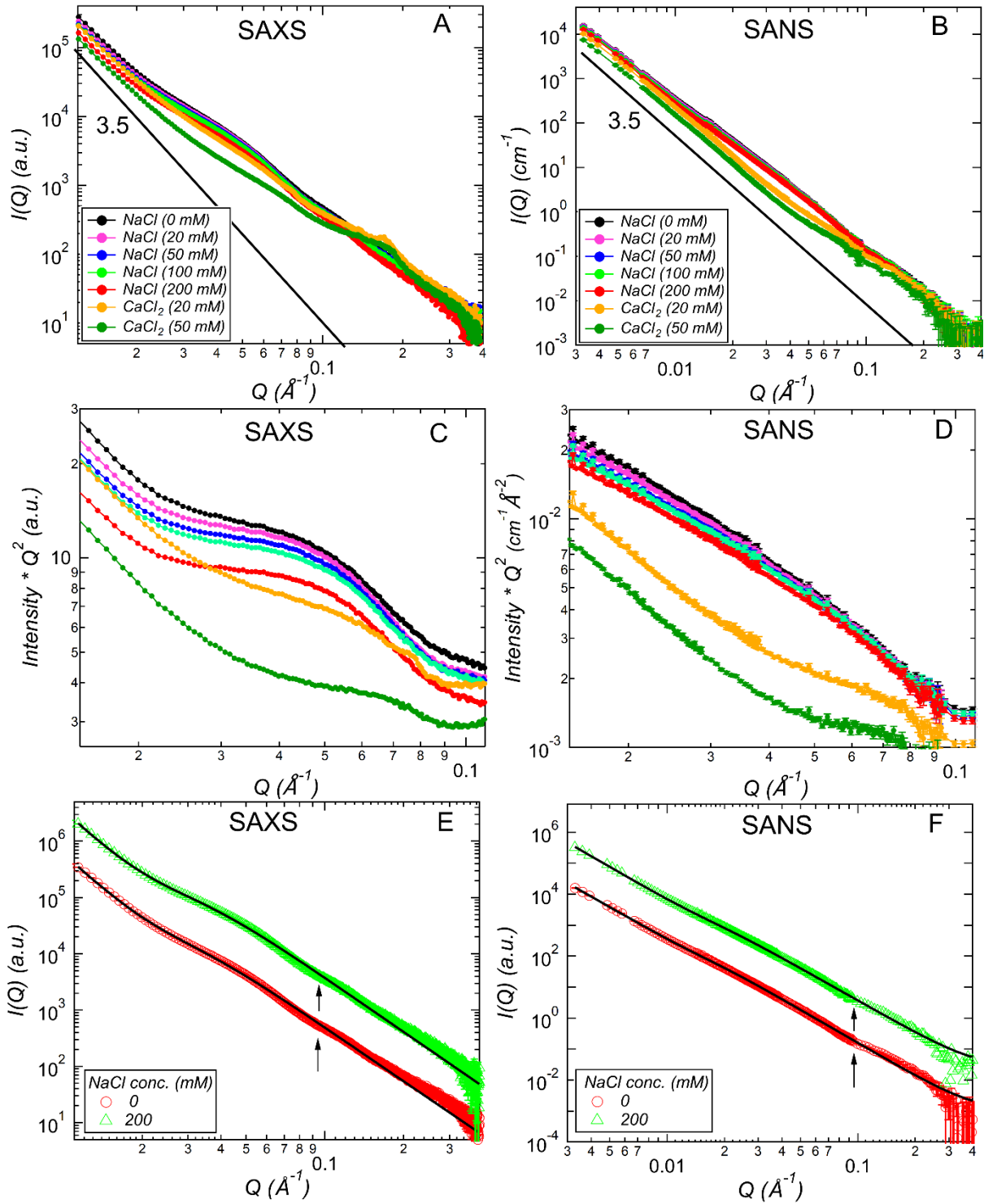


Fig 3.6: SAXS (A) and SANS (B) profiles of QPI gels that formed in the presence of various concentrations of NaCl and CaCl₂. The power-law scattering found in different Q regions are also indicated with a power-law exponent. (C) and (D) are the Kratky plots of SAXS and SANS profiles of QPI gels. Symbols are the same as in A and B. (E) and (F) are SAXS (E) and SANS (F) profiles of QPI gels containing 0 and 200 mM NaCl. Solid black lines are the correlation

length model fits using equation (2). In (E) and (F), scattering curves were arbitrary vertically shifted to avoid overlap.

3.5. Conclusions

In this study, the thermal induced gelation of QPI, as influenced by the addition of various concentrations of NaCl and CaCl₂, was studied. Small and large deformation rheology demonstrated that the addition of salts could promote a sol-gel transition, with the gelation occurring at lower temperatures with increasing salt concentration. All protein gels exhibited weak gel characteristics. Greater complex modulus (G^*) and breaking stress was achieved in the QPI gels with the addition of higher concentration of either salt. Large scale microstructural features of the QPI before and after heat treatment were characterised by CLSM and USANS while their nanostructures were probed by SAXS and SANS. SAXS and SANS results showed that the internal structure of QPI was not changed after heat treatment. However, addition of 200 mM NaCl and CaCl₂ (20 and 50 mM) caused a marked reduction in scattering intensity and alteration of scattering features. This could be attributed to protein aggregation and micro-phase separation. The mismatch between the SAXS and the SANS profiles suggested the existence of compact protein inhomogeneities in QPI gels. CLSM showed all QPI gels were made of a space-spanning fractal-like network. USANS results implied that the change of QPI structure mainly occurred at the micron scale after heat treatment. The gels containing 0-200 mM NaCl showed a similar mass fractal structure with $d_f=2$. For QPI gels containing 20 and 50 mM CaCl₂, large protein agglomerates ($R_g=2.5$ or $4.0 \mu\text{m}$) were identified with a more compact and denser structure; however, those large protein blobs tend to be phase separated as observed in CLSM, which might account for their weak gel strength. Finally, this work showed the gelation behaviour, gel strength, and gel structure of the QPI can be tuned by addition of mono- and divalent ions at neutral pH. This work also shows that USANS, SANS, and SAXS are excellent techniques in probing the hierarchical structure of plant protein gels. Future work can be conducted to investigate the effect of salt addition on the characteristics of quinoa protein gels obtained by other methods such as enzymatic crosslinking or high hydrostatic pressure treatment.

4. Impact of incorporations of various polysaccharides on rheological and microstructural characteristics of heat-induced quinoa protein isolate gels

4.1. Abstract

This study aimed to investigate the properties of heat-induced gels (85 °C for 30 min) of quinoa protein isolate (QPI) in the presence and absence of various polysaccharides including guar gum (GG), locust bean gum (LBG), and xanthan gum (XG) at pH 7. For this purpose, samples with three gum concentrations (0.05, 0.1, and 0.2 wt%) at a fixed QPI concentration (10 wt%) and a fixed ionic strength (50 mM NaCl) were studied in terms of their gelation behaviour, small and large deformation rheological properties, water holding capabilities, and microstructural characteristics. Rheological measurements revealed that all polysaccharides incorporation could improve gel strength (complex modulus, G^*) and breaking stress, accelerate gel formations, and more stiffer gels were obtained at greater polysaccharide concentrations. The XG exhibited the most gel strengthening effect followed by LBG and GG. Incorporation of 0.2 wt% XG led to a 15 folds increase in G^* compared to the control. Confocal laser scanning microscopy observation revealed that the polysaccharides also altered gel microstructures, with the gels containing XG showing the most compact gel structures. The findings of this study may provide useful information for the fabrication of novel QPI based food gel products with improved texture.

4.2. Introduction

Animal proteins have been dominated in the Western diet for a long time, as they have a high amino acid score, easier digestibility, and greater water solubility for the required nutrition of humans (Day et al., 2021). However, meat production has a significant impact on environment and contributes to greenhouse gas emission (Niva et al., 2017). Making food production more sustainable in order to feed fast growing population, one solution is to increasingly investigate and utilize novel plant protein sources and decrease the consumption of animal-based food (Sá et al., 2020b). Recently, extensive efforts have been devoted to developing plant protein based food such as meat substitutes, infant formulae, and dairy alternatives, and some of them still commercially available (Le Roux et al., 2020; Mäkinen et al., 2016; Sethi et al., 2016). Quinoa (*Chenopodium quinoa*) is a pseudocereal and being an important protein and nutritional resource for the people from its origin, South America (Dakhili et al., 2019). The total protein

content in quinoa seeds varies from 12 to 23% (based on dry weight) depending on variety and origin (Dakhili et al., 2019). Quinoa protein isolates (QPI) have a significant amount of all essential amino acids, and it is mainly composed of 11S globulins (37%), 2S albumins (35%), and small amount of prolamins (0.5-7.0%) (Abugoch et al., 2008; Shen et al., 2021).

Among all these technical functionalities of proteins, gelation is considered as one of the most important attributes, as it play important roles in textures of various food products such as yoghurt, sausage, meat analogue and tofu-like products. As globular proteins, QPI can form gels under heat treatment. Upon heating above the denaturation temperature of the QPI (~ 75 °C), compact protein structures start to unfold and hydrophobic amino acid groups that were buried inside of the proteins are exposed, leading to protein aggregations through hydrophobic interactions (Kaspchak, de Oliveira, et al., 2017). When the protein concentration is greater than the minimum protein concentration required for the gelation, these protein aggregates can further grow to large clusters and finally formed a three dimensional interconnected network structure (Chen et al., 2017). Previous studies suggested that the QPI gelation kinetics and the resultant gel characteristics such as gel strength are strongly related to extraction procedure, temperature, pH, and ionic strength (Kaspchak, de Oliveira, et al., 2017; Ruiz, Opazo-Navarrete, et al., 2016). For example, a previous study indicated that protein fractions of lower molecular weight became more prominent as the extraction pH increased from 8 to 11. Thus, only QPI obtained from extractions at pH 8 and pH 9 can form self-supporting gels (Ruiz, Opazo-Navarrete, et al., 2016).

Compared to animal and dairy derived proteins, most of plant protein gels exhibited a weak gel strength, as they are mostly formed by non-covalent interactions (Sun & Arntfield, 2012). This limit their applications in food and pharmaceutical products and thus improvement of gel strength is needed. Incorporation of polysaccharides into protein gels is one of most commonly used strategies to enhance the protein gel strength and microstructure (Cortez-Trejo et al., 2021). Depending on the nature of proteins and polysaccharides as well as pH, temperature, and ionic strength, interactions between proteins and polysaccharides can be either through electrostatic attraction or intermolecular repulsion (Ye, 2008). The latter may lead to thermodynamic incompatibility or depletion-flocculation phenomena, resulting in a phase separation (Hemar et al., 2001). Both types of interactions have been reported to lead to the improvement of gelation properties (Bertrand & Turgeon, 2007; Bryant & McClements, 2000b). For example, H. Zhao et al. (2020) found that the mechanical properties of Ca_2SO_4

induced soy protein isolate gels were significantly improved after additions of 0.5% (w/v) of konjac gum, gellan gum, and curdlan gum.

Guar gum (GG) is a neutral polysaccharide obtained from seeds of the plant *Cyamopsis tetragonoloba*, a member of the Leguminosae family (George et al., 2019; Mudgil et al., 2014). In terms of structure, GG has a linear backbone of mannose units with branched chains constituting galactose units (Mudgil et al., 2014). The galactose to mannose ratio is 1:2, therefore the degree of branching is ~ 50%. The higher hydrogen bonding and hydration property of guar gum are due to a large degree of branching (Thombare et al., 2016). Locust bean gum (LBG) has a galactose to mannose ratio of 1:4 and also belongs to the galactomannan family (Prajapati et al., 2013; Sébastien et al., 2014). Like GG, LBG is also a non-ionic neutral gum (Prajapati et al., 2013). Xanthan gum (XG) is an anionic polysaccharide generated by bacterial of the genus *Xanthomonas* (Garcia-Ochoa et al., 2000). XG produces a viscous solution and has been used extensively as a stabiliser or thickener in many food applications (Niknezhad et al., 2015). XG comprises a linear cellulose backbone substituted with a trisaccharide side chain containing glucose, mannose, and gluconate as well as acetyl and pyruvate groups (Kumar et al., 2018). Owing to different molecular structural characteristics (e.g. molecular weight and degree of branching) of GG, LBG, and XG; their hydration and self-association behaviour in water as well as interactions with proteins could be different. Thus, the incorporations of different polysaccharides may result in QPI gels with different rheological properties, water-holding capacities, and microstructural characteristics.

Most studies on properties of polysaccharide-protein mixtures to fabricate composite gels are focused on animal or dairy-derived proteins, and such studies on emerging plant proteins are limited. Therefore, the aim of this work is to study the gelation behaviour and microstructural characteristics of heat-induced QPI gels in the presence of three polysaccharides-GG, LBG, and XG at three concentrations. This study will provide useful information for developing QPI gel-based food products.

4.3. Materials and Methods

4.3.1. Materials

Quinoa seeds (*Chenopodium quinoa*) were kindly provided from Kiwi Quinoa, and they were locally grown and processed in Taihape, New Zealand. Chemicals including HCl, NaOH, NaCl, petroleum ether, and sodium azide were purchased from Sigma-Aldrich (USA) and were of analytical grade. Polysaccharides including guar gum (GG, purity: 92%, Mw: ~1000 kDa), locust bean gum (LBG, purity: 92%, Mw:~ 1200 kDa), and xanthan gum (XG, purity:90%, Mw:~2000 kDa) were obtained from DuPont Danisco, Inc. (Singapore). Milli-Q water was used for all the sample preparation.

4.3.2. Preparation of quinoa protein isolate (QPI)

The quinoa protein isolate (QPI) was obtained according to our previous studies (Yang et al., 2022; Zhang et al., 2021). The raw quinoa seeds were pulverised using a coffee grinder (Coffee and spice grinder, Breville, New Zealand) and sieved through a 500 µm sieve (Endecotts, UK). The ground quinoa flour was soaked and stirred continuously in petroleum ether for 24 h in a ratio of 1:5 (w/w) and then dried in a fume hood at ~20 °C for 15 h. Defatted quinoa flour was then soaked in 0.5 M NaCl solution containing 0.02 wt% sodium azide, with a weight ratio of quinoa flour to NaCl solution 1:10. Under magnetic stirring, the pH of the suspension was then adjusted to 8 with 1M NaOH and kept stirring overnight to maximize the protein extraction at 20 °C. pH was regularly check and adjusted when necessary. Thereafter, the suspension was centrifuged at 10000×g at 20 °C (Sigma, 6-16KS with rotor 12356, Germany) for 15 min, and the supernatant was collected. The residual fat layer on the surface of the supernatant was carefully removed by a wooden spatula. This centrifugation step was repeated twice until the supernatant exhibited low turbidity. After that, the pH of the supernatant was adjusted to 4.5 using 1M HCl, before centrifugating at 10000×g at 20 °C for 15 min to recover the precipitated protein. The collected protein pellets were thoroughly washed with Milli-Q water and centrifuged under the same conditions for three times until the electrical conductivity became lower than 40 µS/cm. The pellets were then redispersed to Milli-Q water containing 0.02 wt% sodium azide at pH 7 under magnetically stirring overnight. Finally, The QPI solution was frozen at -20 °C for 48 h , before being lyophilised using a freeze dryer (Labconco, Model 7753034, USA) for 5 days. A pestle and mortar was used to grind the dried sample to fine

powder. The obtained QPI powder was stored in sealed plastic containers and kept in a desiccator avoiding sunlight for further use. The proximate analyses of QPI were conducted at the Nutrition Laboratory of Massey University (School of Food and Advanced Technology, Palmerston North, New Zealand). The protein, fat, ash, and moisture contents of the QPI powder were 91.6 %, 2.9 %, 2.8 %, and 2.7 %, respectively.

4.3.3. Sample preparations

The QPI stock solution (12.5wt%) was prepared by dispersing the QPI powder in Milli-Q water containing 0.02 wt% sodium azide under stirring for 24 h to allow the protein hydration and solubilisation. To prevent microorganisms growth, sodium azide was added. Polysaccharides stock solution (1.0 wt%) was prepared by dispersing the GG, LBG, or XG powder in Milli-Q water containing 0.02 wt% sodium azide under stirring for ~5 h. Polysaccharides stock solution was left overnight at 20 °C to enable full hydration. The gum-QPI mixtures were prepared by mixing an appropriate amount of QPI stock solution, different polysaccharide stock solution, 1 M NaCl solution, and Milli-Q water containing 0.02% sodium azide to a total protein concentration of 10 wt%. The ionic strength of all samples was fixed at 50 mM NaCl in order to promote gelation of QPI-gum composites by diminishing electrostatic repulsions between protein molecules (Yang et al., 2022). All dispersions were gently mixed under magnetic stirring for 2 h at 20 °C, and the pH was regularly checked and adjusted to 7 using 1 M HCl or 1 M NaOH.

4.3.4. Confocal Laser Scanning Microscopy (CLSM)

CLSM was used to observe the microstructures of various QPI dispersions and gels. In brief, a few drops of 1% fast green dye were added and mixed with QPI dispersions and then vortex mixed for 15 seconds at 20 °C. Thereafter, aliquots of each sample were carefully transferred into a glass slide with a cavity and covered with a glass coverslip. In the case of QPI gels, to prevent water evaporation (Wang et al., 2019), nail polish was used to seal the coverslip edges before transferring into an oven (Labserve, Australia) pre-set at 85 °C for 30 min. The samples were observed at a wavelength of 630 nm under a confocal laser scanning microscope (Leica TCS SP5, Leica Microsystems) attached with a 100 × oil immersion objective lens. The Image J software (version 1.51k, NIH, USA) was used to process all images.

4.3.5. Rheological characterisations

Dynamic rheological measurements were conducted using a DHR-3 stress-controlled rheometer (TA instruments, USA) equipped with a stainless steel plate-plate geometry (diameter: 40 mm, gap: 1 mm). Aliquots of QPI dispersions were carefully transferred onto the bottom plate using a plastic dropper. The samples were then carefully trimmed before adding the low viscosity mineral oil (M5904, Sigma Aldrich, USA) around the edge of the sample to prevent evaporation during the rheological measurements. The following rheological protocols were conducted in a sequence: firstly, a *temperature sweep* was performed during which the sample was heated from 25 to 85 °C at 1 °C/min, maintained at 85 °C for 30 min, before decreasing to 25 °C at 1 °C/min. During this step, the gel formation was monitored by recording evolution of storage modulus G' and loss modulus G'' at a fixed frequency of 1 Hz and a fixed strain of 1%. Secondly, to investigate viscoelasticity of heat induced gels, a *frequency sweep* was carried out at a constant strain 1% while the frequency was changed from 0.01 to 30 Hz. Finally, large deformation rheological properties of samples were characterised by a *strain sweep* test, and the frequency was fixed at 1 Hz, while the strain amplitude was varied from 0.1% to 1000%. All the frequency and strain sweep measurements were performed at 25 °C.

4.3.6. Water holding capacity (WHC)

The water holding capacity was determined according to H. Zhao et al. (2020) with slight modifications. QPI dispersions (10 wt%, 2 g each) were transferred to Eppendorf tubes and heated in a water bath pre-set at 85 °C for 30 min to form gels. The gels were left on bench to allow temperature to equilibrate to room temperature (~ 20 °C). Thereafter, the gels formed in the tubes were centrifuged at 4000 ×g for 20 min at 20 °C (Heraeus Pico 17 centrifuge, Thermo scientific, USA). WHC (%) was calculated as the weight ratios of the water left in gels after centrifugation to that of the water in the original samples before centrifugation.

4.3.7. Statistical analysis

All measurements were conducted twice with duplicated samples, and the data was represented as the mean ± standard deviation. Analysis of variance (ANOVA) was conducted with the

SPSS software (version 21.0, IBM, NY, USA) using the Least Significant Difference (LSD) test at the significance level $P < 0.05$.

4.4. Results and Discussion

4.4.1. Microstructural characteristics revealed by CLSM

Confocal laser scanning microscopy (CLSM) has been commonly employed to characterise the microstructural characteristics of protein-polysaccharide mixtures (Cortez-Trejo et al., 2021). Confocal micrographs of QPI dispersions containing different polysaccharides including guar gum (GG), locust bean gum (LBG), and xanthan gum (XG) at various concentrations before (sol) and after (gel) heat treatment are shown in Fig. 4.1. Protein stained with fast green appear as green, while the polysaccharides rich zones and voids in between the protein particles appeared in dark. For all QPI samples, interconnected protein network structures were formed after heat treatment, which resulted in gel characteristics as agreed with previous studies on heat induced QPI gels (Kaspchak, de Oliveira, et al., 2017; Ruiz, Opazo-Navarrete, et al., 2016; Yang et al., 2022). Incorporation of all the polysaccharides made structures heterogenous by forming large protein particles, and these heterogeneities being more prominent in heat treated samples. Heat treatment results in protein denaturation, which enhances the exposing of hydrophobic groups, thus promoting protein-protein interactions through hydrophobic interactions (Sun & Arntfield, 2012). Further, at all polysaccharide concentrations, XG additions induced formation of largest protein aggregates and micro-phase separation followed by that of LBG and GG. Similar observations have been made in heat-induced WPI gel in the presence of XG (Bertrand & Turgeon, 2007), NaCl-induced cold set gels of soy protein isolate containing LBG and GG (Brito-Oliveira et al., 2020), and acid induced soy milk gels adding with GG, LBG, and XG (Pang et al., 2020). This was attributed to the fact that the mixtures of proteins and polysaccharides are incompatible because of their low mixing entropy (Cortez-Trejo et al., 2021).

QPI carry a negative charge at pH 7, as the isoelectric point of QPI is $\sim 4.5-5.0$ (Shen et al., 2021). The addition of both neutral (GG and LBG) and anionic polysaccharides (XG) could induce various degree of incompatibility (Cortez-Trejo et al., 2021). For examples, rheological properties and structural characteristics of soy protein gel at pH ~ 7 containing GG and LBG (0.1-0.3%) were evaluated by Brito-Oliveira, Cavini, Ferreira, Moraes and Pinho (Brito-Oliveira et al., 2020). The authors also observed that the microstructure became more heterogenous with the addition of GG and LBG, while the latter induced more predominant

phase separation. The authors explained this by the strong self-association of LBG due to its less branched structure (branching ~25%) than GG (branching 50%) as above discussion. Likewise, Bertrand and Turgeon (2007) found that the incorporation of XG into WPI gel at pH 6.0 and 6.5 destroyed the connectivity of the protein network because of incompatibility of these polymers at these gelling conditions. It can be seen from Fig. 4.1 that the protein network structure became more heterogenous with the increase in polysaccharides concentrations. This observation is supported by a number of previous studies (Brito-Oliveira et al., 2020; Pang et al., 2020). In addition, it has been suggested that within a certain range, the gel strength increased with the increase in the degree of incompatibility or micro-phase separation (Bertrand & Turgeon, 2007; TAN et al., 2007). The incorporation of polysaccharides may also enhance network via depletion flocculation or steric exclusion mechanisms (Hemar et al., 2001). Protein-solvent interactions are considerably suppressed by incorporation of polysaccharide thus promoting the protein-protein interactions (Tseng & Xiong, 2009).

It is worth noting that even at $\text{pH} > \text{pI}$ where QPI carry a negative charge, the electrostatic attraction can also occur between anionic gums (like XG) and cationic amino acids located in some protein patches of QPI (Cortez-Trejo et al., 2021). While for neutral gums like GG and LGB, they can only form hydrogen bonding with proteins. The electrostatic association is likely to occur between QPI and XG, and these interactions could give rise to a more compact and denser structures and great gel strength particularly at higher concentration of XG (0.2%). A similar observation has been found in bigeye snapper surimi containing another anionic polysaccharide-gellan gum (Petcharat & Benjakul, 2018). The great gel strength and a higher degree of micro-phase separation in QPI-XG gel could be also ascribed to a high molecular weight of XG. It has been suggested that the polysaccharide with a high molecular weight or longer chain such as XG could occupy much larger hydrodynamic volume, facilitating them to interact with other polymers (Yang et al., 2021b). Ozel et al. (2017) found that owing to a higher molecular weight, XG generated more compact structures than tragacanth gum in the WPI gels at pH 7. In another study working on galactomannan-soy protein gels at pH 7, Sónia R. Monteiro et al. (2013) found that the incorporation of the galactomannan with larger molecular weight gave rise to more extensive phase separation, lower gelation temperature, and greater gel stiffness. The authors explained this by the enhancement of protein-protein interactions (via. hydrophobic interactions and hydrogen bonding) and polysaccharide-polysaccharide interactions (via. molecular entanglement) in each phase.

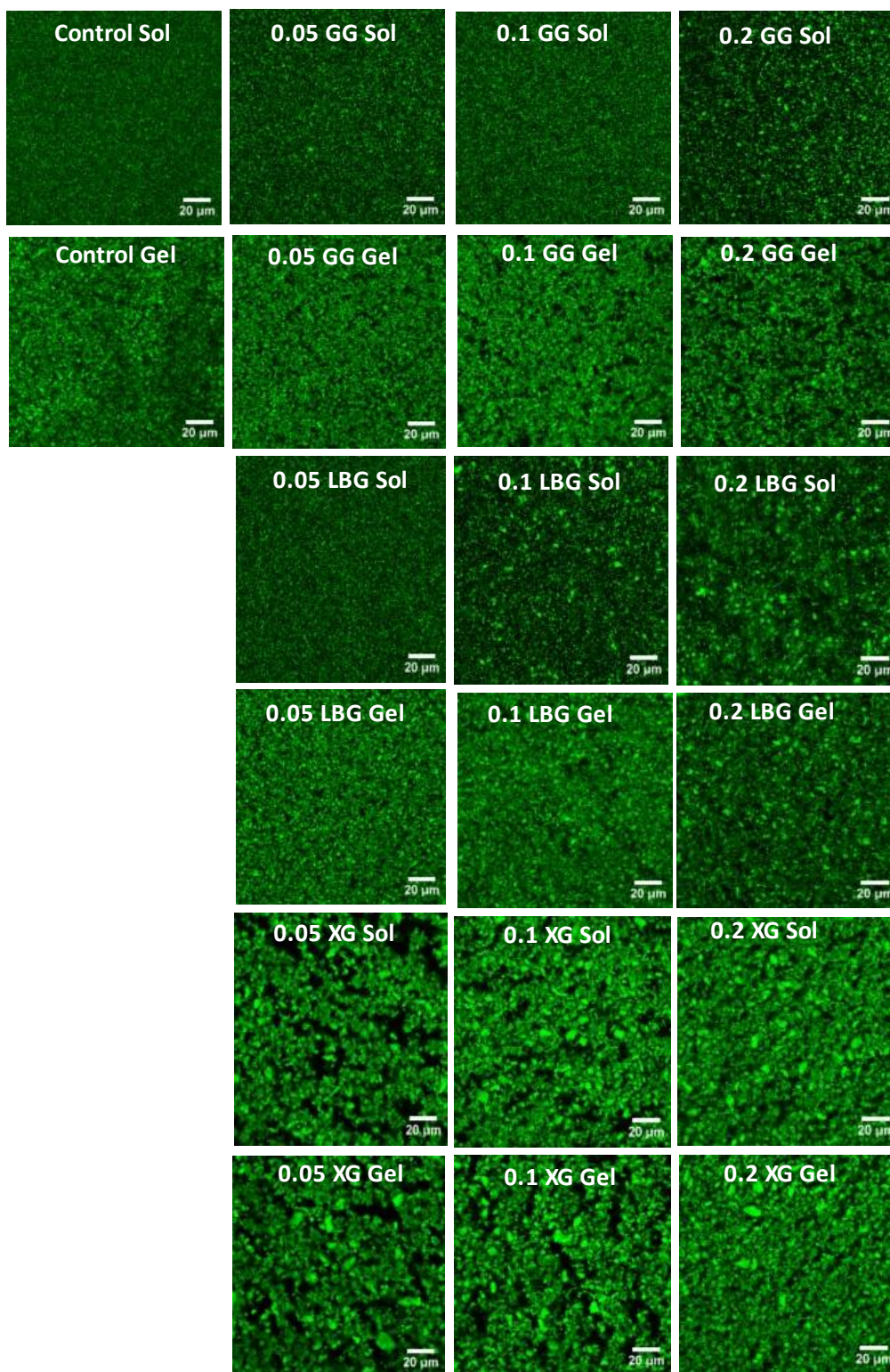


Fig 4.1: Confocal laser scanning micrographs of 10 wt% QPI dispersions and gels in the absence and presence of guar gum, locust bean gum, and xanthan gum at 0.05 wt%, 0.1 wt%, and 0.2 wt%. The gels were formed by heating at 85 °C for 30 min

4.4.2. Effect of polysaccharides incorporation on the rheological properties during gelation

Viscoelastic properties of the QPI dispersion in the presence of GG, LBG, and XG at various concentrations during heat-induced gelation were monitored by small dynamic oscillatory deformation measurement. Storage modulus (G') and loss modulus (G'') as a function of temperature are recorded and presented in Fig. 4.2. The G' and G'' indicate the elastic and viscous component of QPI gels, respectively. Qualitatively, all the samples displayed a similar behaviour and both G' and G'' increased throughout the entire course of heat treatment (temperature increase, maintaining, and decrease). The onset of gelation, T_{gel} , when G' reached 1 Pa (Lucey & Singh, 1997) during the temperature ramp stage are shown in Fig. 4.3. Note that at time zero, G' values of the QPI dispersion in the presence of XG are higher than 1 Pa, thus the T_{gel} for those samples cannot be determined using this method. This also indicates that the sol-gel transition occurred rapidly in the presence of XG at room temperature, which could be due to a high water binding and gel forming capacity of XG at 25 °C (Fig. S1, refer to section 8 Appendices). Generally, for both GG and LBG, the T_{gel} was considerably decreased with the increase in concentrations of polysaccharides. At the same concentration, LBG exhibited a larger reduction in T_{gel} than that of GG. For example, compared to the control, incorporation of 0.2 wt% of GG and LBG into QPI dispersion resulted in a decrease of T_{gel} from ~70 °C to ~52 °C and ~32 °C, respectively. Similar gelation behaviours have been found in previous gelation studies of various plant proteins with adding polysaccharides. Pang et al. (2020) found that T_{gel} of acid induced soymilk gels decreased from ~13 min to ~8.5 min, ~8.0 min, and ~7.6 min, respectively in the presence of 0.10% GG, LBG, and XG, respectively. In another study working on Ca_2SO_4 induced soy protein isolate gels, H. Zhao et al. (2020) indicated that gelation occurred earlier when added with 0.3 and 0.5% of konjac gum, gellan gum, and curdlan gum. It has been suggested that the incorporation of polysaccharides can improve interactions among proteins, thus facilitating gelling of protein-gum dispersions at lower temperatures (Tseng & Xiong, 2009). Owing to strong water binding capacities of polysaccharides, protein-protein interactions are promoted and is accompanied with a decrease of protein-water association, leading to an earlier aggregation and gelation in QPI-gum composites (Luo et al., 2021). Molecular interactions between polysaccharides and proteins may affect rheological properties and microstructural characteristics of the final composite gels. Due to a charge screening effect of NaCl and neutral nature of GG and LBG, inclusions of polysaccharides did not induce significant changes on surface charges of the QPI as revealed

by zeta-potential measurements (results not shown). Nevertheless, further studies are required to probe non-covalent interactions between polysaccharides and proteins (if any) using Fourier-transform infrared spectroscopy (FTIR) and/or nuclear magnetic resonance (NMR). In addition, differential scanning calorimetry (DSC) can be used to examine the effect of polysaccharides addition on unfolding/denaturation of the QPI.

Despite both GG and LBG are galactomannans, LBG exhibited a less degree of branching (~25%) than that of GG (~50%) (Cortez-Trejo et al., 2021). Therefore, LBG demonstrated a higher capacity to self-associate and showed more incompatible with proteins, thereby promoting the protein-protein interactions to a greater extent (Brito-Oliveira et al., 2020). This could give rise to the greater T_{gel} reduction in the presence of LBG than GG. Alternatively, lower branching of LBG might improve the integration in the QPI protein network, resulting in a more prominent increase of G' with the increase in temperature (Fig. 4.2). Future studies such as staining proteins and polysaccharides with different dyes in CLSM experiments and/or directly probe protein-polysaccharide interactions at a molecular level using FTIR/DSC/NMR may help to understand the underlying mechanism.

At the latter stage of temperature ramping and holding at 85 °C, both G' and G'' progressively increased but at a much lower rate. This indicated that the unfolding and denaturation of protein molecules occurred progressively and hydrophobic amino acids group that were buried inside of the protein were increasingly exposed to induce protein aggregation. When the protein concentration beyond the critical concentration for gelation, protein aggregates are further grown into large clusters and eventually to form an interconnected three-dimensional network structure. Similar trend of G' and G'' versus heating temperature have been found in previous reports on rheological studies of heat-induced QPI gels (Kaspchak, de Oliveira, et al., 2017; Yang et al., 2022). The heat-induced gelation is one of the most common gelation route for globular proteins and similar gelation behaviours have been also found in previous studies on whey protein isolates (WPI) (Diedericks et al., 2021), pea protein isolates (Sun & Arntfield, 2012), and faba bean protein isolates (Langton et al., 2020). When the temperature is decreased, all the QPI gels showed an increase in G' and G'' , which is likely due to the formation or enhancement of covalent and non-covalent bonds such as hydrogen bond and disulfide bond among proteins, as well as the interactions between protein-polysaccharides (Yang et al., 2021b; H. Zhao et al., 2020).

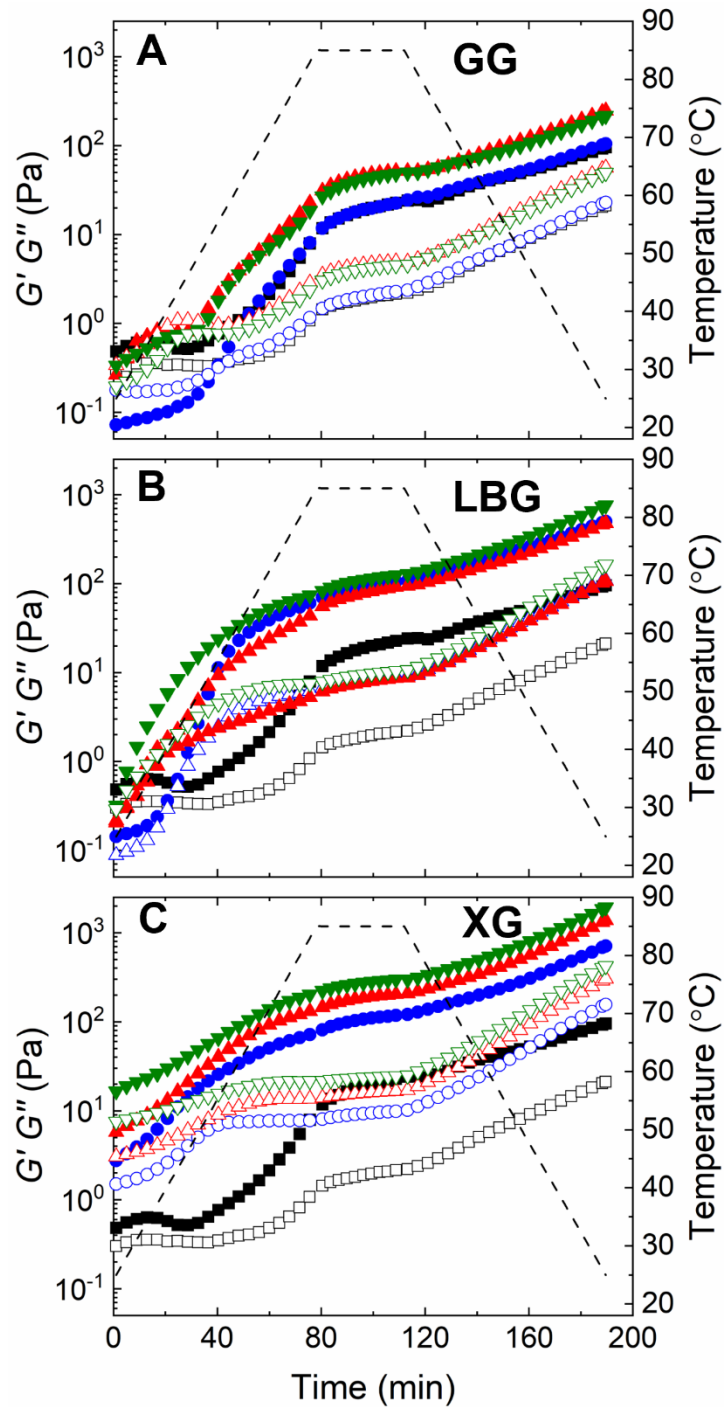


Fig 4.2: The evolution of G' (solid symbols) and G'' (open symbols) for 10 wt% QPI dispersions during heat-induced gelation in the absence and presence of guar gum (A), locust bean gum (B), and xanthan gum (C). Gums concentrations: 0 wt% (\blacksquare), 0.05wt% (\bullet), 0.1wt% (\blacktriangle), and 0.2wt% (\blacktriangledown).

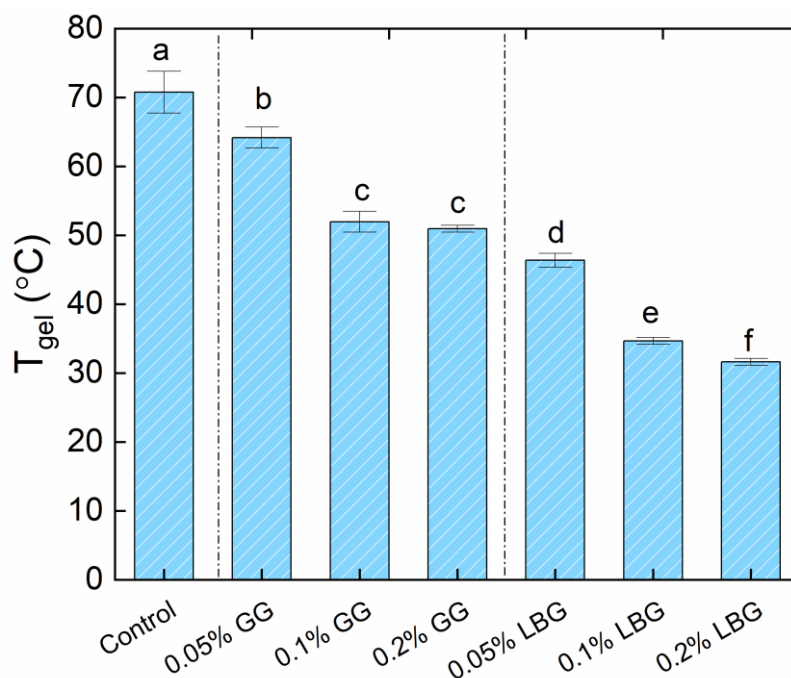


Fig 4.3: The gelation temperature T_{gel} of the QPI gels containing guar gum and locust bean gum at 0 wt%, 0.05 wt%, 0.1 wt%, and 0.2 wt%. Different letters above columns indicate significant differences.

4.4.3. Effect of polysaccharides incorporation on the rheological properties after gelation

At the end of temperature sweep measurements, the small and large deformation rheological properties of QPI gels in the presence of different gums at various concentrations were characterised by the frequency sweep and strain sweep measurement and the results are demonstrated in Fig. 4.4. A constant strain of 1% was applied in all the frequency sweep measurements to ensure the strain is well within the Linear Viscoelastic Region (LVER) region. G' and G'' as a function of frequency for all QPI gels are shown in Fig. 4.4A, B, and C. For all the QPI samples, G' is greater than G'' over the whole frequency range and both are slightly dependent of frequency, demonstrating typical characteristics of weak gels (Sun & Arntfield, 2012; Wang et al., 2019). To allow better comparison of gel strength among different QPI gels, the complex modulus G^* at 1 Hz which takes into account the contribution from both G' and G'' at this frequency are presented in Fig. 4A. Compared to control, the gel strength is increased in the presence of all the polysaccharides and greater gel strength is achieved at higher polysaccharide concentrations. Further, the effect of gel strengthening is strongly related to the type of polysaccharides. Incorporating XG resulted in highest gel strength at all gum

concentrations followed by LBG and GG. For instance, in the presence of 0.2% XG, 0.2% LBG, or 0.2% GG, the value of G^* increased ~15, ~7, and ~2 folds than the control sample, respectively. The greatest gel strength in the QPI gels containing XG could be attributed to the largest protein aggregates and prominent phase separation as revealed by CLSM. The improvement of gel strength of protein gels upon addition of polysaccharides have been found in many previous studies (Brito-Oliveira et al., 2017; Brito-Oliveira et al., 2020; Zhuang et al., 2010; Zhuang et al., 2020). The degree of enhancement in gel strength are affected by intrinsic factors such as the nature, conformation, and concentration of the protein and polysaccharide and by extrinsic factors including heating temperature, pH, and ionic strength (Cortez-Trejo et al., 2021).

In the case of large deformation rheology, the dependence of G' and G'' with applied strain for all QPI samples are presented in Fig. 4.4D, E, and F. At lower strains, G' and G'' are independent of the applied strain until reaching a critical strain value, which is defined as the LVER region. Above this point, G' and G'' begin to deviate from plateau and G' decreased more steeply than G'' with further increase in the applied strain. Eventually, crossover of G' and G'' occurs, and beyond this point G'' is greater than G' , indicating network structure of gels is broken down and start to flow. The stress at this crossover point ($G' = G''$) is defined as breaking or yield stress. To better examine the large deformation rheological properties differences among the various QPI gels containing different polysaccharides, the breaking stress (BS) for the different samples is summarized in Fig. 4.5B. Generally, the breaking stress increased with the increase in polysaccharide concentration in a polysaccharide dependent manner, following the nearly same trend as G^* (1 Hz). For example, QPI gels containing XG exhibited greatest value of BS, indicating these gels are more resistant toward structural rearrangement and yield when subjected to large oscillatory deformation. In summary, the small and large deformation rheological behaviour correlate well with the microstructural characteristics (e.g. size of protein aggregates, extent of microstructural separation, and structural inhomogeneities) as revealed by CLSM.

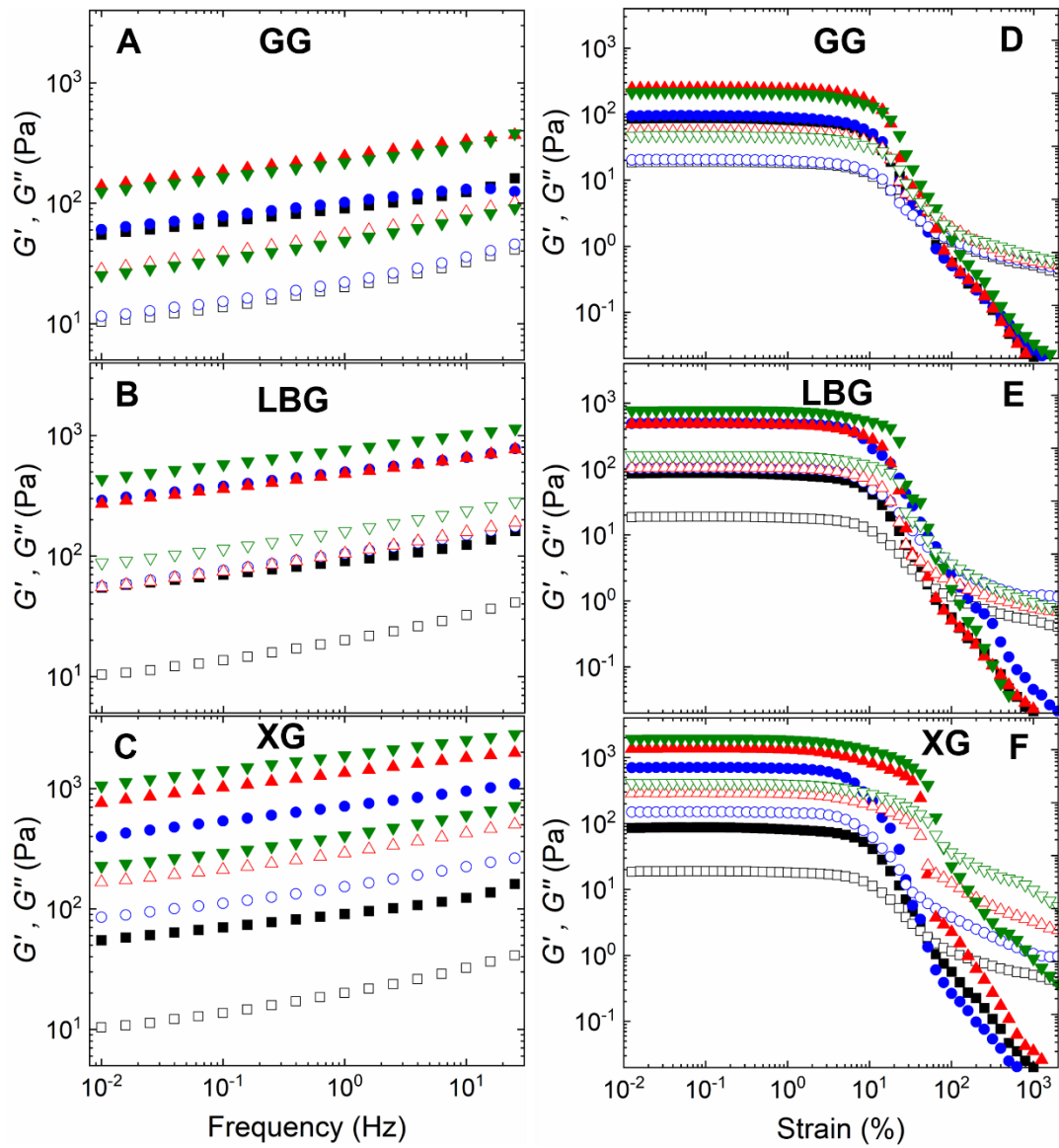


Fig 4.4: The dependence of frequency (A, B, C) and strain amplitude (D, E, F) on G' (solid symbols) and G'' (open symbols) for QPI dispersions at 10 wt% with various concentrations of polysaccharides incorporation measured at 25 °C. Gums concentrations: 0 wt% (■), 0.05wt% (●), 0.1wt% (▲), and 0.2wt% (▼).

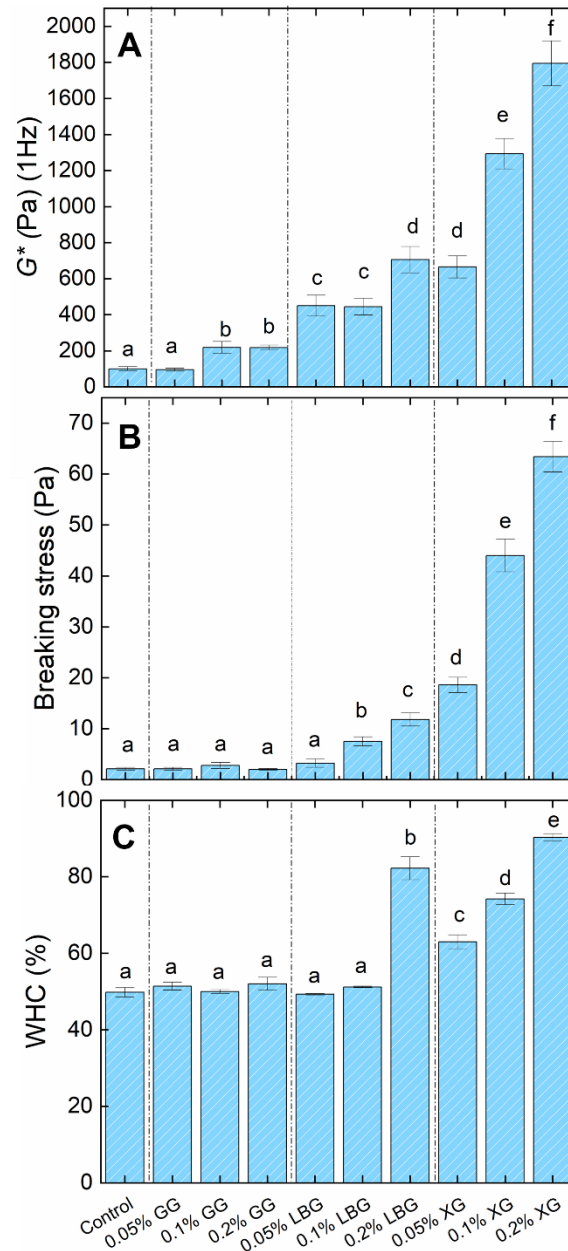


Fig 4.5: Complex modulus G^* (1 Hz) (A), breaking stress (B), and water holding capacity (C) of the QPI gels containing guar gum, locust bean gum, and xanthan gum at 0 wt%, 0.05 wt%, 0.1 wt%, and 0.2 wt%. Different letters above columns indicate a significant difference.

4.4.4. Impact of polysaccharides addition on the WHC

The WHC (%) of QPI gels in the presence and absence of various polysaccharides at different concentrations is shown in Fig. 4.5C. Incorporation of GG did not induce changes in WHC, while the additions of 0.2wt% LBG and XG (at all concentrations) markedly improved the WHC. For example, the WHC increased from ~50 % to ~90 % after adding 0.2 wt% XG to the

QPI gel. WHC is closely related to compactness of structural arrangements within the network and a high WHC typically resulted in a greater gel strength (Cortez-Trejo et al., 2021; Zhuang et al., 2020). This is also observed in the present study that the compact structure induced by XG addition particularly at 0.1 and 0.2 wt% (Fig. 4.1) could entrap water tightly and could not easily be disrupted by centrifugation force, which was responsible for the high WHC and stiffer gels. It could be attributed to the fact that QPI-XG co-polymers have a strong water absorption and swelling capacity and prevent the water channels formation between proteins, leading to a compact network of QPI proteins and great WHC (Hemar et al., 2011; Zhuang et al., 2020). Similar findings were also found in previous studies that the incorporation of 0.05% XG significantly improved the WHC and gel strength of soy milk gels (Pang et al., 2020).

4.5. Conclusions

GG, LBG, and XG have been extensively used in food products for modifying textures and improving stabilities. In the current study, the impact of their incorporations on the rheological properties and microstructural characteristics of heat-induced QPI gels were evaluated. The gel strength and network structures were improved by addition of abovementioned polysaccharides, as evidenced by the increase in G' and G'' during and after gelation. The gel strength and microstructural features are strongly dependent on the polysaccharide used, which might be attributed to different extents of demixing and/or interactions between the QPI and polysaccharides. Owing to a high molecular weight and anionic nature, XG is most effective in improving the gel strength followed by LBG and GG. Since LBG has a lower degree of branching than GG, it has a higher capacity to self-associate or it is more compatible with the QPI, resulting in stronger gels. In addition, the gel formation is accelerated by incorporating polysaccharides, as reflected in the decrease in the gelation temperature, T_{gel} . For all polysaccharides, the complex modulus, breaking stress, WHC were progressively improved with increasing incorporation of polysaccharides. Various extents of polysaccharide-protein demixing were observed by CLSM with QPI gels containing XG displaying the most prominent micro-phase separation. The gel structures became more compact and denser with increasing addition of XG. Nevertheless, further studies are needed to understand molecular interactions between polysaccharides and the QPI. The finding obtained from this study could be useful for development of food products containing QPI gels with desirable gel stiffness, textures, and microstructures. Finally, different polysaccharides and food ingredients (e.g. small saccharides and salts) might co-exist in QPI gel based food products. Therefore, it may be worth

investigating the impact of other polysaccharides (e.g. kappa and iota-carrageenan and alginate) (Ren et al., 2021; Sow et al., 2018), gelatine (Yin et al., 2021), small sugars (e.g. sucrose) (D. Yang et al., 2020; Yang et al., 2018), and salts (e.g. NaCl and CaCl₂) (Brito-Oliveira et al., 2020; Zhou & Yang, 2019) on the rheological properties and microstructural characteristics of QPI gels.

5. Impact of pH and protein concentrations on the thermal gelation behaviour of quinoa protein isolates and whey protein isolates dispersions

5.1. Abstract

This study aimed to investigate the impact of pH and protein concentration of heat-induced (95 °C for 30 min) quinoa protein isolate and whey protein isolate dispersions. For this purpose, samples (QPI and WPI) with four different concentrations (3 wt%, 5 wt%, 7 wt% and 10 wt%) at various pH (pH 3, pH 5, pH 7) were studied in terms of their gelation behaviour, small and large deformation rheological properties and microstructural characteristics. Rheological measurements revealed that increase in the concentration of the QPI and WPI dispersions individually, could improve gel strength (complex modulus, G^*), breaking stress and accelerate gel formations. However, at all pHs WPI showed higher G' than QPI. In addition, concentrations resulted in higher G' for both QPI and WPI, regardless of pH. For QPI, highest G' were obtained at pH 5 but WPI showed higher G' at pH 7. Confocal laser scanning microscopy revealed that higher concentration (10 wt%) of QPI gels, large aggregates are formed at pH 5, which may lead to a higher gel strength as revealed by rheological measurement. In case of WPI gels, the microstructure of gels was found to be homogenous and dense at pH 7 and pH 3 revealing higher gel strength as compared to QPI at same pH. The finding of this study may provide useful information for the fabrication of QPI-WPI hybrid gels.

5.2. Introduction

The United Nations has assigned 2013 as the International Year of Quinoa, with the goal of drawing worldwide attention to the role of quinoa contributing to food security, nutrition, and poverty eradication (Burlingame et al., 2012; Nowak et al., 2016; Vilcacundo & Hernández-Ledesma, 2017). Quinoa seeds have a protein content of approximately 12 to 25% depending on the variety (Abugoch et al., 2008; Dakhili et al., 2019). Quinoa protein isolates (QPI) have shown versatile techno-functional properties including gelation, emulsification, and foaming (Abugoch James, 2009; Abugoch et al., 2008; Bhargava et al., 2006; Comai et al., 2011; Elsohaimy et al., 2015). QPI contains all nine essential amino acid with the high amount of lysine and methionine (Abugoch James, 2009; Koziol, 1992; Wright et al., 2002). It is also rich

in antioxidants such as polyphenols (Repo-Carrasco-Valencia et al., 2010; Repo-Carrasco-Valencia & Serna, 2011). It also contains minerals such as iron and calcium in substantial amount (Ando et al., 2002). QPI is also considered as gluten free due to a low content of prolamin (Thanapornpoonpong et al., 2008; Turkut et al., 2016). Based on our previous study, QPI shows excellent gelation properties at 10 wt% in the presence of monovalent salt (NaCl) or divalent salt (CaCl₂) (Yang et al., 2022).

Whey protein isolate (WPI) is mostly made up of beta-lactoglobulin, alpha-lactalbumin, and bovine serum albumin, and is a by-product of the cheese-making process (Liang et al., 2020; Xiao et al., 2021). WPI contains all nine essential amino acids, so it is regarded as a high-quality protein source (Krissansen, 2007). Because of its excellent gelation, emulsification, foaming, thickening, water retention properties, WPI is widely employed as a functional ingredient in the food industry (Bryant & McClements, 1998). Heat-induced gelation of WPI has been extensively studied and WPI gels are mainly formed by non-covalent interactions such as hydrophobic interactions and disulphide bonds through thiol-disulphide exchange (Brodkorb et al., 2016; Martin et al., 2014; Nguyen, Balakrishnan, et al., 2016; Nguyen, Nicolai, et al., 2016; Nicolai, 2019; Nicolai et al., 2011). At same protein concentrations and pH, WPI generally forms a stronger gel than plant proteins such as soy protein (Jose et al., 2016) and pea protein (Kornet et al., 2021; Wong et al., 2013).

Previous studies demonstrated that plant protein gels typically have large aggregates and form coarse network after heat treatment (Chen et al., 2022; Kristensen et al., 2021; Munialo, van der Linden, et al., 2014). However, homogenous fine-stranded networks are formed by nano-sized aggregates of whey proteins upon heating at low ionic strength and at neutral pH (Wagner et al., 2020). In addition, quinoa proteins and WPI may display differences in unfolding and aggregation behaviour, leading to different gelation properties. Therefore, it is essential to compare the gelation behaviour and microstructural characteristics of heat-induced QPI and WPI gels to understand their gelation behaviour from microstructural perspective. These differences may enable revealing the structure-texture correlations of these two globular proteins and further guide into formations of hybrid gels.

In this chapter, heat induced gelation of QPI and WPI were studied at three different pHs (pH 3, pH 5 and pH 7) at various concentrations (3 wt%, 5 wt%, 7 wt% and 10 wt%). The mechanical properties of the QPI or WPI gels were investigated using small and large

oscillatory deformation rheology. The microstructural characteristics of the gels were probed via confocal laser scanning microscopy.

5.3. Materials and method

5.3.1. Materials

Quinoa seeds (*Chenopodium quinoa*) were kindly provided from Kiwi Quinoa (Taihape, New Zealand). The protein, fat, ash and moisture content of the QPI powder were 91.6%, 4.9%, 2.8% and 0.7%, respectively based on the dry weight. Whey protein isolate (WPI 895) is kindly provided by Fonterra Co-operative Group (Auckland, New Zealand). According to the supplier, the protein, fat, ash, carbohydrate and moisture content of WPI powder were 92%, 0.9%, 1.6%, 0.3% and 5.2%, respectively, based on the dry weight. Sodium chloride (NaCl), petroleum ether, sodium azide, HCl, NaOH, 1% fast green and low viscosity mineral oil were of analytical grades and obtained from Sigma Aldrich (Auckland, New Zealand). Milli-Q water (Millipore, USA) was used in all sample preparations.

5.3.2. Preparation of quinoa protein isolate (QPI)

Please refer to the Chapter 4, section 3.2.

5.3.3. Sample preparations

Stock solutions of QPI and WPI (12.5 wt%) was prepared by dispersing QPI powder or WPI powder in Milli-Q water containing 0.02% sodium azide under gentle stirring for 24 h to enable protein hydration. Sodium azide was used as a preservative. The samples were prepared by mixing different aliquots of protein stock solutions, 1 M NaCl solution, and Milli-Q water containing 0.02% sodium azide. The 100 mM NaCl was added in all the samples to reduce electrostatic repulsions between proteins and promote gelation (Bryant & McClements, 2000a). Afterwards, samples were adjusted to pH 7, pH 5 and pH 3, respectively using 4M NaOH or 4M HCl and were gently stirred for 24 h at 20 °C and the pH was regularly checked and adjusted using 1M NaOH or 1M HCl if needed. The final protein concentration was 10 wt%.

5.3.4. Rheological measurements

To perform small and large deformation oscillatory rheological measurements, a rotational DHR-3 stress-controlled rheometer (TA Instruments, USA) with a parallel plate geometry (diameter 40 mm, gap 1 mm) was used. Samples were carefully transferred onto the bottom plate using a plastic dropper. To prevent the evaporation low viscosity mineral oil (M 5904, Sigma Aldrich, USA) was added to the edge of the geometry. The rheological measurements were carried out using the following procedure: 1) A temperature sweep was carried out by heating the sample from 20 °C to 95 °C at a rate of 1 °C/min, holding at 95 °C for 30 min and cooling down to 20 °C at a rate of 1 °C/min at a constant frequency (1 Hz) and strain amplitude (1 %); 2) a frequency sweep was measured at a constant strain of 1 % where the frequency was varied from 0.01 to 100 Hz; 3) a strain sweep was initiated with a strain varied from 0.1 % to 10000 % with a constant temperature (20 °C) and frequency (1 Hz). All measurements were conducted at least in triplicates.

5.3.5. Confocal laser scanning microscopy (CLSM)

CLSM was used to observe microstructures of dispersion and gel samples for both QPI and WPI. Samples were prepared in the similar way as for rheological measurements. Few drops of 1 % Fast Green (Sigma Aldrich, USA) were added in prepared samples and were vortex for 10 seconds at 20 °C. A sample was added into a cavity of the slide and then covered with a coverslip. To avoid any evaporation, nail polish was used to seal the edges of slide. An oven (Labserve, Australia) was used at 95 °C for 30 min to gel the samples. The samples were observed at a wavelength of 630 nm under a confocal laser scanning microscope (Leica TCS SP5, Leica Microsystems) attached with a 100× oil immersion objective lens. To process all the images, Image J software (version 1.51k, NIH, USA) was used.

5.3.6. Statistical analysis

All the measurements were conducted at least twice with triplicate samples and the data was represented as the mean \pm standard deviation. Analysis of variance (ANOVA) was conducted with MINITAB software (version 19.2020.1, PA, USA) using the Least Significant Difference (LSD) test at the significance level $P < 0.05$.

5.4. Result and discussion

5.4.1. Thermally induced gelation of QPI and WPI at pH 3, pH 5, and pH 7

The viscoelastic property of QPI or WPI dispersions at various concentrations was measured using small deformation rheological measurements. Fig. 5.1 represents the evolution of storage modulus (G'), loss modulus (G'') and temperature of QPI and WPI samples as a function of time. At each pH, as the concentration of the QPI and WPI increases, the G' and G'' of each sample also increases. During the temperature ramp and temperature holding stage, the protein molecules denature, and hydrophobic groups initially buried inside of protein molecules are exposed to form protein aggregates and networks (Mession et al., 2013; Wijayanti et al., 2014; Yang et al., 2022; Zhang et al., 2017). The gradual increase in the G' and G'' during the temperature decrease from 95 °C to 25 °C is due to the formation of covalent and non-covalent bonds such as hydrophobic interactions and hydrogen bonds at all three pH (Felix et al., 2021; H. Zhao et al., 2020).

For QPI samples at pH 7, as the temperature is increased, QPI start to denature and form aggregates and eventually the gel network. From Fig. 5.1A, it can be seen that all the samples displayed similar behaviour and both G' and G'' increased throughout entire heat treatment from 25 °C to 95 °C; maintaining 95 °C for 30 min and decreasing from 95 °C to 25 °C. Similar rise in G' were also reported by Langton et al. (2020) when heating faba bean protein isolate (15 wt%, 2% NaCl, pH 7) at 95 °C following a similar temperature profile. Chen et al. (2017) reported, when heating soy protein isolate (SPI) at 90 °C (50 mM NaCl, pH 6.4) at a concentration ranging from 0.5 wt% to 9.5 wt%, the G' increases during heating. The increase in protein concentration results in an increase in G' as the temperature increased during gelation process. The gelation temperature (T_{gel}) can be defined as the temperature at which the G' reached 1 Pa (Lucey & Singh, 1997). As the concentration of the QPI increased from 3 wt% to 10 wt%, the T_{gel} decreased from ~94.4 °C to ~55.9 °C, respectively (Fig 5.1D). Kaspchak, Oliveira, et al. (2017) also reported the decrease in gelation temperature from ~87.6 °C to ~77.8 °C as the concentration of the QPI increased from 10 wt% to 15 wt% at pH 7.

At pH 5, the increase in G' with the concentration can be seen in Fig. 5.1B. Similar results were also reported for soy proteins and pea proteins (concentration was increased from 3 wt% to 10 wt%, heated from 20 °C to 90 °C at pH 5.8) (Silva et al., 2019). The electrostatic repulsion decreases at pH 5 as it is close to the isoelectric point of QPI (~4.5) (Puppo & Añón, 1998). As

the QPI concentration increases, the gelation temperature decreases at pH 5. The increase in G' was observed by Renkema et al. (2002) for 12 wt% soy protein isolate at pH 5.2 when heated from 20 °C to 95 °C (0.5 M NaCl). It is expected that when the pH is close to isoelectric point, hydrophobic interaction plays important role in the formation of gels. Tanger et al. (2022) also reported that 80 %- 100 % hydrophobic interactions are responsible for pea protein gelation at pH 4.5 for 15 wt% pea protein isolate when heated from 25 °C to 95 °C and cooled down to 25 °C containing 0.3 M NaCl. Note that at pH 5, G' values of 10 wt% QPI and 7 wt% QPI, were higher than 1 Pa at time zero, thus the T_{gel} for these samples cannot be determined (Fig 1D). It could be due to the sol-gel transition occurred rapidly at higher concentrations of QPI and when the pH close to isoelectric point (~4.5) (Mäkinen et al., 2016). The T_{gel} decreased from ~68 °C to ~46 °C when the protein concentration is increased from 3 wt% to 5 wt%.

At pH 3, from Fig. 5.1C it can be seen that G' is increased as the QPI concentration increased from 3 wt% to 10 wt%. The higher G' at pH 3 when compared with pH 7 could be due to electrostatic interactions. The QPI solution becomes positively charged once it is below the isoelectric point of QPI (~4.5) (Kaspchak, Oliveira, et al., 2017), which promotes the formation of gel with higher G' as compared with QPI at pH 7 (Wang et al., 2019). Renkema et al. (2002) also found higher G' of 12 wt% soy protein isolate at pH 3.8 as compared with pH 5.2 and 7.6 at 95 °C in the presence of 0.2 M NaCl. In addition, as the QPI concentration increased from 3 wt% to 10 wt%, the T_{gel} decreased from ~47.8 °C to ~30 °C as shown in Fig. 5.1D. Similar results were also found by Kaspchak, Oliveira, et al. (2017): as QPI concentration increased from 10 wt% to 15 wt%, the T_{gel} decreased from 82.4°C to 75.4 °C at pH 3.5. At pH 3, T_{gel} occurred at lower temperatures than at pH 5 and pH 7; this implies that T_{gel} was also pH dependent (Fig. 5.1D).

For WPI samples, as the concentration of the dispersion increased, the G' and G'' also increased for pH 7, pH 5 and pH 3 samples as shown in Fig. 5.1E, F and G. The increase in G' with increasing concentrations was due to disulphide interchange reaction during the temperature ramp from 25 °C to 95 °C (Dunkerley & Zadow, 1984; Shimada & Cheftel, 1989; To et al., 1985). During the cooling from 95 °C to 25 °C, there is continuous protein network formation caused by decreasing mobility of whey proteins with decreasing temperature, which accelerates non-covalent bond formation between protein molecules (Ramos et al., 2012). Hydrogen bonds and van der Waals forces were responsible for gradual but steady increase in the G' during cooling from 95 °C to 25°C (de la Fuente et al., 2002; He et al., 2021). A sudden increase in G' can be seen at ~70 min and ~80 min for pH 7 and pH 3 respectively in Fig 5.1E and 1G. A

strong electrostatic repulsion between whey protein molecules could be expected at pH 7 and pH 3, leading to higher solubility and thus higher G' (Monahan et al., 1995). A higher gel strength of WPI found at alkaline pH (7-9) (Errington & Foegeding, 1998; Leksrisompong et al., 2012; Tang et al., 1995) and acidic pH (3-4) (Kinsella & Whitehead, 1989; Lorenzen & Schrader, 2006) was possibly due to formations of disulphide bonds. During heat induced aggregation of whey protein, partial unfolding of monomers and buried hydrophobic groups and thiol groups are exposed. This triggers thiol/disulphide exchange reaction between whey proteins, which has been reported in previous studies (Iametti et al., 1995; McSwiney et al., 1994; Sawyer, 1968; Watanabe & Klostermeyer, 1976).

Comparing with pH 3 and pH 7, G' of the gels formed at pH 5 were low. However, as the protein concentration was increased from 3 wt% to 10 wt% the G' increased. After sudden increase at ~60 min, a gradual increase in G' is observed as the temperature increases for pH 5 samples. A similar result was also observed by Puyol et al. (2001) when the protein concentration is increased from 2.5% w/v to 10% w/v (pH 6.7, 100 mM NaCl). At pH 5, the G' is the lowest for WPI. It could be due to that pH 5 is close to the isoelectric point (4.6) of WPI, resulting in low protein solubility (De Wit, 1989). According to Lorenzen and Schrader (2006), at pH 5 a small net charge and a small number of intermolecular bonds showing less electrostatic interaction between protein resulting in insufficient gel formation at a protein concentration of 11.25% WPI when heated at 75°C for 45 min. But they also claimed that differences in production process and composition of WPI may lead to a completely different result. At pH 4.5, loss of dispersibility can result in the formation of insoluble whey protein aggregates (10 wt% WPI, pH 4.5, 90 °C) (Cornacchia et al., 2014). Leksrisompong and Foegeding (2011) studied heat induced gelation of 7 wt% WPI (80 °C) at different heating rate from 0.2 °C/min to 20 °C/min. They found that at lower heating rate (2 °C/min), the sample at pH 4.5 shows lower G' as compared with samples at pH 3, pH 7 or pH 8, which could be due to the micro-phase separation observed at pH 4.5 (close to the isoelectric point of WPI). Therefore, the aggregates formed at pH 4.5 had more time to sediment at lower heating rate, resulting in a lower gel rigidity. This might be another reason for the lower G' of WPI found at pH 5, since the heating rate used in our study was slow (1 °C/ min). From Fig. 5.1H, as the WPI concentration increased from 3 wt% to 10 wt% at pH 7, pH 5 and pH 3, the T_{gel} decreased from ~86 °C to ~76 °C; ~93 °C to ~79 °C; and ~95 °C to ~85 °C, respectively. The decrease in T_{gel} with increase in protein concentration could be due to net charge density of protein is larger at lower protein concentration (Thomar & Nicolai, 2016).

The gel strength and gelation temperature of the quinoa protein isolate is different from whey protein isolate. The gelation of QPI and WPI showed different pH dependent behaviour. The highest G' of quinoa is observed at pH 5, however, the highest G' is found at pH 7 for WPI. This could be due to non-covalent bonds such as electrostatic interaction, hydrophobic bonds and hydrogen bonds are mainly responsible for gelation of QPI, while covalent interactions such as disulphide bonds played more critical roles in the formation of WPI gels. For example, at pH 7, the gelation of WPI gels could be mainly contributed to covalent disulphide bridges (Lorenzen & Schrader, 2006). However, at pH 5 that is near pI of WPI, gelation could be significantly reduced due to lower protein solubility and formation of large aggregates (Lorenzen & Schrader, 2006; Singh & Havea, 2003). At pH 3, it is suggested that the gelation of WPI is mainly governed by hydrophobic bonds (de la Fuente et al., 2002; Doi, 1993; Resch et al., 2005).

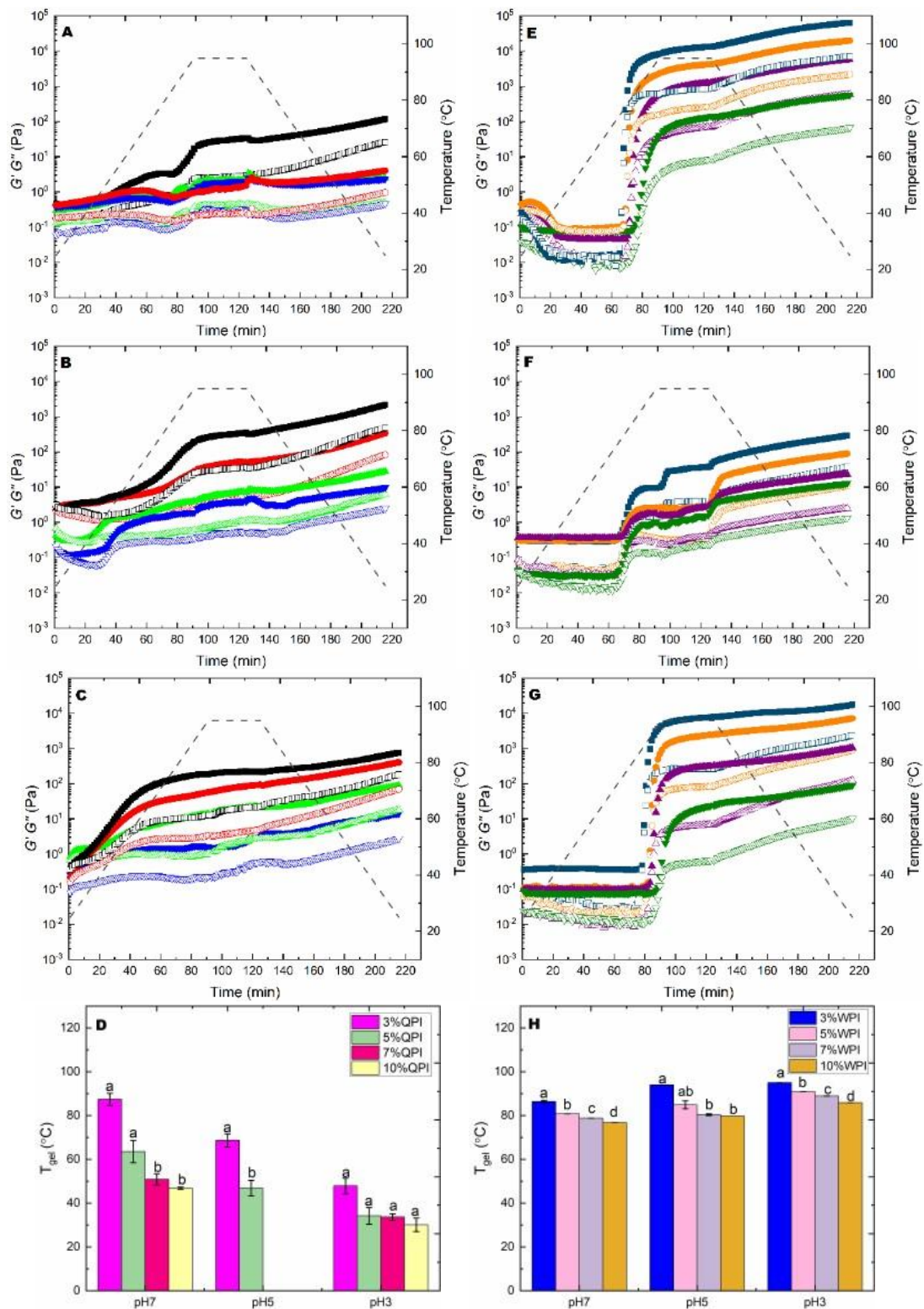


Fig 5.1: The evolution of G' (solid symbols) and G'' (open symbols) for QPI (A- pH 7; B- pH 5; C- pH 3) and WPI (E- pH 7; F- pH 5; G- pH 3) dispersion during heat-induced gelation in presence of NaCl (100 mM). D- T_{gel} of QPI; H- T_{gel} of WPI. QPI concentrations: 10 wt% (■), 7 wt% (●), 5 wt% (▲), 3 wt% (▼); WPI concentrations: 10 wt% (■), 7 wt% (●), 5 wt% (▲), 3 wt% (▼). Means that do not share a letter are significantly different.

5.4.2. Thermally induced gelation of QPI, and WPI after gelation at pH 7, pH 5 and pH 3.

The viscoelastic response of all the QPI and WPI gels as a function of frequency are shown in Fig. 5.2. In all the frequency sweep measurements, a constant strain of 1% was applied to ensure that the strain used was in the Linear Viscoelastic Region (LVER). G' is greater than G'' for all QPI and WPI samples over the entire frequency range, and both are modestly frequency dependant, indicating typical characteristics of weak gels (Sun & Arntfield, 2012; Yang et al., 2022). The complex modulus (G^*) at 1 Hz, which takes into account the contribution from both G' and G'' at this frequency, is plotted in Fig. 5.2D and 5.2H to allow for a better comparison of gel strength among different QPI and WPI gels, respectively. The gel strength is increased with increasing concentrations for both QPI and WPI. For QPI gels, the G^* increased from ~19 to ~750 Pa at pH 3; from ~8 to ~1793 Pa at pH 5, and from ~2 to ~127 Pa at pH 7 as the concentration is increased from 3 wt% to 10 wt%. For QPI gels (10 wt%), the G^* showed the highest value at pH 5 (~1793 Pa), followed by pH 3 (~750 Pa) and pH 7 (~127 Pa). The highest G^* of QPI (10 wt%) at pH 5 could be attributed to extensive protein aggregation as compared with other pHs. This is confirmed by the CLSM observations in Fig. 5.4 and 5.5.

Regarding WPI gels, G^* increased from ~94 to ~16096 Pa for pH 3; from ~12 to ~291 Pa for pH 5 and from ~511 to ~72557 Pa for pH 7 respectively, when the concentration is increased from 3 wt% to 10 wt%. For WPI gels (10 wt%), G^* has the highest value at pH 7 (~72557 Pa), followed by pH 3 (~16096 Pa), and pH 5 (~291 Pa). It can be observed that WPI shows higher G' at all pHs when compared with QPI. And the higher G' of whey protein may be due to higher extent of inter- or intra-molecular crosslinking by covalent and non-covalent bonds (Errington & Foegeding, 1998; Havea et al., 2009). On the other hand, it has been suggested that covalent interactions such as disulphide bond did not significantly contribute to the formation of quinoa protein gels and noncovalent interactions, such as hydrogen bonding or hydrophobic interactions, are primarily responsible for the gel network's strength (Ruiz, Xiao, et al., 2016; Yang et al., 2022). Similar results were reported for WPI when compared with rapeseed protein isolates at pH 3, pH 5, and pH 7 by Ainis et al. (2018).

Large deformation rheological properties of QPI and WPI gels were studied by strain sweep measurements and results are shown in Fig. 5.3. It can be observed that G' and G'' were independent of strain amplitude at small strains, indicating the presence of substantial linear

viscoelastic regions in QPI and WPI gels. This also confirmed that the 1% strain used in the temperature and frequency sweep measurements was within the linear viscoelastic region (LVER). Increasing in strain amplitude leads to a decrease in G' and G'' , suggesting strain thinning behaviour of the gels (Hamedi et al., 2022). The stress at the crossover point ($G' = G''$) is defined as breaking stress. The breaking stress of the QPI and WPI at different pH were plotted in Fig. 5.3D and H. The breaking stress is increased from ~1 to ~21 Pa for pH 3; from ~0.2 to ~27 Pa for pH 5 and from ~0.2 to ~1 Pa for pH 7 as the concentration of QPI is increased from 3 wt% to 10 wt%. The breaking stress of 10 wt% QPI is the highest at pH 5. In the case of WPI (3 wt% to 10 wt%), breaking stress increased from ~114 to 896 Pa for pH 3; from ~2.6 to 19 Pa for pH 5 and from ~510 to 15019 Pa for pH 7. The highest breaking stress for WPI was observed at 10 wt% pH 7. In general, breaking stress is increased as the protein concentration is increased. Similar results were also reported in Diedericks et al. (2021) for Bambara groundnut protein isolate and whey protein isolate (12 wt%, pH 3, pH 5 and pH 7, no salt). Furthermore, the change of breaking stress with pH at the same protein concentration is similar to that of G^* (1 Hz) (Fig. 5.2D and H), indicating large deformation rheological properties are consistent with small deformation rheological properties .

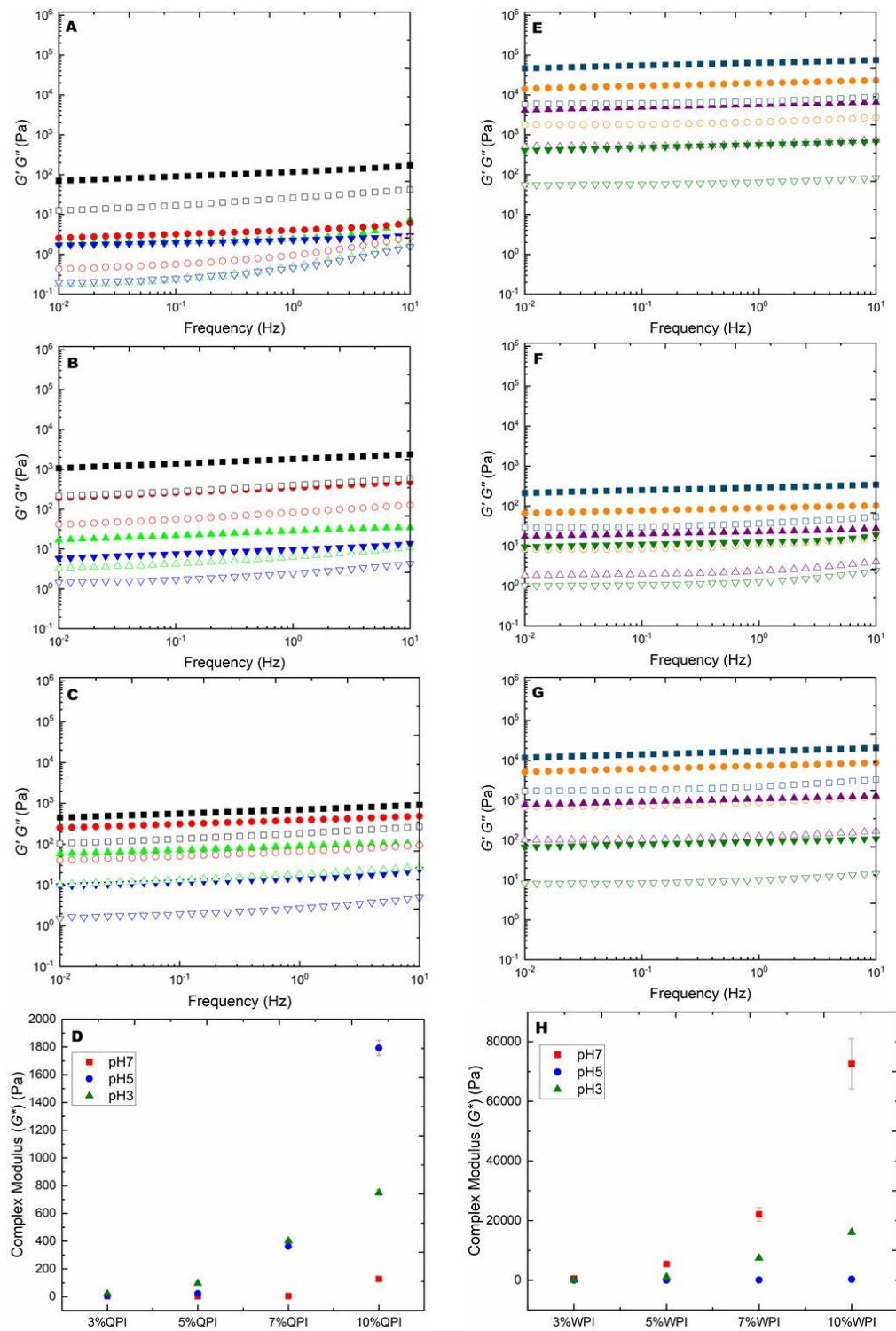


Fig 5.2: G' (solid symbols) and G'' (open symbols) as a function of frequency for QPI (A- pH 7; B- pH 5; C- pH 3) and WPI (E- pH 7; F- pH 5; G- pH 3) gels after heat-induced gelation in the presence of NaCl (100 mM). D- Complex modulus (G^* (1Hz)) of QPI and H- Complex Modulus (G^* (1Hz)) of WPI as a function of protein concentrations. QPI concentrations: 10 wt% (■), 7 wt% (●), 5 wt% (▲), 3 wt% (▼); WPI concentrations: 10 wt% (■), 7 wt% (●), 5 wt% (▲), 3 wt% (▼).

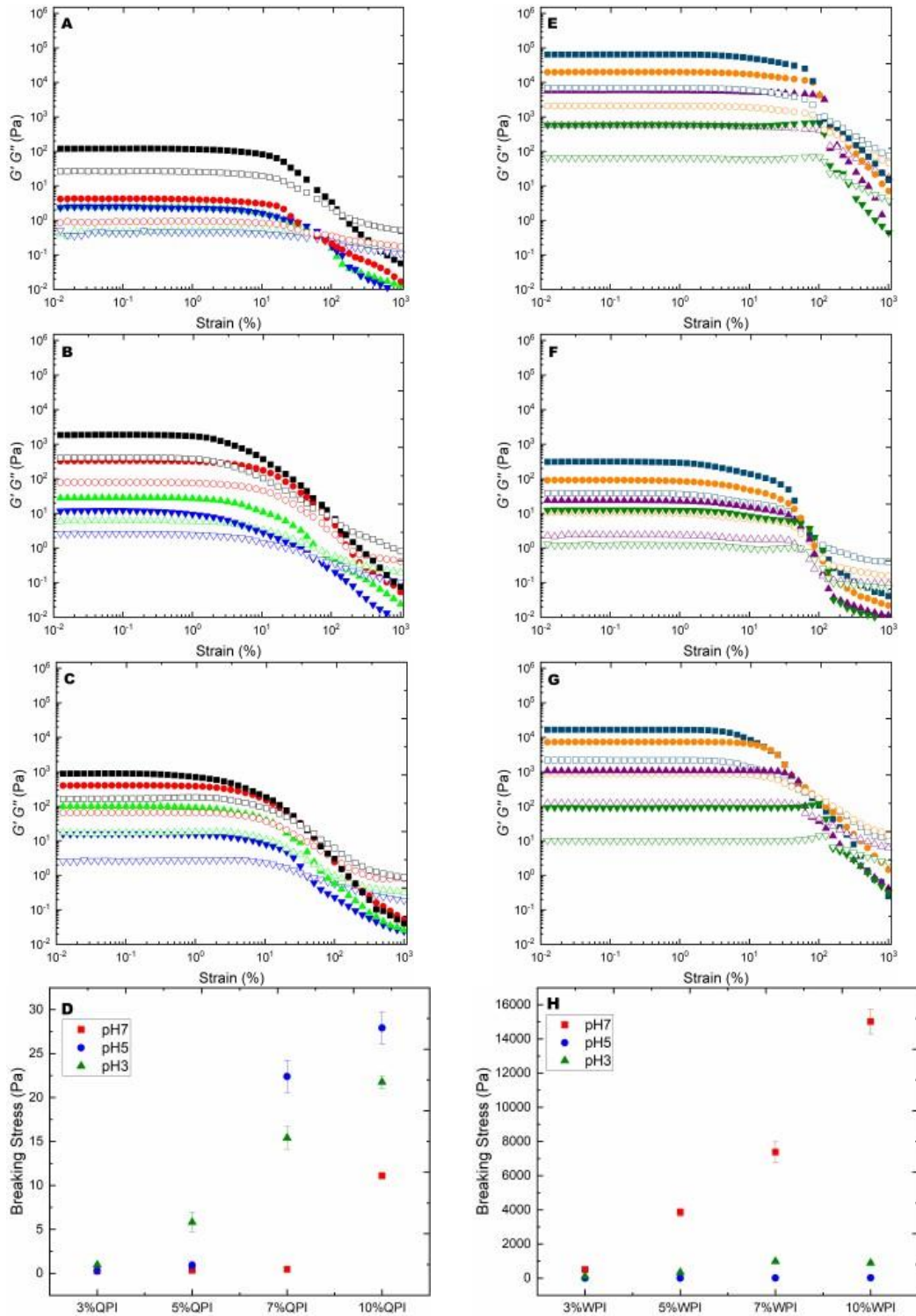


Fig 5.3: The dependence of G' (solid symbols) and G'' (open symbols) on strain amplitude for QPI (A- pH 7; B- pH 5; C- pH 3) and WPI (E- pH 7; F- pH 5; G- pH 3) dispersion during heat-induced gelation in the presence of NaCl (100 mM). D- Breaking Stress of QPI and H- Breaking Stress of WPI as a function of protein concentrations. QPI concentrations: 10 wt% (■), 7 wt% (●), 5 wt% (▲), 3 wt% (▼); WPI concentrations: 10 wt% (■), 7 wt% (●), 5 wt% (▲), 3 wt% (▼).

5.4.3. Microstructural characteristics of QPI and WPI gels as revealed by CLSM

The microstructural characteristics of QPI and WPI dispersions at pH 3, pH 5 and pH 7 before and after heat treatment were probed by CLSM and micrographs are shown Fig. 5.4 and Fig. 5.5, respectively. The pores between protein particles are black while the proteins stained by Fast Green are green. From Fig. 5.4, at pH 3, as the QPI concentration increases, the solution tends to become more homogenous along with some aggregates. At pH 5, QPI at higher concentrations have more aggregates than at lower concentration. For WPI, the microstructure at pH 7 and pH 3 of the solution was homogenous at all the concentrations although some small aggregates can be observed. At pH 5, less amount of protein is detected in CLSM for WPI as compared with pH 7 and pH 3.

Fig. 5.5 shows the microstructure of the samples after heat treatment. At pH 5 and pH 3, as the QPI concentration is increased the gel microstructure becomes denser. At pH 3 and pH 5, a network connected by aggregated protein with voids in between was observed (Fig. 5.5). These aggregates can be referred to building blocks that connect to each other and form space spanning network (Ainis et al., 2018). The increase in the space spanning network formed at pH 3 and pH 5 for QPI after heat-treatment is in agreement with rheological results. At higher concentration of QPI gel (10 wt%) large aggregates are formed at pH 5 due to low electrostatic interaction at pH close to isoelectric point (Luo et al., 2021; Puppo & Añón, 1998). The denser and more aggregated network formed at pH 5 agrees with higher gel strength as revealed by rheology. However, samples at pH 7 could not be determined due to failure of the CLSM equipment during the time of the experiment.

For WPI at pH 7 and pH 3, the microstructure of the gel was found to be homogenous and dense after heat treatment. According to Langton and Hermansson (1992), Krebs et al. (2007) and Nicolai and Durand (2013), homogenous and fine stranded network of WPI gels is formed when the pH is above or below isoelectric point. McCann et al. (2018) found out that 12 wt% WPI at pH 7 also formed homogenous protein network when heated at 95°C for 60 min. Similar observations were also obtained for 6 wt% and 18 wt% whey protein gels (Comfort & Howell, 2002; Roesch & Corredig, 2005). Heat-treated WPI gels at pH 3 showed ordered structure and filaments of the protein with some small pores (Fig. 5) (Brodkorb et al., 2016). Similar results were observed of filamentous structure at pH 2 for β -lactoglobulin (10 wt%) (Jung et al., 2008). At pH 5, WPI gels were not homogenous and particularly at higher concentration (10 wt%),

spherical aggregates were formed. The formation of spherical aggregates at pH 5 for WPI was found by TEM for 10g/L WPI (85°C for 15 min at pH 5) (Schmitt et al., 2007).

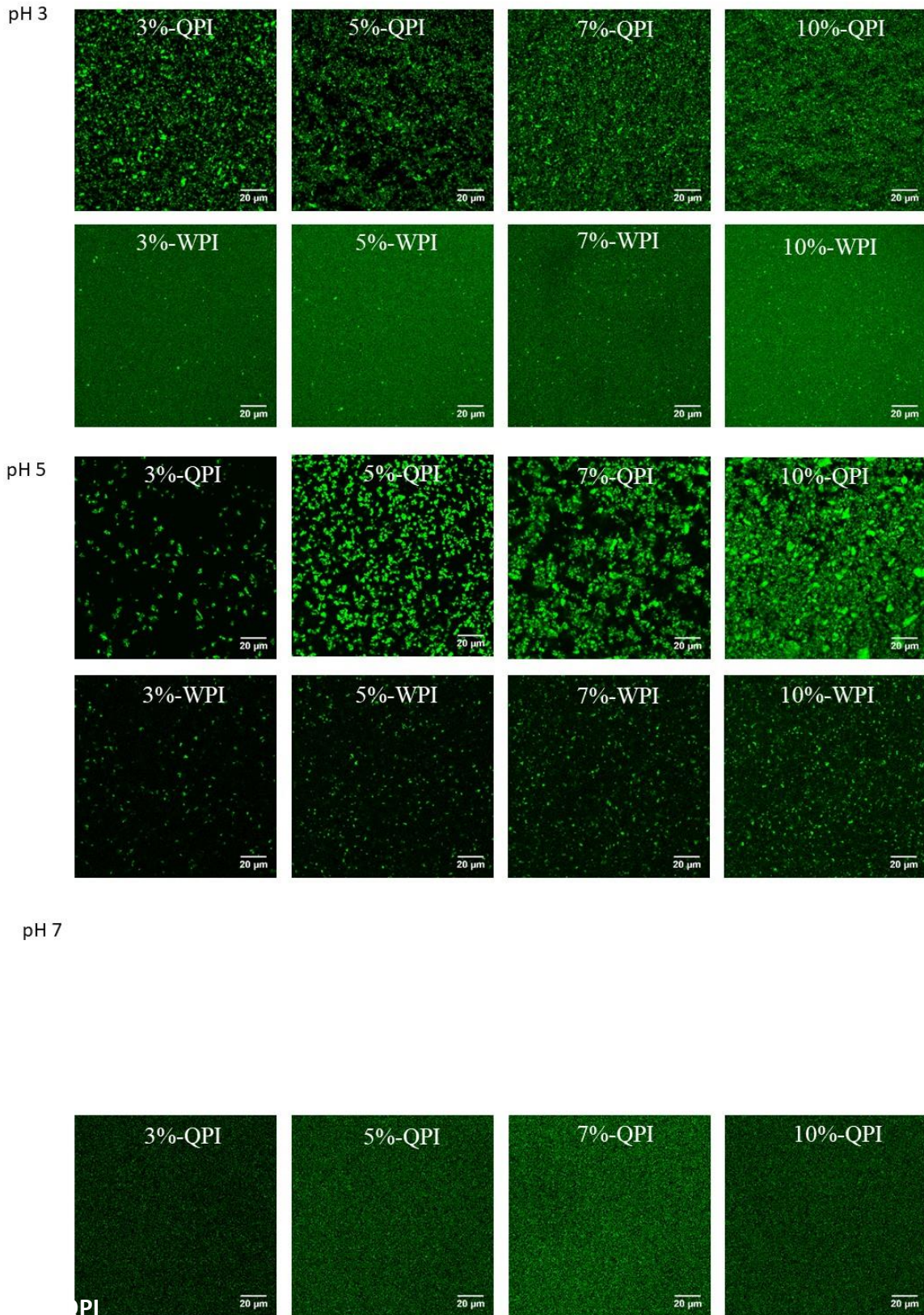


Fig 5.4: CLSM images of QPI, and WPI at pH 7, pH 5 and pH 3 before heat treatment (100x magnification).

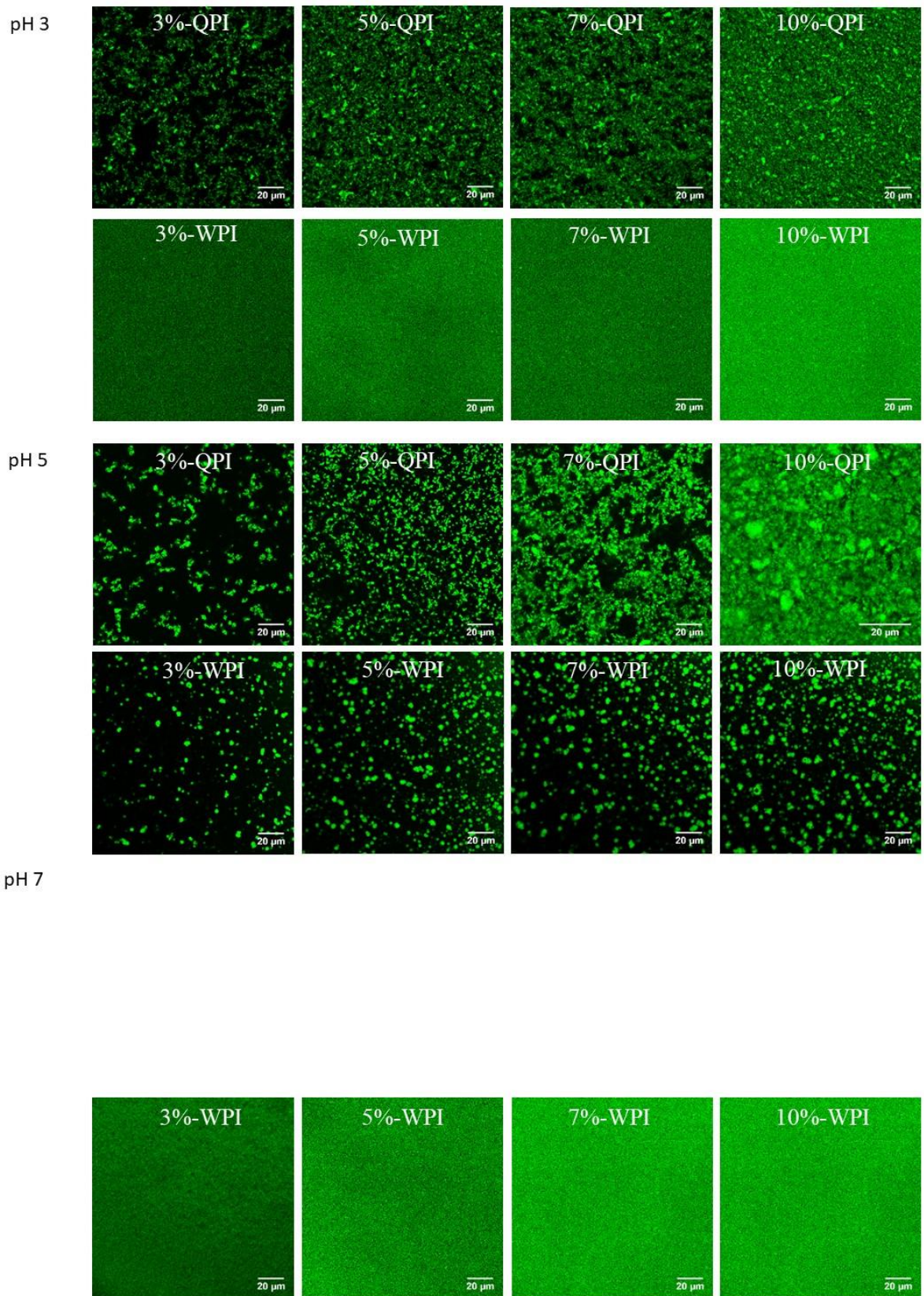


Fig 5.5: CLSM images of QPI, and WPI at pH 7, pH 5 and pH 3 after heat treatment (100x magnification).

5.5. Conclusion and future work

In this chapter, the effect of protein concentrations and pH on the thermal gelation of QPI and WPI was investigated. The gel strength and microstructure of the quinoa protein gel and whey protein gel were different at various pH and also dependent on the protein concentration. For QPI, highest G' was found at pH 5 followed by pH 3 and pH 7. But for WPI, the highest G' was found at pH 7 followed by pH 3 and pH 5. At all pHs, WPI showed higher G' than QPI. For both QPI and WPI irrespective of pH, higher protein concentrations led to higher G' . The thiol disulphide interchange reaction may be responsible for the higher G' in WPI gels, however hydrophobic bonds and electrostatic interaction could play more important roles in the gelation of quinoa protein isolate. Furthermore, the higher protein concentration accelerates gel formation, as evidenced by the lower gelation temperature (T_{gel}) of QPI and WPI at all the pHs. For both QPI and WPI gels, the G^* (1 Hz) and breaking stress increased as the protein concentration increased. Nonetheless, further studies are necessary to understand the thermal denaturation temperature, enthalpy, and peak temperature of proteins using DSC. The enthalpy change in the protein can be used to indicate protein interactions such as hydrogen bonds, hydrophobic interactions, and van der Waals forces. In addition, intermolecular forces responsible for gelation of quinoa protein and whey protein at different pH can be determined by measuring solubilities of gels in various denaturants solutions such as urea, SDS and 2-mercaptoethanol. In terms of microstructural characterisation, other microscopic techniques such as TEM and SEM could be employed to further probe the microstructures of QPI and WPI gels at a higher resolution. The finding from this study shows that the gel strength and microstructural characteristics of QPI and WPI gels can be tailored by adjusting pH and protein concentrations. Further studies can be conducted to fabricate QPI-WPI hybrid gels that may have potential applications in food products such as sausage and yoghurt.

6. Conclusions and future work recommendation

6.1. Conclusions

This project sets out to study the heat-induced gelation properties of quinoa protein isolates with addition of monovalent salt (NaCl) and divalent salt (CaCl₂); different types of polysaccharides (guar gum, locust bean gum, xanthan gum) with different concentration; and to investigate the differences of gelation behaviour between whey protein isolate and quinoa protein isolate at various pHs (pH 3, pH 5 and pH 7). The findings of the project are concluded below.

The heat induced gelation of QPI is significantly affected by the addition of various amounts of NaCl and CaCl₂. It was shown by small- and large-deformation rheology that salt addition enhances a sol-gel transition, with the gelation taking place at lower temperatures with increasing salt concentration. The nanostructure of QPI was not modified after heat treatment, according to SAXS and SANS findings. The addition of 200 mM NaCl and CaCl₂ (20 and 50 mM) resulted in a significant decrease in the scattering intensity, which could be attributed to the protein aggregation and microphase separation. The difference between the SAXS and SANS profiles revealed that the presence of protein inhomogeneities in QPI gels. CLSM revealed that all QPI gels were composed of a space-spanning fractal-like network. Finally, this work showed that the gelation behaviour, gel structure and gel strength of the QPI can be tuned by the addition of NaCl and CaCl₂ at neutral pH.

The incorporation of polysaccharides (guar gum, locust bean gum and xanthan gum) changed the gelation kinetics of QPI gels and led to an increased QPI gel strength, as demonstrated by increases in G' and G'' during and after gelation. Due to varying degrees of demixing and/or interactions between the QPI and polysaccharides, the gel strength and microstructural characteristics are significantly dependent on the polysaccharide utilised. It was found that XG showed highest gel strength followed by LBG and GG at the same gum concentration. The water holding capacity, breaking stress, gel strength and complex modulus progressively increased with the increasing concentration of polysaccharides. As revealed by CLSM, significant microphase separations occurred in the QPI-XG gels. Microstructure of the gels with addition of GG and LBG was also observed to be heterogeneous however, LBG showed a more predominant micro-phase separation. This could be explained by the fact that LBG has

strong self-association capabilities as LBG (~25 % branching) has less degree of branching than GG (~ 50% branching).

QPI and WPI showed different gelation behaviour and gel strength at the different protein concentrations (3 wt%, 5 wt%, 7 wt%, 10 wt%) and different pH (pH 3, pH 5, pH 7). At all the concentrations and pHs, WPI had a stronger gel strength than QPI. The higher G' in WPI gels can be attributed to disulphide bridges and hydrophobic interactions. The highest G' for WPI was observed at pH 7 followed by pH 3 and pH 5. Higher gel strength at pH 7 for WPI was mainly due to covalent disulphide bridges. In the case of QPI gels, a highest gel strength was obtained at pH 5 followed by pH 3 and pH 7 due to significant protein aggregation close to the isoelectric point of QPI (pI ~4.5). This study revealed that QPI and WPI showed different gelation behaviour despite both can be considered as globular proteins.

6.2.Future work recommendation

- Based on the findings of this study, some future directions are provided below. pH plays an important role in determination gelation behaviour of QPI. We studied gelation of QPI containing monovalent and divalent salt at neutral pH. However, it would be of great interest to study the gelation of behaviour of QPI with addition of NaCl and CaCl₂ at different pH values such as pH 3, pH 5 (near pI of QPI) and at an alkaline pH (pH 9)
- In this study, the heat treatment is used to induce the formation of QPI gels. Future work can be conducted to investigate the impact of salt addition and pH on the QPI gels induced by other methods such as high hydrostatic pressure.
- In this project additions of polysaccharides i.e., guar gum, locust bean gum and xanthan gum on the gelation of QPI was studied. It would be interesting to use other commonly industry used polysaccharides such as starch, kappa-carrageenan, iota-carrageenan, and gelatine to find out the compatibility of QPI with these polysaccharides. This could be useful for the development of food products containing QPI gels with desired texture and structures.
- Future work can be conducted to reveal molecular interactions between QPI and polysaccharides using DSC and FTIR.

- Future work can be carried out on creating hybrid gels by blending QPI and WPI. The effect of salt additions and pH on the gelation behaviour, gel strength, and microstructures of hybrid gels can also be studied.
- Molecular forces that involved in heat induced QPI gel formations including non-covalent interactions (e.g., hydrophobic interactions and hydrogen bond) and covalent interactions (e.g., disulfide bond) can be better quantified by measuring protein solubilities or rheological properties changes in the presence of urea, thiourea, SDS, or 2-Mercaptoethanol.

7. References

- Abugoch James, L. E. (2009). Quinoa (*Chenopodium quinoa* Willd.): Composition, Chemistry, Nutritional, and Functional Properties. In *Advances in food and nutrition research* (Vol. 58, pp. 1-31). Academic Press.
- Abugoch, L. (2009). Quinoa (*Chenopodium quinoa* WILLD.): Composition. *Chemistry*.
- Abugoch, L., Castro, E., Tapia, C., Añón, M. C., Gajardo, P., & Villarroel, A. (2009). Stability of quinoa flour proteins (*Chenopodium quinoa* Willd.) during storage. *International Journal of Food Science & Technology*, *44*(10), 2013-2020.
- Abugoch, L. E., Romero, N., Tapia, C. A., Silva, J., & Rivera, M. (2008). Study of some physicochemical and functional properties of quinoa (*Chenopodium quinoa* Willd) protein isolates. *Journal of Agricultural and Food Chemistry*, *56*(12), 4745-4750.
- Agoub, A. A., Smith, A. M., Giannouli, P., Richardson, R. K., & Morris, E. R. (2007). “Melt-in-the-mouth” gels from mixtures of xanthan and konjac glucomannan under acidic conditions: A rheological and calorimetric study of the mechanism of synergistic gelation. *Carbohydrate polymers*, *69*(4), 713-724.
- Aguilera, J. (1992). Generation of engineered structures in gels. *Physical chemistry of foods*, 387-421.
- Ahamed, N. T., Singhal, R. S., Kulkarni, P. R., & Pal, M. (1996). Physicochemical and functional properties of *Chenopodium quinoa* starch. *Carbohydrate polymers*, *31*(1-2), 99-103.
- Ainis, W. N., Ersch, C., & Ipsen, R. (2018). Partial replacement of whey proteins by rapeseed proteins in heat-induced gelled systems: Effect of pH. *Food Hydrocolloids*, *77*, 397-406.
- Akharume, F. U., Aluko, R. E., & Adedeji, A. A. (2021). Modification of plant proteins for improved functionality: A review. *Comprehensive Reviews in Food Science and Food Safety*, *20*(1), 198-224.
- Ako, K., Nicolai, T., Durand, D., & Brotons, G. (2009). Micro-phase separation explains the abrupt structural change of denatured globular protein gels on varying the ionic strength or the pH. *Soft Matter*, *5*(20), 4033-4041.
- Alrosan, M., Tan, T.-C., Mat Easa, A., Gammoh, S., & Alu'datt, M. H. (2022). Recent updates on lentil and quinoa protein-based dairy protein alternatives: Nutrition, technologies, and challenges. *Food chemistry*, *383*, 132386.

- Alting, A. C. (2003). *Cold gelation of globular proteins* S.n.]. [S.l.].
- Alting, A. C., Hamer, R. J., de Kruif, C. G., & Visschers, R. W. (2003). Cold-Set Globular Protein Gels: Interactions, Structure and Rheology as a Function of Protein Concentration. *Journal of Agricultural and Food Chemistry*, 51(10), 3150-3156.
- Ando, H., Chen, Y.-c., Tang, H., Shimizu, M., Watanabe, K., & Mitsunaga, T. (2002). Food components in fractions of quinoa seed. *Food Science and Technology Research*, 8(1), 80-84.
- Anklam, E. (2005). H.-D. Belitz, W. Grosch, P. Schieberle: Food Chemistry.
- Anon. (2007). Reference Manual for US Whey Products. *US Dairy Export Council, Arlington, VA*.
- Auty, M. (2013). Confocal microscopy: principles and applications to food microstructures. In *Food microstructures* (pp. 96-P98). Elsevier.
- Avanza, M., Puppo, M., & Añón, M. (2005). Rheological characterization of amaranth protein gels. *Food Hydrocolloids*, 19(5), 889-898.
- Bağdatlı, A. (2018). The Influence Of Quinoa (*Chenopodium Quinoa* Willd.) Flour On The Physicochemical, Textural and Sensorial Properties Of Beef Meatball. *Italian Journal of Food Science*, 30(2).
- Balandrán-Quintana, R. R., Mendoza-Wilson, A. M., Ramos-Clamont Montfort, G., & Huerta-Ocampo, J. Á. (2019). Plant based Protein. In C. M. Galanakis (Ed.), *Proteins: Sustainable Source, Processing and Applications* (pp. 97-130). Academic Press.
- Bale, H. D., & Schmidt, P. W. (1984). Small-angle X-ray-scattering investigation of submicroscopic porosity with fractal properties. *Physical Review Letters*, 53(6), 596.
- Bamdad, F., Song, Y., & Chen, L. (2012). Hydrogel particles and other novel protein-based methods for food ingredient and nutraceutical delivery systems. In *Encapsulation technologies and delivery systems for food ingredients and nutraceuticals* (pp. 412-450). Elsevier.
- Banc, A., Charbonneau, C., Dahesh, M., Appavou, M.-S., Fu, Z., Morel, M.-H., & Ramos, L. (2016). Small angle neutron scattering contrast variation reveals heterogeneities of interactions in protein gels. *Soft Matter*, 12(24), 5340-5352.
- Bansal, N., & Bhandari, B. (2016). Functional Milk Proteins: Production and Utilization—Whey-Based Ingredients. In P. L. H. McSweeney & J. A. O'Mahony (Eds.), *Advanced Dairy Chemistry: Volume 1B: Proteins: Applied Aspects* (pp. 67-98). Springer New York.

- Barak, S., & Mudgil, D. (2014). Locust bean gum: Processing, properties and food applications—A review. *International Journal of Biological Macromolecules*, 66, 74-80.
- Barba de la Rosa, A. P., Gueguen, J., Paredes-Lopez, O., & Viroben, G. (1992). Fractionation procedures, electrophoretic characterization, and amino acid composition of amaranth seed proteins. *Journal of Agricultural and Food Chemistry*, 40(6), 931-936.
- Barbut, S. (1995). Effects of calcium level on the structure of pre-heated whey protein isolate gels. *LWT-Food Science and Technology*, 28(6), 598-603.
- Barbut, S., & Foegeding, E. (1993). Ca²⁺-induced gelation of pre-heated whey protein isolate. *Journal of Food Science*, 58(4), 867-871.
- Beaucage, G. (1995). Approximations leading to a unified exponential/power-law approach to small-angle scattering. *Journal of Applied Crystallography*, 28(6), 717-728.
- Beaucage, G., & Schaefer, D. W. (1994). Structural studies of complex systems using small-angle scattering: a unified Guinier/power-law approach. *Journal of non-crystalline solids*, 172, 797-805.
- BeMiller, J. N., & Whistler, R. L. (2012). *Industrial gums: polysaccharides and their derivatives*. Academic Press.
- Bercea, M., & Morariu, S. (2020). Real-time monitoring the order-disorder conformational transition of xanthan gum. *Journal of Molecular Liquids*, 309, 113168.
- Bernstein, F. C., Koetzle, T. F., Williams, G. J., Meyer Jr, E. F., Brice, M. D., Rodgers, J. R., Kennard, O., Shimanouchi, T., & Tasumi, M. (1977). The Protein Data Bank: a computer-based archival file for macromolecular structures. *Journal of molecular biology*, 112(3), 535-542.
- Bertrand, M.-E., & Turgeon, S. L. (2007). Improved gelling properties of whey protein isolate by addition of xanthan gum. *Food Hydrocolloids*, 21(2), 159-166.
- Bhargava, A., Shukla, S., & Ohri, D. (2006). Chenopodium quinoa—an Indian perspective. *Industrial crops and products*, 23(1), 73-87.
- Bi, C.-h., Li, D., Wang, L.-j., & Adhikari, B. (2013). Viscoelastic properties and fractal analysis of acid-induced SPI gels at different ionic strength. *Carbohydrate polymers*, 92(1), 98-105.
- Bohrer, B. M. (2019). An investigation of the formulation and nutritional composition of modern meat analogue products. *Food Science and Human Wellness*, 8(4), 320-329.

- Brinegar, C., & Goundan, S. (1993). Isolation and characterization of chenopodin, the 11S seed storage protein of quinoa (*Chenopodium quinoa*). *Journal of Agricultural and Food Chemistry*, *41*(2), 182-185.
- Brito-Oliveira, T. C., Bispo, M., Moraes, I. C., Campanella, O. H., & Pinho, S. C. (2017). Stability of curcumin encapsulated in solid lipid microparticles incorporated in cold-set emulsion filled gels of soy protein isolate and xanthan gum. *Food Research International*, *102*, 759-767.
- Brito-Oliveira, T. C., Cavini, A. C. M., Ferreira, L. S., Moraes, I. C., & Pinho, S. C. (2020). Microstructural and rheological characterization of NaCl-induced gels of soy protein isolate and the effects of incorporating different galactomannans. *Food Structure*, *26*, 100158.
- Brodkorb, A., Croguennec, T., Bouhallab, S., & Kehoe, J. J. (2016). Heat-induced denaturation, aggregation and gelation of whey proteins. In *Advanced dairy chemistry* (pp. 155-178). Springer.
- Brown, J. R. (1977). Serum albumin: amino acid sequence. In *Albumin: Structure, Function and Uses* (pp. 27-52b). Elsevier.
- Bruin, A. d. (1964a). Investigation of the food value of quinoa and canihua seed. *Journal of Food Science*, *29*(6), 872-876.
- Bruin, A. d. (1964b). Investigation of the food value of quinoa and cañihua seed. *Journal of Food Science*, *29*(6), 872-876.
- Bryant, C., & McClements, D. (2000a). Influence of NaCl and CaCl₂ on cold-set gelation of heat-denatured whey protein. *Journal of Food Science*, *65*(5), 801-804.
- Bryant, C., & McClements, D. (2000b). Influence of xanthan gum on physical characteristics of heat-denatured whey protein solutions and gels. *Food Hydrocolloids*, *14*(4), 383-390.
- Bryant, C. M., & McClements, D. J. (1998). Molecular basis of protein functionality with special consideration of cold-set gels derived from heat-denatured whey. *Trends in Food Science & Technology*, *9*(4), 143-151.
- Bui, B., Saasen, A., Maxey, J., Ozbayoglu, M. E., Miska, S. Z., Yu, M., & Takach, N. E. (2012). Viscoelastic properties of oil-based drilling fluids. *Annual Transactions of the Nordic Rheology Society*, *20*, 33-47.
- Bulaj, G. (2005). Formation of disulfide bonds in proteins and peptides. *Biotechnology Advances*, *23*(1), 87-92.

- Burgos-Díaz, C., Rubilar, M., Morales, E., Medina, C., Acevedo, F., Marqués, A. M., & Shene, C. (2016). Naturally occurring protein–polysaccharide complexes from linseed (*Linum usitatissimum*) as bioemulsifiers. *European Journal of Lipid Science and Technology*, *118*(2), 165-174.
- Burlingame, B., Charrondiere, U. R., Dernini, S., Stadlmayr, B., & Mondovì, S. (2012). Food biodiversity and sustainable diets: Implications of applications for food production and processing. In *Green technologies in food production and processing* (pp. 643-657). Springer.
- Callisaya, A., Carlos, J., Alvarado, K., & Antonio, J. (2009). Aislados Proteínicos de granos altoandinos Chenopodiaceas; quinoa “*Chenopodium Quinoa*”-Cañahua “*Chenopodium Pallidicaule*” por Precipitación Isoeléctrica. *Revista Boliviana de Química*, *26*(1), 12-20.
- Campbell, L., Rempel, C. B., & Wanasundara, J. P. (2016). Canola/rapeseed protein: Future opportunities and directions—Workshop proceedings of IRC 2015.
- Canabady-Rochelle, L.-S., Sanchez, C., Mellema, M., & Banon, S. (2009). Study of Calcium–Soy protein interactions by isothermal titration calorimetry and pH cycle. *Journal of Agricultural and Food Chemistry*, *57*(13), 5939-5947.
- Canette, A., & Briandet, R. (2014). MICROSCOPY | Confocal Laser Scanning Microscopy. In *Encyclopedia of Food Microbiology* (pp. np). Elsevier.
- Carmen, M. (1984). Acclimatization of quinoa (*Chenopodium quinoa* Willd.) and canihua (*Chenopodium pallidicaule* Aellen) to Finland. *Annales Agriculturae Fenniae*,
- Chen, D., Kuzmenko, I., Ilavsky, J., Pinho, L., & Campanella, O. (2022). Structural evolution during gelation of pea and whey proteins envisaged by time-resolved ultra-small-angle x-ray scattering (USAXS). *Food Hydrocolloids*, *126*, 107449.
- Chen, D., Zhu, X., Ilavsky, J., Whitmer, T., Hatzakis, E., Jones, O. G., & Campanella, O. H. (2021). Polyphenols Weaken Pea Protein Gel by Formation of Large Aggregates with Diminished Noncovalent Interactions. *Biomacromolecules*, *22*(2), 1001-1014.
- Chen, J., & Dickinson, E. (2000). On the temperature reversibility of the viscoelasticity of acid-induced sodium caseinate emulsion gels. *International Dairy Journal*, *10*(8), 541-549.
- Chen, N., Zhao, M., Chassenieux, C., & Nicolai, T. (2016). Thermal aggregation and gelation of soy globulin at neutral pH. *Food Hydrocolloids*, *61*, 740-746.
- Chen, N., Zhao, M., Chassenieux, C., & Nicolai, T. (2017). The effect of adding NaCl on thermal aggregation and gelation of soy protein isolate. *Food Hydrocolloids*, *70*, 88-95.

- Cheng, J., Xie, S., Yin, Y., Feng, X., Wang, S., Guo, M., & Ni, C. (2017). Physiochemical, texture properties, and the microstructure of set yogurt using whey protein–sodium tripolyphosphate aggregates as thickening agents. *Journal of the Science of Food and Agriculture*, 97(9), 2819-2825.
- Chodankar, S., Aswal, V., Kohlbrecher, J., Vavrin, R., & Wagh, A. (2008). Structural evolution during protein denaturation as induced by different methods. *Physical Review E*, 77(3), 031901.
- Chu, B., & Hsiao, B. S. (2001). Small-Angle X-ray Scattering of Polymers. *Chemical reviews*, 101(6), 1727-1762.
- Chudzikowski, R. (1971). Guar gum and its applications. *J Soc Cosmet Chem*, 22(1), 43.
- Chun, J.-Y., Hong, G.-P., Surassmo, S., Weiss, J., Min, S.-G., & Choi, M.-J. (2014). Study of the phase separation behaviour of native or preheated WPI with polysaccharides. *Polymer*, 55(16), 4379-4384.
- Clark, A. (1992). Gels and gelling. *Physical chemistry of foods*, 7, 263-305.
- Clark, A., Kavanagh, G., & Ross-Murphy, S. (2001). Globular protein gelation—theory and experiment. *Food Hydrocolloids*, 15(4-6), 383-400.
- Comai, S., Bertazzo, A., Costa, C. V., & Allegri, G. (2011). Quinoa: Protein and nonprotein tryptophan in comparison with other cereal and legume flours and bread. In *Flour and Breads and their Fortification in Health and Disease Prevention* (pp. 113-125). Elsevier.
- Comfort, S., & Howell, N. K. (2002). Gelation properties of soya and whey protein isolate mixtures. *Food Hydrocolloids*, 16(6), 661-672.
- Cornacchia, L., Forquenot de la Fortelle, C., & Venema, P. (2014). Heat-Induced Aggregation of Whey Proteins in Aqueous Solutions below Their Isoelectric Point. *Journal of Agricultural and Food Chemistry*, 62(3), 733-741.
- Cortez-Trejo, M. C., Gaytán-Martínez, M., Reyes-Vega, M. L., & Mendoza, S. (2021). Protein-gum-based gels: Effect of gum addition on microstructure, rheological properties, and water retention capacity. *Trends in Food Science & Technology*, 116, 303-317.
- Costanzo, S., Banc, A., Louhichi, A., Chauveau, E., Wu, B., Morel, M.-H., & Ramos, L. (2020). Tailoring the viscoelasticity of polymer gels of gluten proteins through solvent quality. *Macromolecules*, 53(21), 9470-9479.
- Creighton, T. E. (1997). Protein folding coupled to disulphide bond formation. *Biological Chemistry-Hoppe Seyler*, 378(8), 731-744.

- Dakhili, S., Abdolalizadeh, L., Hosseini, S. M., Shojaee-Aliabadi, S., & Mirmoghtadaie, L. (2019). Quinoa protein: Composition, structure and functional properties. *Food chemistry*, 299, 125161.
- Damodaran, S. (1996). Amino acids, peptides, and proteins. *Food Science and Technology- New York- Marcel Dekker*, 321-430.
- Damodaran, S., Parkin, K. L., & Fennema, O. R. (2007). *Fennema's food chemistry*. CRC press.
- Dapčević-Hadnađev, T., Hadnađev, M., Lazaridou, A., Moschakis, T., & Biliaderis, C. G. (2018). Hempseed meal protein isolates prepared by different isolation techniques. Part II. gelation properties at different ionic strengths. *Food Hydrocolloids*, 81, 481-489.
- Day, L., Cakebread, J. A., & Loveday, S. M. (2021). Food proteins from animals and plants: Differences in the nutritional and functional properties. *Trends in Food Science & Technology*.
- De Kruif, C., & Tuinier, R. (2001). Polysaccharide protein interactions. *Food Hydrocolloids*, 15(4-6), 555-563.
- de la Fuente, M. A., Singh, H., & Hemar, Y. (2002). Recent advances in the characterisation of heat-induced aggregates and intermediates of whey proteins. *Trends in Food Science & Technology*, 13(8), 262-274.
- De La Vega, G. (2006). *The Royal Commentaries of the Incas and General History of Peru, Abridged*. Hackett Publishing.
- de Vries, J. (2004). Hydrocolloid gelling agents and their applications. In *Gums and Stabilisers for the Food Industry 12* (pp. 23-31).
- De Wit, J. (1989). Functional properties of whey proteins. *Developments in dairy chemistry. 4. Functional milk proteins.*, 285-321.
- Del Castillo, C., Mahy, G., & Winkel, T. (2008). La quinoa en Bolivie: une culture ancestrale devenue culture de rente" bio-équitable". *BASE*.
- Deželak, M., Zarnkow, M., Becker, T., & Košir, I. J. (2014). Processing of bottom-fermented gluten-free beer-like beverages based on buckwheat and quinoa malt with chemical and sensory characterization. *Journal of the Institute of Brewing*, 120(4), 360-370.
- Diedericks, C. F., Stolten, V., Jideani, V. A., Venema, P., & van der Linden, E. (2021). Effect of pH and mixing ratios on the synergistic enhancement of Bambara groundnut-whey protein gels. *Food Hydrocolloids*, 117, 106702.
- Dijkink, B., Speranza, L., Paltsidis, D., & Vereijken, J. (2007). Air dispersion of starch–protein mixtures: A predictive tool for air classification performance. *Powder technology*, 172(2), 113-119.

- Dini, A., Rastrelli, L., Saturnino, P., & Schettino, O. (1992). A compositional study of *Chenopodium quinoa* seeds. *Food/Nahrung*, *36*(4), 400-404.
- Doi, E. (1993). Gels and gelling of globular proteins. *Trends in Food Science & Technology*, *4*(1), 1-5.
- Dong, X. Y., Guo, L. L., Wei, F., Li, J. F., Jiang, M. L., Li, G. M., Zhao, Y. D., & Chen, H. (2011). Some characteristics and functional properties of rapeseed protein prepared by ultrasonication, ultrafiltration and isoelectric precipitation. *Journal of the Science of Food and Agriculture*, *91*(8), 1488-1498.
- Doublier, J.-L., Garnier, C., Renard, D., & Sanchez, C. (2000). Protein–polysaccharide interactions. *Current Opinion in Colloid & Interface Science*, *5*(3-4), 202-214.
- Drake, M. A., Chen, X. Q., Tamarapu, S., & Leenanon, B. (2000). Soy Protein Fortification Affects Sensory, Chemical, and Microbiological Properties of Dairy Yogurts. *Journal of Food Science*, *65*(7), 1244-1247.
- Ducel, V., Saulnier, P., Richard, J., & Boury, F. (2005). Plant protein–polysaccharide interactions in solutions: application of soft particle analysis and light scattering measurements. *Colloids and Surfaces B: Biointerfaces*, *41*(2-3), 95-102.
- Dunkerley, J., & Zadow, J. (1984). The effect of calcium and cysteine hydrochloride on the firmness of heat coagula formed from cheddar whey protein concentrates. *Australian Journal of Dairy Technology*, *39*(1), 44.
- Dürrenberger, M. B., Handschin, S., Conde-Petit, B., & Escher, F. (2001). Visualization of food structure by confocal laser scanning microscopy (CLSM). *LWT-Food Science and Technology*, *34*(1), 11-17.
- Eleya, M. O., Ko, S., & Gunasekaran, S. (2004). Scaling and fractal analysis of viscoelastic properties of heat-induced protein gels. *Food Hydrocolloids*, *18*(2), 315-323.
- Elsohaimy, S., Refaay, T., & Zaytoun, M. (2015). Physicochemical and functional properties of quinoa protein isolate. *Annals of Agricultural Sciences*, *60*(2), 297-305.
- Erik van der, L., & Foegeding, E. A. (2009). Gelation: Principles, Models and Applications to Proteins. In S. Kasapis, I. T. Norton, & J. B. Ubbink (Eds.), *Modern Biopolymer Science* (pp. 29-91). Academic Press.
- Errington, A. D., & Foegeding, E. A. (1998). Factors determining fracture stress and strain of fine-stranded whey protein gels. *Journal of Agricultural and Food Chemistry*, *46*(8), 2963-2967.

- Felix, M., Camacho-Ocaña, Z., López-Castejón, M. L., & Ruiz-Domínguez, M. (2021). Rheological properties of quinoa-based gels. An alternative for vegan diets. *Food Hydrocolloids*, *120*, 106827.
- Fernández-López, J., Lucas-González, R., Roldán-Verdú, A., Viuda-Martos, M., Sayas-Barberá, E., Ballester-Sánchez, J., Haros, C. M., & Pérez-Álvarez, J. A. (2020). Effects of black quinoa wet-milling coproducts on the quality properties of bologna-type sausages during cold storage. *Foods*, *9*(3), 274.
- Fernández-López, J., Lucas-González, R., Viuda-Martos, M., Sayas-Barberá, E., Ballester-Sánchez, J., Haros, C. M., Martínez-Mayoral, A., & Pérez-Álvarez, J. A. (2020). Chemical and technological properties of bologna-type sausages with added black quinoa wet-milling coproducts as binder replacer. *Food chemistry*, *310*, 125936.
- Ferrando, M., & Spiess, W. (2000). Confocal scanning laser microscopy. A powerful tool in food science Revision: Microscopía láser confocal de barrido. Una potente herramienta en la ciencia de los alimentos. *Food Science and Technology International*, *6*(4), 267-284.
- Fitzsimons, S. M., Mulvihill, D. M., & Morris, E. R. (2007). Denaturation and aggregation processes in thermal gelation of whey proteins resolved by differential scanning calorimetry. *Food Hydrocolloids*, *21*(4), 638-644.
- Fleddermann, M., Fechner, A., Röbber, A., Bähr, M., Pastor, A., Liebert, F., & Jahreis, G. (2013). Nutritional evaluation of rapeseed protein compared to soy protein for quality, plasma amino acids, and nitrogen balance—a randomized cross-over intervention study in humans. *Clinical Nutrition*, *32*(4), 519-526.
- Foegeding, E. A., Bowland, E. L., & Hardin, C. C. (1995). Factors that determine the fracture properties and microstructure of globular protein gels. *Food Hydrocolloids*, *9*(4), 237-249.
- Fox, P. F., McSweeney, P. L., & Paul, L. (1998). *Dairy chemistry and biochemistry*.
- Franck, A. (2004). Understanding rheology of structured fluids. *Book of TA instruments*, 1-17.
- Galani, D., & Owusu Apenten, R. K. (1999). Heat-induced denaturation and aggregation of β -Lactoglobulin: kinetics of formation of hydrophobic and disulphide-linked aggregates. *International Journal of Food Science & Technology*, *34*(5-6), 467-476.
- Gallagher, E., Gormley, T. R., & Arendt, E. K. (2004). Recent advances in the formulation of gluten-free cereal-based products. *Trends in Food Science & Technology*, *15*(3), 143-152.
- Galloway, J. (2017). Quinoa, the new crop that might be a goldmine. *Stuff*

- Gangurde, H., Chordiya, M., Patil, P., & Baste, N. (2011). Whey protein. *Scholars' Research Journal*, 1(2).
- García-Ochoa, F., Santos, V., Casas, J., & Gómez, E. (2000). Xanthan gum: production, recovery, and properties. *Biotechnology Advances*, 18(7), 549-579.
- García, M., Condori, B., & Castillo, C. D. (2015). Agroecological and agronomic cultural practices of quinoa in South America. *Quinoa: Improvement and sustainable production*, 25-46.
- George, A., Shah, P. A., & Shrivastav, P. S. (2019). Guar gum: Versatile natural polymer for drug delivery applications. *European Polymer Journal*, 112, 722-735.
- Gezimati, J., Singh, H., & Creamer, L. K. (1996). Heat-induced interactions and gelation of mixtures of bovine β -lactoglobulin and serum albumin. *Journal of Agricultural and Food Chemistry*, 44(3), 804-810.
- Giancone, T., Torrieri, E., Masi, P., & Michon, C. (2009). Protein–polysaccharide interactions: Phase behaviour of pectin–soy flour mixture. *Food Hydrocolloids*, 23(5), 1263-1269.
- Gilbert, E. P. (2019). Small Angle X-Ray and Neutron Scattering in Food Colloids. *Current Opinion in Colloid & Interface Science*.
- Gilbert, E. P., Schulz, J. C., & Noakes, T. J. (2006). ‘Quokka’—the small-angle neutron scattering instrument at OPAL. *Physica B: Condensed Matter*, 385, 1180-1182.
- Goldstein, J. I., Newbury, D. E., Michael, J. R., Ritchie, N. W., Scott, J. H. J., & Joy, D. C. (2017). *Scanning electron microscopy and X-ray microanalysis*. Springer.
- González, J. A., Eisa, S. S., Hussin, S., & Prado, F. E. (2015). Quinoa: an Incan crop to face global changes in agriculture. *Quinoa: Improvement and sustainable production*, 1-18.
- Gosal, W. S., & Ross-Murphy, S. B. (2000). Globular protein gelation. *Current Opinion in Colloid & Interface Science*, 5(3), 188-194.
- Guasch-Ferré, M., Zong, G., Willett, W. C., Zock, P. L., Wanders, A. J., Hu, F. B., & Sun, Q. (2019). Associations of monounsaturated fatty acids from plant and animal sources with total and cause-specific mortality in two US prospective cohort studies. *Circulation research*, 124(8), 1266-1275.
- Guerreo-Ochoa, M. R., Pedreschi, R., & Chirinos, R. (2015). Optimised methodology for the extraction of protein from quinoa (*Chenopodium quinoa* Willd.). *International Journal of Food Science & Technology*, 50(8), 1815-1822.
- Gunasekaran, S., & Ak, M. M. (2000). Dynamic oscillatory shear testing of foods — selected applications. *Trends in Food Science & Technology*, 11(3), 115-127.

- Gupta, A., Sharma, S., & Reddy Surasani, V. K. (2021). Quinoa protein isolate supplemented pasta: Nutritional, physical, textural and morphological characterization. *LWT*, *135*, 110045.
- Gutiérrez, C., Rubilar, M., Jara, C., Verdugo, M., Sineiro, J., & Shene, C. (2010). Flaxseed and flaxseed cake as a source of compounds for food industry. *Journal of soil science and plant nutrition*, *10*(4), 454-463.
- Habibi, H., & Khosravi-Darani, K. (2017). Effective variables on production and structure of xanthan gum and its food applications: A review. *Biocatalysis and Agricultural Biotechnology*, *10*, 130-140.
- Hamed, F., Razavi, S. M. A., & Sharif, A. (2022). Structural, morphological and rheological characterisation of bovine serum albumin–cress seed gum complex coacervate. *International Journal of Food Science & Technology*.
- Hammouda, B., Ho, D. L., & Kline, S. (2004). Insight into clustering in poly (ethylene oxide) solutions. *Macromolecules*, *37*(18), 6932-6937.
- Havea, P., Singh, H., Creamer, L. K., & Campanella, O. H. (1998). Electrophoretic characterization of the protein products formed during heat treatment of whey protein concentrate solutions. *Journal of Dairy Research*, *65*(1), 79-91.
- Havea, P., Watkinson, P., & Kuhn-Sherlock, B. (2009). Heat-Induced Whey Protein Gels: Protein–Protein Interactions and Functional Properties. *Journal of Agricultural and Food Chemistry*, *57*(4), 1506-1512.
- He, R., He, H.-Y., Chao, D., Ju, X., & Aluko, R. (2014). Effects of high pressure and heat treatments on physicochemical and gelation properties of rapeseed protein isolate. *Food and Bioprocess Technology*, *7*(5), 1344-1353.
- He, Z., Ma, T., Zhang, W., Su, E., Cao, F., Huang, M., & Wang, Y. (2021). Heat-induced gel formation by whey protein isolate-Lycium barbarum polysaccharides at varying pHs. *Food Hydrocolloids*, *115*, 106607.
- Hemar, Y., Lebreton, S., Xu, M., & Day, L. (2011). Small-deformation rheology investigation of rehydrated cell wall particles–xanthan mixtures. *Food Hydrocolloids*, *25*(4), 668-676.
- Hemar, Y., Tamehana, M., Munro, P., & Singh, H. (2001). Influence of xanthan gum on the formation and stability of sodium caseinate oil-in-water emulsions. *Food Hydrocolloids*, *15*(4-6), 513-519.
- Hermansson, A.-M. (1994). Microstructure of protein gels related to functionality. In *Protein structure-function relationships in foods* (pp. 22-42). Springer.

- Hettiarachchy, N. S., & Ziegler, G. R. (1994). *Protein functionality in food systems*. CRC Press.
- Higgins, T. (1984). Synthesis and regulation of major proteins in seeds. *Annual Review of Plant Physiology*, 35(1), 191-221.
- Hines, M. E., & Foegeding, E. A. (1993). Interactions of .alpha.-lactalbumin and bovine serum albumin with .beta.-lactoglobulin in thermally induced gelation. *Journal of Agricultural and Food Chemistry*, 41(3), 341-346.
- Hiroi, T., Hirosawa, K., Okazumi, Y., Pingali, S. V., & Shibayama, M. (2020). Mechanism of heat-induced gelation for ovalbumin under acidic conditions and the effect of peptides. *Polymer Journal*, 52(11), 1263-1272.
- Hiroi, T., Okazumi, Y., Littrell, K. C., Narita, Y., Tanaka, N., & Shibayama, M. (2016). Mechanism of heat-induced gelation for ovalbumin and its N-terminus cleaved form. *Polymer*, 93, 152-158.
- Hoffmann, M. A., & van Mil, P. J. (1997). Heat-induced aggregation of β -lactoglobulin: role of the free thiol group and disulfide bonds. *Journal of Agricultural and Food Chemistry*, 45(8), 2942-2948.
- Hollamby, M. J. (2013). Practical applications of small-angle neutron scattering. *Physical chemistry chemical physics*, 15(26), 10566-10579.
- Hongsprabhas, P., & Barbut, S. (1997). Effect of gelation temperature on Ca²⁺-induced gelation of whey protein isolate. *LWT-Food Science and Technology*, 30(1), 45-49.
- Hou, J.-J., Guo, J., Wang, J.-M., He, X.-T., Yuan, Y., Yin, S.-W., & Yang, X.-Q. (2015). Edible double-network gels based on soy protein and sugar beet pectin with hierarchical microstructure. *Food Hydrocolloids*, 50, 94-101.
- Hu, B., Chen, Q., Cai, Q., Fan, Y., Wilde, P. J., Rong, Z., & Zeng, X. (2017). Gelation of soybean protein and polysaccharides delays digestion. *Food chemistry*, 221, 1598-1605.
- Hu, H., Fan, X., Zhou, Z., Xu, X., Fan, G., Wang, L., Huang, X., Pan, S., & Zhu, L. (2013). Acid-induced gelation behavior of soybean protein isolate with high intensity ultrasonic pre-treatments. *Ultrasonics Sonochemistry*, 20(1), 187-195.
- Huffman, L. M., & de Barros Ferreira, L. (2011). Whey-based ingredients. *Dairy ingredients for food processing*, 1, 179-198.
- Hunnicutt, J. W., Hardy, R. W., Williford, J., & McDonald, J. M. (1994). Saturated fatty acid-induced insulin resistance in rat adipocytes. *Diabetes*, 43(4), 540-545.

- Iametti, S., Cairoli, S., De Gregori, B., & Bonomi, F. (1995). Modifications of High-Order Structures upon Heating of β -Lactoglobulin: Dependence on the Protein Concentration. *Journal of Agricultural and Food Chemistry*, *43*(1), 53-58.
- Ikeda, S., Foegeding, E. A., & Hagiwara, T. (1999). Rheological study on the fractal nature of the protein gel structure. *Langmuir*, *15*(25), 8584-8589.
- Ilavsky, J., & Jemian, P. R. (2009). Irena: tool suite for modeling and analysis of small-angle scattering. *Journal of Applied Crystallography*, *42*(2), 347-353.
- Jancurová, M., Minarovičová, L., & Dandar, A. (2009). Quinoa—a review. *Czech Journal of Food Sciences*, *27*(2), 71-79.
- Jeanes, A., Pittsley, J., & Senti, F. (1961). Polysaccharide B-1459: a new hydrocolloid polyelectrolyte produced from glucose by bacterial fermentation. *Journal of Applied Polymer Science*, *5*(17), 519-526.
- Jenness, R., Wong, N. P., Marth, E. H., & Keeney, M. (1988). *Fundamentals of dairy chemistry*. Springer Science & Business Media.
- Jeyarajah, S., & Allen, J. C. (1994). Calcium binding and salt-induced structural changes of native and preheated β -lactoglobulin. *Journal of Agricultural and Food Chemistry*, *42*(1), 80-85.
- Joo, S.-I., Kim, J.-E., & Lee, S.-P. (2011). Physicochemical properties of whole soybean curd prepared by microbial transglutaminase. *Food Science and Biotechnology*, *20*(2), 437.
- Jose, J., Pouvreau, L., & Martin, A. H. (2016). Mixing whey and soy proteins: Consequences for the gel mechanical response and water holding. *Food Hydrocolloids*, *60*, 216-224.
- Jung, J.-M., Savin, G., Pouzot, M., Schmitt, C., & Mezzenga, R. (2008). Structure of Heat-Induced β -Lactoglobulin Aggregates and their Complexes with Sodium-Dodecyl Sulfate. *Biomacromolecules*, *9*(9), 2477-2486.
- Kale, S. N., & Deore, S. L. (2017). Emulsion micro emulsion and nano emulsion: a review. *Systematic Reviews in Pharmacy*, *8*(1), 39.
- Kang, K., & Pettitt, D. (1993). Xanthan, gellan, welan, and rhamosan. In *Industrial gums* (pp. 341-397). Elsevier.
- Kaspchak, E., de Oliveira, M. A. S., Simas, F. F., Franco, C. R. C., Silveira, J. L. M., Mafra, M. R., & Igarashi-Mafra, L. (2017). Determination of heat-set gelation capacity of a quinoa protein isolate (*Chenopodium quinoa*) by dynamic oscillatory rheological analysis. *Food chemistry*, *232*, 263-271.
- Kaspchak, E., Oliveira, M. A. S. d., Simas, F. F., Franco, C. R. C., Silveira, J. L. M., Mafra, M. R., & Igarashi-Mafra, L. (2017). Determination of heat-set gelation capacity of a

- quinoa protein isolate (*Chenopodium quinoa*) by dynamic oscillatory rheological analysis. *Food chemistry*, 232, 263-271.
- Kaushik, P., Dowling, K., Barrow, C. J., & Adhikari, B. (2015). Complex coacervation between flaxseed protein isolate and flaxseed gum. *Food Research International*, 72, 91-97.
- Kavanagh, G. M., Clark, A. H., & Ross-Murphy, S. B. (2000). Heat-induced gelation of globular proteins: part 3. Molecular studies on low pH β -lactoglobulin gels. *International Journal of Biological Macromolecules*, 28(1), 41-50.
- Kayitmazer, A. B. (2017). Thermodynamics of complex coacervation. *Advances in colloid and interface science*, 239, 169-177.
- Khan, K. (2016). *Wheat: chemistry and technology*. Elsevier.
- Kilara, A. (1984). Standardization of methodology for evaluating whey proteins. *Journal of Dairy Science*, 67(11), 2734-2744.
- Kilara, A., & Vaghela, M. N. (2018). Whey protein. In R. Y. Yada (Ed.), *Proteins in Food Processing (Second Edition)* (pp. 93-126). Woodhead Publishing.
- Kim, S.-G., Yoo, W., & Yoo, B. (2014). Effect of thickener type on the rheological properties of hot thickened soups suitable for elderly people with swallowing difficulty. *Preventive nutrition and food science*, 19(4), 358.
- Kinsella, J., & Whitehead, D. (1989). Proteins in whey: chemical, physical, and functional properties. *Advances in food and nutrition research*, 33, 343-438.
- Kinsella, J. E., & Melachouris, N. (1976). Functional properties of proteins in foods: a survey. *Critical Reviews in Food Science & Nutrition*, 7(3), 219-280.
- Kinsella, J. E., & Morr, C. V. (1984). Milk proteins: physicochemical and functional properties. *Critical Reviews in Food Science & Nutrition*, 21(3), 197-262.
- Kizilay, E., Kayitmazer, A. B., & Dubin, P. L. (2011). Complexation and coacervation of polyelectrolytes with oppositely charged colloids. *Advances in colloid and interface science*, 167(1-2), 24-37.
- Klassen, D. R., Elmer, C. M., & Nickerson, M. T. (2011). Associative phase separation involving canola protein isolate with both sulphated and carboxylated polysaccharides. *Food chemistry*, 126(3), 1094-1101.
- Kline, S. R. (2006). Reduction and analysis of SANS and USANS data using IGOR Pro. *Journal of Applied Crystallography*, 39(6), 895-900.
- Klost, M., Brzeski, C., & Drusch, S. (2020). Effect of protein aggregation on rheological properties of pea protein gels. *Food Hydrocolloids*, 108, 106036.

- Klost, M., & Drusch, S. (2019). Structure formation and rheological properties of pea protein-based gels. *Food Hydrocolloids*, *94*, 622-630.
- Konishi, Y., Hirano, S., Tsuboi, H., & Wada, M. (2004). Distribution of minerals in quinoa (*Chenopodium quinoa* Willd.) seeds. *Bioscience, biotechnology, and biochemistry*, *68*(1), 231-234.
- Kornet, R., Shek, C., Venema, P., Jan van der Goot, A., Meinders, M., & van der Linden, E. (2021). Substitution of whey protein by pea protein is facilitated by specific fractionation routes. *Food Hydrocolloids*, *117*, 106691.
- Kozioł, M. (1992). Chemical composition and nutritional evaluation of quinoa (*Chenopodium quinoa* Willd.). *Journal of food composition and analysis*, *5*(1), 35-68.
- Krebs, M. R., Devlin, G. L., & Donald, A. (2007). Protein particulates: another generic form of protein aggregation? *Biophysical journal*, *92*(4), 1336-1342.
- Krissansen, G. W. (2007). Emerging health properties of whey proteins and their clinical implications. *Journal of the American college of Nutrition*, *26*(6), 713S-723S.
- Kristensen, H. T., Denon, Q., Tavernier, I., Gregersen, S. B., Hammershøj, M., Van der Meeren, P., Dewettinck, K., & Dalsgaard, T. K. (2021). Improved food functional properties of pea protein isolate in blends and co-precipitates with whey protein isolate. *Food Hydrocolloids*, *113*, 106556.
- Kulkarni, V. S., & Shaw, C. (2015). *Essential chemistry for formulators of semisolid and liquid dosages*. Academic Press.
- Kumar, A., Rao, K. M., & Han, S. S. (2018). Application of xanthan gum as polysaccharide in tissue engineering: A review. *Carbohydrate polymers*, *180*, 128-144.
- Kundu, S., Chinchalikar, A. J., Das, K., Aswal, V., & Kohlbrecher, J. (2013). Fe³⁺ ion induced protein gelation: Small-angle neutron scattering study. *Chemical Physics Letters*, *584*, 172-176.
- Laneuville, S., Paquin, P., & Turgeon, S. (2000). Effect of preparation conditions on the characteristics of whey protein—xanthan gum complexes. *Food Hydrocolloids*, *14*(4), 305-314.
- Langton, M., Ehsanzamir, S., Karkehabadi, S., Feng, X., Johansson, M., & Johansson, D. P. (2020). Gelation of faba bean proteins—Effect of extraction method, pH and NaCl. *Food Hydrocolloids*, *103*, 105622.
- Langton, M., & Hermansson, A.-M. (1992). Fine-stranded and particulate gels of β -lactoglobulin and whey protein at varying pH. *Food Hydrocolloids*, *5*(6), 523-539.

- Le Priol, L., Dagmey, A., Morandat, S., Saleh, K., El Kirat, K., & Nesterenko, A. (2019). Comparative study of plant protein extracts as wall materials for the improvement of the oxidative stability of sunflower oil by microencapsulation. *Food Hydrocolloids*, *95*, 105-115.
- Le Roux, L., Chacon, R., Dupont, D., Jeantet, R., Deglaire, A., & Nau, F. (2020). In vitro static digestion reveals how plant proteins modulate model infant formula digestibility. *Food Research International*, *130*, 108917.
- Leksrisonpong, P. N., & Foegeding, E. A. (2011). How Micro-Phase Separation Alters the Heating Rate Effects on Globular Protein Gelation. *Journal of Food Science*, *76*(3), E318-E327.
- Leksrisonpong, P. N., Lanier, T. C., & Foegeding, E. A. (2012). Effects of Heating Rate and pH on Fracture and Water-Holding Properties of Globular Protein Gels as Explained by Micro-Phase Separation. *Journal of Food Science*, *77*(2), E60-E67.
- Li, T., Senesi, A. J., & Lee, B. (2016). Small angle X-ray scattering for nanoparticle research. *Chemical reviews*, *116*(18), 11128-11180.
- Li, X., Cheng, Y., Yi, C., Hua, Y., Yang, C., & Cui, S. (2009). Effect of ionic strength on the heat-induced soy protein aggregation and the phase separation of soy protein aggregate/dextran mixtures. *Food Hydrocolloids*, *23*(3), 1015-1023.
- Li, Z., Yang, Z., Otter, D., Rehm, C., Li, N., Zhou, P., & Hemar, Y. (2018). Rheological and structural properties of coagulated milks reconstituted in D2O: Comparison between rennet and a tamarillo enzyme (tamarillin). *Food Hydrocolloids*, *79*, 170-178.
- Liang, X., Ma, C., Yan, X., Zeng, H., McClements, D. J., Liu, X., & Liu, F. (2020). Structure, rheology and functionality of whey protein emulsion gels: Effects of double cross-linking with transglutaminase and calcium ions. *Food Hydrocolloids*, *102*, 105569.
- Lindeboom, N., Chang, P. R., Falk, K. C., & Tyler, R. T. (2005). Characteristics of starch from eight quinoa lines. *Cereal chemistry*, *82*(2), 216-222.
- López-Alarcón, C. A., Cerdán-Leal, M. A., Beristain, C. I., Pascual-Pineda, L. A., Azuara, E., & Jiménez-Fernández, M. (2019). The potential use of modified quinoa protein isolates in cupcakes: physicochemical properties, structure and stability of cupcakes. *Food & function*, *10*(7), 4432-4439.
- Lopez-Rubio, A., & Gilbert, E. P. (2009). Neutron scattering: a natural tool for food science and technology research. *Trends in Food Science & Technology*, *20*(11-12), 576-586.

- López, D. N., Galante, M., Robson, M., Boeris, V., & Spelzini, D. (2018). Amaranth, quinoa and chia protein isolates: Physicochemical and structural properties. *International Journal of Biological Macromolecules*, *109*, 152-159.
- Lopez, M. J., & Mohiuddin, S. S. (2021). Biochemistry, Essential Amino Acids. *StatPearls [Internet]*.
- Lorenzen, P. C., & Schrader, K. (2006). A comparative study of the gelation properties of whey protein concentrate and whey protein isolate. *Le lait*, *86*(4), 259-271.
- Lowry, O., Rosebrough, N., Farr, A., & Randall, R. (1951). Protein estimation by Lowry's method. *J Biol Chem*, *193*, 265.
- Lucey, J., & Singh, H. (1997). Formation and physical properties of acid milk gels: a review. *Food Research International*, *30*(7), 529-542.
- Luo, L., Zhang, R., Palmer, J., Hemar, Y., & Yang, Z. (2021). Impact of High Hydrostatic Pressure on the Gelation Behavior and Microstructure of Quinoa Protein Isolate Dispersions. *ACS Food Science & Technology*, *1*(11), 2144-2151.
- Lytle, T. K., Radhakrishna, M., & Sing, C. E. (2016). High charge density coacervate assembly via hybrid Monte Carlo single chain in mean field theory. *Macromolecules*, *49*(24), 9693-9705.
- Ma, K. K., Greis, M., Lu, J., Nolden, A. A., McClements, D. J., & Kinchla, A. J. (2022). Functional Performance of Plant Proteins. *Foods*, *11*(4), 594.
- Mäkinen, O. E., Zannini, E., Koehler, P., & Arendt, E. K. (2016). Heat-denaturation and aggregation of quinoa (*Chenopodium quinoa*) globulins as affected by the pH value. *Food chemistry*, *196*, 17-24.
- Maltais, A., Remondetto, G. E., & Subirade, M. (2008). Mechanisms involved in the formation and structure of soya protein cold-set gels: A molecular and supramolecular investigation. *Food Hydrocolloids*, *22*(4), 550-559.
- Mansfeld, J., Vriend, G., Dijkstra, B. W., Veltman, O. R., Van den Burg, B., Venema, G., Ulbrich-Hofmann, R., & Eijsink, V. G. (1997). Extreme stabilization of a thermolysin-like protease by an engineered disulfide bond. *Journal of Biological Chemistry*, *272*(17), 11152-11156.
- Martin, A. H., Nieuwland, M., & de Jong, G. A. (2014). Characterization of heat-set gels from RuBisCO in comparison to those from other proteins. *Journal of Agricultural and Food Chemistry*, *62*(44), 10783-10791.
- Martin, J. E. (1986). Scattering exponents for polydisperse surface and mass fractals. *Journal of Applied Crystallography*, *19*(1), 25-27.

- Matthews, B. W. (2001). Hydrophobic interactions in proteins. *e LS*.
- McCann, T. H., Guyon, L., Fischer, P., & Day, L. (2018). Rheological properties and microstructure of soy-whey protein. *Food Hydrocolloids*, 82, 434-441.
- McClements, D. J. (2004). *Food emulsions: principles, practices, and techniques*. CRC press.
- McClements, D. J., Decker, E. A., Park, Y., & Weiss, J. (2009). Structural design principles for delivery of bioactive components in nutraceuticals and functional foods. *Critical reviews in food science and nutrition*, 49(6), 577-606.
- McClements, D. J., & Keogh, M. K. (1995). Physical properties of cold-setting gels formed from heat-denatured whey protein isolate. *Journal of the Science of Food and Agriculture*, 69(1), 7-14.
- McClements, D. J., Newman, E., & McClements, I. F. (2019). Plant-based milks: A review of the science underpinning their design, fabrication, and performance. *Comprehensive Reviews in Food Science and Food Safety*, 18(6), 2047-2067.
- McSwiney, M., Singh, H., & Campanella, O. H. (1994). Thermal aggregation and gelation of bovine β -lactoglobulin. *Food Hydrocolloids*, 8(5), 441-453.
- Mehalebi, S., Nicolai, T., & Durand, D. (2008). The influence of electrostatic interaction on the structure and the shear modulus of heat-set globular protein gels. *Soft Matter*, 4(4), 893-900.
- Mession, J.-L., Chihi, M. L., Sok, N., & Saurel, R. (2015). Effect of globular pea proteins fractionation on their heat-induced aggregation and acid cold-set gelation. *Food Hydrocolloids*, 46, 233-243.
- Mession, J.-L., Sok, N., Assifaoui, A., & Saurel, R. (2013). Thermal Denaturation of Pea Globulins (*Pisum sativum* L.)—Molecular Interactions Leading to Heat-Induced Protein Aggregation. *Journal of Agricultural and Food Chemistry*, 61(6), 1196-1204.
- Mezger, T. (2020). The rheology handbook. In *The rheology handbook* (pp. 17-18). Vincentz Network.
- Mezzenga, R., & Fischer, P. (2013). The self-assembly, aggregation and phase transitions of food protein systems in one, two and three dimensions. *Reports on Progress in Physics*, 76(4), 046601.
- Milas, M., & Rinaudo, M. (1986). Properties of xanthan gum in aqueous solutions: Role of the conformational transition. *Carbohydrate Research*, 158, 191-204.
- Mitchell, J. R. (1980). THE RHEOLOGY OF GELS. *Journal of Texture Studies*, 11(4), 315-337.

- Mohammadi, M., Sadeghnia, N., Azizi, M.-H., Neyestani, T.-R., & Mortazavian, A. M. (2014). Development of gluten-free flat bread using hydrocolloids: Xanthan and CMC. *Journal of Industrial and Engineering Chemistry*, 20(4), 1812-1818.
- Monahan, F. J., German, J. B., & Kinsella, J. E. (1995). Effect of pH and temperature on protein unfolding and thiol/disulfide interchange reactions during heat-induced gelation of whey proteins. *Journal of Agricultural and Food Chemistry*, 43(1), 46-52.
- Monteiro, S. R., & Lopes-da-Silva, J. A. (2017). Effect of the molecular weight of a neutral polysaccharide on soy protein gelation. *Food Research International*, 102, 14-24.
- Monteiro, S. R., Rebelo, S., da Cruz e Silva, O. A. B., & Lopes-da-Silva, J. A. (2013). The influence of galactomannans with different amount of galactose side chains on the gelation of soy proteins at neutral pH. *Food Hydrocolloids*, 33(2), 349-360.
- Monteiro, S. R., Rebelo, S., e Silva, O. A. d. C., & Lopes-da-Silva, J. A. (2013). The influence of galactomannans with different amount of galactose side chains on the gelation of soy proteins at neutral pH. *Food Hydrocolloids*, 33(2), 349-360.
- Montellano Duran, N., Spelzini, D., & Boeris, V. (2019). Characterization of acid – Induced gels of quinoa proteins and carrageenan. *LWT*, 108, 39-47.
- Montero, P., & Borderías, A. J. (1988). Fundamentos de la funcionalidad de las proteínas en alimentos. *Revista de agroquímica y tecnología de alimentos*, 28(2), 159-169.
- Mortensen, A., Aguilar, F., Crebelli, R., Di Domenico, A., Frutos, M. J., Galtier, P., Gott, D., Gundert-Remy, U., & Lambré, C. (2017). Re-evaluation of locust bean gum (E 410) as a food additive. *Efsa Journal*, 15(1), e04646.
- Mudgil, D., Barak, S., & Khatkar, B. S. (2014). Guar gum: processing, properties and food applications—a review. *Journal of food science and technology*, 51(3), 409-418.
- Mulvihill, D., & Donovan, M. (1987). Whey proteins and their thermal denaturation—a review. *Irish Journal of Food Science and Technology*, 11(1), 43-75.
- Mulvihill, D., & Ennis, M. (2003). Functional milk proteins: production and utilization. In *Advanced dairy chemistry—1 Proteins* (pp. 1175-1228). Springer.
- Munialo, C. D., Martin, A. H., van der Linden, E., & de Jongh, H. H. J. (2014). Fibril Formation from Pea Protein and Subsequent Gel Formation. *Journal of Agricultural and Food Chemistry*, 62(11), 2418-2427.
- Munialo, C. D., van der Linden, E., & de Jongh, H. H. (2014). The ability to store energy in pea protein gels is set by network dimensions smaller than 50 nm. *Food Research International*, 64, 482-491.

- Murphy, K. S., & Matanguihan, J. (2015). *Quinoa: Improvement and sustainable production*. John Wiley & Sons.
- Nadathur, S., Wanasundara, J. P., & Scanlin, L. (2016). *Sustainable protein sources*. Academic Press.
- Nasrollahzadeh, M., Nezafat, Z., Shafiei, N., & Soleimani, F. (2021). *Polysaccharides in food industry*. Elsevier: Iran.
- Navruz-Varli, S., & Sanlier, N. (2016). Nutritional and health benefits of quinoa (*Chenopodium quinoa* Willd.). *Journal of Cereal Science*, *69*, 371-376.
- Nguyen, B. T., Balakrishnan, G., Jacquette, B., Nicolai, T., Chassenieux, C., Schmitt, C., & Bovetto, L. (2016). Inhibition and promotion of heat-induced gelation of whey proteins in the presence of calcium by addition of sodium caseinate. *Biomacromolecules*, *17*(11), 3800-3807.
- Nguyen, B. T., Chassenieux, C., Nicolai, T., & Schmitt, C. (2017). Effect of the pH and NaCl on the microstructure and rheology of mixtures of whey protein isolate and casein micelles upon heating. *Food Hydrocolloids*, *70*, 114-122.
- Nguyen, B. T., Nicolai, T., Chassenieux, C., Schmitt, C., & Bovetto, L. (2016). Heat-induced gelation of mixtures of whey protein isolate and sodium caseinate between pH 5.8 and pH 6.6. *Food Hydrocolloids*, *61*, 433-441.
- Nicolai, T. (2019). Gelation of food protein-protein mixtures. *Advances in colloid and interface science*, *270*, 147-164.
- Nicolai, T., Britten, M., & Schmitt, C. (2011). β -Lactoglobulin and WPI aggregates: Formation, structure and applications. *Food Hydrocolloids*, *25*(8), 1945-1962.
- Nicolai, T., & Chassenieux, C. (2019). Heat-induced gelation of plant globulins. *Current Opinion in Food Science*, *27*, 18-22.
- Nicolai, T., & Durand, D. (2013). Controlled food protein aggregation for new functionality. *Current Opinion in Colloid & Interface Science*, *18*(4), 249-256.
- Nieto-Nieto, T. V., Wang, Y. X., Ozimek, L., & Chen, L. (2014). Effects of partial hydrolysis on structure and gelling properties of oat globular proteins. *Food Research International*, *55*, 418-425.
- Niknezhad, S. V., Asadollahi, M. A., Zamani, A., Biria, D., & Doostmohammadi, M. (2015). Optimization of xanthan gum production using cheese whey and response surface methodology. *Food Science and Biotechnology*, *24*(2), 453-460.

- Niva, M., Vainio, A., & Jallinoja, P. (2017). Barriers to increasing plant protein consumption in Western populations. In *Vegetarian and plant-based diets in health and disease prevention* (pp. 157-171). Elsevier.
- Nordgård, C. T., & Draget, K. I. (2021). Alginates. In G. O. Phillips & P. A. Williams (Eds.), *Handbook of Hydrocolloids (Third Edition)* (pp. 805-829). Woodhead Publishing.
- Nowak, V., Du, J., & Charrondièrre, U. R. (2016). Assessment of the nutritional composition of quinoa (*Chenopodium quinoa* Willd.). *Food chemistry*, 193, 47-54.
- Núñez, L. (1974). *La agricultura prehistórica en los Andes meridionales*. Editorial Orbe.
- Nyman, M., & Fullmer, L. (2015). Small Angle X-Ray Scattering of Group V polyoxometalates. *Trends in Polyoxometalates Research*, 151-170.
- Ogungbenle, H. N. (2003). Nutritional evaluation and functional properties of quinoa (*Chenopodium quinoa*) flour. *International journal of food sciences and nutrition*, 54(2), 153-158.
- Oldfield, D. J., Singh, H., Taylor, M. W., & Pearce, K. N. (1998). Kinetics of denaturation and aggregation of whey proteins in skim milk heated in an ultra-high temperature (UHT) pilot plant. *International Dairy Journal*, 8(4), 311-318.
- Opazo-Navarrete, Schutyser, Boom, & Janssen. (2018). Effect of pre-treatment on in vitro gastric digestion of quinoa protein (*Chenopodium quinoa* Willd.) obtained by wet and dry fractionation. *International journal of food sciences and nutrition*, 69(1), 1-11.
- Oshodi, A., Ipinmoroti, K., & Adeyeye, E. (1997). Functional properties of some varieties of African yam bean (*Sphenostylis stenocarpa*) flour—III. *International journal of food sciences and nutrition*, 48(4), 243-250.
- Ouyang, H., Kilcawley, K. N., Miao, S., Fenelon, M., Kelly, A., & Sheehan, J. J. (2021). Exploring the potential of polysaccharides or plant proteins as structuring agents to design cheeses with sensory properties focused toward consumers in East and Southeast Asia: a review. *Critical reviews in food science and nutrition*, 1-14.
- Ozel, B., Cikrikci, S., Aydin, O., & Oztop, M. H. (2017). Polysaccharide blended whey protein isolate-(WPI) hydrogels: A physicochemical and controlled release study. *Food Hydrocolloids*, 71, 35-46.
- Özer, C. O., & Secen, S. M. (2018). Effects of quinoa flour on lipid and protein oxidation in raw and cooked beef burger during long term frozen storage. *Food Science and Technology*, 38, 221-227.
- Pak, C. W., Kosno, M., Holehouse, A. S., Padrick, S. B., Mittal, A., Ali, R., Yunus, A. A., Liu, D. R., Pappu, R. V., & Rosen, M. K. (2016). Sequence determinants of intracellular

- phase separation by complex coacervation of a disordered protein. *Molecular cell*, 63(1), 72-85.
- Pang, Z., Luo, Y., Li, B., Zhang, M., & Liu, X. (2020). Effect of different hydrocolloids on tribological and rheological behaviors of soymilk gels. *Food Hydrocolloids*, 101, 105558.
- Papalamprou, E. M., Doxastakis, G. I., & Kiosseoglou, V. (2010). Chickpea protein isolates obtained by wet extraction as emulsifying agents. *Journal of the Science of Food and Agriculture*, 90(2), 304-313.
- Pasquier, J., Brûlet, A., Boire, A., Jamme, F., Perez, J., Bizien, T., Lutton, E., & Boué, F. (2019). Monitoring food structure during digestion using small-angle scattering and imaging techniques. *Colloids and Surfaces A: Physicochemical and Engineering Aspects*, 570, 96-106.
- Pathan, S., & Siddiqui, R. A. (2022). Nutritional Composition and Bioactive Components in Quinoa (*Chenopodium quinoa* Willd.) Greens: A Review. *Nutrients*, 14(3), 558.
- Pathania, S., Parmar, P., & Tiwari, B. K. (2019). Stability of protein during processing and storage. In C. M. Galanakis (Ed.), *Proteins: Sustainable Source, Processing and Applications* (pp. 295-330). Academic Press.
- Patole, S., Cheng, L., & Yang, Z. (2022). Impact of incorporations of various polysaccharides on rheological and microstructural characteristics of heat-induced quinoa protein isolate gels. *Food Biophysics*, 1-10.
- Paul, G. L. (2009). The rationale for consuming protein blends in sports nutrition. *Journal of the American college of Nutrition*, 28(sup4), 464S-472S.
- Pawley, J. (2006). *Handbook of biological confocal microscopy* (Vol. 236). Springer Science & Business Media.
- Pechtold, L. A., Boddé, H. E., Junginger, H. E., Koerten, H. K., & Bouwstra, J. A. (2001). X-ray microanalysis of cryopreserved human skin to study the effect of iontophoresis on percutaneous ion transport1. *Pharmaceutical research*, 18(7), 1012-1017.
- Pedersen, J. S. (1997). Analysis of small-angle scattering data from colloids and polymer solutions: modeling and least-squares fitting. *Advances in colloid and interface science*, 70, 171-210.
- Pelegrine, D. H. G., & Gasparetto, C. A. (2005). Whey proteins solubility as function of temperature and pH. *LWT - Food Science and Technology*, 38(1), 77-80.

- Pelgrom, P. J., Vissers, A. M., Boom, R. M., & Schutyser, M. A. (2013). Dry fractionation for production of functional pea protein concentrates. *Food Research International*, *53*(1), 232-239.
- Pellegrini, M., Lucas-Gonzalez, R., Sayas-Barberá, E., Fernández-López, J., Pérez-Álvarez, J. A., & Viuda-Martos, M. (2018). Quinoa (*Chenopodium quinoa* Willd) paste as partial fat replacer in the development of reduced fat cooked meat product type pâté: Effect on quality and safety. *CyTA-Journal of Food*, *16*(1), 1079-1088.
- Peña, M., Méndez, B., Guerra, M., & Peña, S. (2015). Development of functional meat products: use of quinoa flour. *Alimentos. Ciencia e Investigacion*, *23*(1), 21-36.
- Petcharat, T., & Benjakul, S. (2018). Effect of gellan incorporation on gel properties of bigeye snapper surimi. *Food Hydrocolloids*, *77*, 746-753.
- Phan-Xuan, T., Durand, D., Nicolai, T., Donato, L., Schmitt, C., & Bovetto, L. (2013). Tuning the structure of protein particles and gels with calcium or sodium ions. *Biomacromolecules*, *14*(6), 1980-1989.
- Phillips, L. G., Whitehead, D. M., & Kinsella, J. (2013). *Structure-function properties of food proteins*. Academic Press.
- Pouzot, M., Durand, D., & Nicolai, T. (2004). Influence of the ionic strength on the structure of heat-set globular protein gels at pH 7. β -lactoglobulin. *Macromolecules*, *37*(23), 8703-8708.
- Pouzot, M., Nicolai, T., Visschers, R., & Weijers, M. (2005). X-ray and light scattering study of the structure of large protein aggregates at neutral pH. *Food Hydrocolloids*, *19*(2), 231-238.
- Prajapati, V. D., Jani, G. K., Moradiya, N. G., Randeria, N. P., & Nagar, B. J. (2013). Locust bean gum: A versatile biopolymer. *Carbohydrate polymers*, *94*(2), 814-821.
- Price, D. L., & Skold, K. (1986). 1. introduction to neutron scattering. In *Methods in Experimental Physics* (Vol. 23, pp. 1-97). Elsevier.
- Puppo, M. C., & Añón, M. C. (1998). Structural Properties of Heat-Induced Soy Protein Gels As Affected by Ionic Strength and pH. *Journal of Agricultural and Food Chemistry*, *46*(9), 3583-3589.
- Puyol, P., Pérez, M. D., & Horne, D. S. (2001). Heat-induced gelation of whey protein isolates (WPI): effect of NaCl and protein concentration. *Food Hydrocolloids*, *15*(3), 233-237.
- Qamar, S., Manrique, Y. J., Parekh, H., & Falconer, J. R. (2020). Nuts, cereals, seeds and legumes proteins derived emulsifiers as a source of plant protein beverages: A review. *Critical reviews in food science and nutrition*, *60*(16), 2742-2762.

- Rabetafika, H. N., Van Remoortel, V., Danthine, S., Paquot, M., & Blecker, C. (2011). Flaxseed proteins: food uses and health benefits. *International Journal of Food Science & Technology*, *46*(2), 221-228.
- Ramos, Ó. L., Pereira, J. O., Silva, S. I., Amorim, M. M., Fernandes, J. C., Lopes-da-Silva, J. A., Pintado, M. E., & Malcata, F. X. (2012). Effect of composition of commercial whey protein preparations upon gelation at various pH values. *Food Research International*, *48*(2), 681-689.
- Ranhotra, G., Gelroth, J., Glaser, B., Lorenz, K., & Johnson, D. (1993). Composition and protein nutritional quality of quinoa. *Cereal chemistry*, *70*, 303-303.
- Rehm, C., Brûlé, A., Freund, A. K., & Kennedy, S. J. (2013). Kookaburra: the ultra-small-angle neutron scattering instrument at OPAL. *Journal of Applied Crystallography*, *46*(6), 1699-1704.
- Rehm, C., Campo, L. d., Brûlé, A., Darmann, F., Bartsch, F., & Berry, A. (2018). Design and performance of the variable-wavelength Bonse–Hart ultra-small-angle neutron scattering diffractometer KOOKABURRA at ANSTO. *Journal of Applied Crystallography*, *51*(1), 1-8.
- Remondetto, G. E., & Subirade, M. (2003). Molecular mechanisms of Fe²⁺-induced β -lactoglobulin cold gelation. *Biopolymers: Original Research on Biomolecules*, *69*(4), 461-469.
- Ren, Z., Li, Z., Chen, Z., Zhang, Y., Lin, X., Weng, W., Yang, H., & Li, B. (2021). Characteristics and application of fish oil-in-water pickering emulsions structured with tea water-insoluble proteins/ κ -carrageenan complexes. *Food Hydrocolloids*, *114*, 106562.
- Renkema, J. M. S., Gruppen, H., & van Vliet, T. (2002). Influence of pH and Ionic Strength on Heat-Induced Formation and Rheological Properties of Soy Protein Gels in Relation to Denaturation and Their Protein Compositions. *Journal of Agricultural and Food Chemistry*, *50*(21), 6064-6071.
- Repo-Carrasco-Valencia, R., Hellström, J. K., Pihlava, J.-M., & Mattila, P. H. (2010). Flavonoids and other phenolic compounds in Andean indigenous grains: Quinoa (*Chenopodium quinoa*), kañiwa (*Chenopodium pallidicaule*) and kiwicha (*Amaranthus caudatus*). *Food chemistry*, *120*(1), 128-133.
- Repo-Carrasco-Valencia, R. A.-M., & Serna, L. A. (2011). Quinoa (*Chenopodium quinoa*, Willd.) as a source of dietary fiber and other functional components. *Food Science and Technology*, *31*(1), 225-230.

- Repo-Carrasco, R., Espinoza, C., & Jacobsen, S.-E. (2003). Nutritional value and use of the Andean crops quinoa (*Chenopodium quinoa*) and kañiwa (*Chenopodium pallidicaule*). *Food Reviews International*, *19*(1-2), 179-189.
- Resch, J. J., Daubert, C. R., & Foegeding, E. A. (2005). β -Lactoglobulin Gelation and Modification: Effect of Selected Acidulants and Heating Conditions. *Journal of Food Science*, *70*(1), C79-C86.
- Rinaudo, M., & Moroni, A. (2009). Rheological behavior of binary and ternary mixtures of polysaccharides in aqueous medium. *Food Hydrocolloids*, *23*(7), 1720-1728.
- Robertson, A. M., Sequeira, A., & Owens, R. G. (2009). Rheological models for blood. In *Cardiovascular mathematics* (pp. 211-241). Springer.
- Roesch, R. R., & Corredig, M. (2005). Heat-Induced Soy–Whey Proteins Interactions: Formation of Soluble and Insoluble Protein Complexes. *Journal of Agricultural and Food Chemistry*, *53*(9), 3476-3482.
- Rojas, W., Pinto, M., Alanoca, C., Gomez Pando, L., Leon-Lobos, P., Alercia, A., Diulgheroff, S., Padulosi, S., & Bazile, D. (2015). Quinoa genetic resources and ex situ conservation.
- Rosalam, S., & England, R. (2006). Review of xanthan gum production from unmodified starches by *Xanthomonas compestris* sp. *Enzyme and Microbial Technology*, *39*(2), 197-207.
- Ross- Murphy, S. B. (1995). Rheological Characterisation of Gels. *Journal of Texture Studies*, *26*(4), 391-400.
- Ruales, J., Grijalva, Y. d., Lopez-Jaramillo, P., & Nair, B. M. (2002). The nutritional quality of an infant food from quinoa and its effect on the plasma level of insulin-like growth factor-1 (IGF-1) in undernourished children. *International journal of food sciences and nutrition*, *53*(2), 143-154.
- Ruales, J., & Nair, B. M. (1992). Nutritional quality of the protein in quinoa (*Chenopodium quinoa*, Willd) seeds. *Plant Foods for Human Nutrition*, *42*(1), 1-11.
- Rubilar, M., Gutiérrez, C., Verdugo, M., Shene, C., & Sineiro, J. (2010). Flaxseed as a source of functional ingredients. *Journal of soil science and plant nutrition*, *10*(3), 373-377.
- Ruiz, Opazo-Navarrete, Meurs, Minor, Sala, Boekel, v., Stieger, & Janssen. (2016). Denaturation and in Vitro Gastric Digestion of Heat-Treated Quinoa Protein Isolates Obtained at Various Extraction pH. *Food Biophysics*, *11*(2), 184-197.
- Ruiz, Xiao, Boekel, v., Minor, & Stieger. (2016). Effect of extraction pH on heat-induced aggregation, gelation and microstructure of protein isolate from quinoa (*Chenopodium quinoa* Willd). *Food chemistry*, *209*, 203-210.

- Ruiz, G. A., Xiao, W., van Boekel, M., Minor, M., & Stieger, M. (2016). Effect of extraction pH on heat-induced aggregation, gelation and microstructure of protein isolate from quinoa (*Chenopodium quinoa* Willd). *Food chemistry*, 209, 203-210.
- Sá, A. G. A., Moreno, Y. M. F., & Carciofi, B. A. M. (2020a). Food processing for the improvement of plant proteins digestibility. *Critical reviews in food science and nutrition*, 60(20), 3367-3386.
- Sá, A. G. A., Moreno, Y. M. F., & Carciofi, B. A. M. (2020b). Plant proteins as high-quality nutritional source for human diet. *Trends in Food Science & Technology*, 97, 170-184.
- Sacks, F. M., Carey, V. J., Anderson, C. A., Miller, E. R., Copeland, T., Charleston, J., Harshfield, B. J., Laranjo, N., McCarron, P., & Swain, J. (2014). Effects of high vs low glycemic index of dietary carbohydrate on cardiovascular disease risk factors and insulin sensitivity: the OmniCarb randomized clinical trial. *Jama*, 312(23), 2531-2541.
- Sacks, F. M., & Katan, M. (2002). Randomized clinical trials on the effects of dietary fat and carbohydrate on plasma lipoproteins and cardiovascular disease. *The American journal of medicine*, 113(9), 13-24.
- Saha, D., & Bhattacharya, S. (2010). Hydrocolloids as thickening and gelling agents in food: a critical review. *Journal of food science and technology*, 47(6), 587-597.
- Sakandar, H., Imran, M., Huma, N., Ahmad, S., Aslam, H., Shakeel, A., & Shoaib, M. (2014). Effects of Polymerized Whey Proteins Isolates on the Quality of Stirred Yoghurt made from Camel Milk. *Food technology*, 54172, 3502157-3507110.
- Sauer, J. D. (1950). The grain amaranths: a survey of their history and classification. *Annals of the Missouri Botanical garden*, 37(4), 561-632.
- Savadkoohi, S., & Farahnaky, A. (2012). Dynamic rheological and thermal study of the heat-induced gelation of tomato-seed proteins. *Journal of Food Engineering*, 113(3), 479-485.
- Sawyer, W. (1968). Heat denaturation of bovine β -lactoglobulins and relevance of disulfide aggregation. *Journal of Dairy Science*, 51(3), 323-329.
- Scanlin, L., & Lewis, K. (2017). Quinoa as a sustainable protein source: production, nutrition, and processing. In *Sustainable protein sources* (pp. 223-238). Elsevier.
- Scanlin, L., & Stone, M. (2009). *Quinoa protein concentrate, production and functionality*.
- Schaefer, D. W., Martin, J. E., Wiltzius, P., & Cannell, D. S. (1984). Fractal geometry of colloidal aggregates. *Physical Review Letters*, 52(26), 2371.

- Schmitt, C., Bovay, C., Rouvet, M., Shojaei-Rami, S., & Kolodziejczyk, E. (2007). Whey protein soluble aggregates from heating with NaCl: physicochemical, interfacial, and foaming properties. *Langmuir*, 23(8), 4155-4166.
- Schmitt, C., Sanchez, C., Desobry-Banon, S., & Hardy, J. (1998). Structure and technofunctional properties of protein-polysaccharide complexes: a review. *Critical reviews in food science and nutrition*, 38(8), 689-753.
- Schokker, E., Singh, H., & Creamer, L. (2000). Heat-induced aggregation of β -lactoglobulin A and B with α -lactalbumin. *International Dairy Journal*, 10(12), 843-853.
- Schutyser, M., Pelgrom, P., Van der Goot, A., & Boom, R. (2015). Dry fractionation for sustainable production of functional legume protein concentrates. *Trends in Food Science & Technology*, 45(2), 327-335.
- Schutyser, M. A. I., & van der Goot, A. J. (2011). The potential of dry fractionation processes for sustainable plant protein production. *Trends in Food Science & Technology*, 22(4), 154-164.
- Sébastien, G., Christophe, B., Mario, A., Pascal, L., Michel, P., & Aurore, R. (2014). Impact of purification and fractionation process on the chemical structure and physical properties of locust bean gum. *Carbohydrate polymers*, 108, 159-168.
- Semenova, M. (2017). Protein-polysaccharide associative interactions in the design of tailor-made colloidal particles. *Current Opinion in Colloid & Interface Science*, 28, 15-21.
- Semenova, M. G., & Dickinson, E. (2010). *Biopolymers in food colloids: Thermodynamics and molecular interactions*. CRC Press.
- Sethi, S., Tyagi, S. K., & Anurag, R. K. (2016). Plant-based milk alternatives an emerging segment of functional beverages: a review. *Journal of food science and technology*, 53(9), 3408-3423.
- Sharif, N., Khoshnoudi-Nia, S., & Jafari, S. M. (2020). Confocal laser scanning microscopy (CLSM) of nanoencapsulated food ingredients. In S. M. Jafari (Ed.), *Characterization of Nanoencapsulated Food Ingredients* (Vol. 4, pp. 131-158). Academic Press.
- Sharma, G., Sharma, S., Kumar, A., Al-Muhtaseb, A. a. H., Naushad, M., Ghfar, A. A., Mola, G. T., & Stadler, F. J. (2018). Guar gum and its composites as potential materials for diverse applications: A review. *Carbohydrate polymers*, 199, 534-545.
- Sheinerman, F. B., Norel, R., & Honig, B. (2000). Electrostatic aspects of protein-protein interactions. *Current Opinion in Structural Biology*, 10(2), 153-159.
- Shen, Y., Tang, X., & Li, Y. (2021). Drying methods affect physicochemical and functional properties of quinoa protein isolate. *Food chemistry*, 339, 127823.

- Shimada, K., & Cheftel, J. C. (1988). Texture characteristics, protein solubility, and sulfhydryl group/disulfide bond contents of heat-induced gels of whey protein isolate. *Journal of Agricultural and Food Chemistry*, 36(5), 1018-1025.
- Shimada, K., & Cheftel, J. C. (1989). Sulfhydryl group/disulfide bond interchange reactions during heat-induced gelation of whey protein isolate. *Journal of Agricultural and Food Chemistry*, 37(1), 161-168.
- Shokry, A. M. (2016). The usage of quinoa flour as a potential ingredient in production of meat burger with functional properties. *Middle East Journal of Applied Sciences*, 6(4), 1128-1137.
- Silva, J. V. C., Cochereau, R., Schmitt, C., Chassenieux, C., & Nicolai, T. (2019). Heat-induced gelation of mixtures of micellar caseins and plant proteins in aqueous solution. *Food Research International*, 116, 1135-1143.
- Singh, H., & Havea, P. (2003). Thermal denaturation, aggregation and gelation of whey proteins. In *Advanced dairy chemistry—1 proteins* (pp. 1261-1287). Springer.
- Singh, T. K., Øiseth, S. K., Lundin, L., & Day, L. (2014). Influence of heat and shear induced protein aggregation on the in vitro digestion rate of whey proteins. *Food & function*, 5(11), 2686-2698.
- Smith, D. M. (1994). *Protein interactions in gels: protein-protein interactions*. Marcel Dekker, New York.
- Smith, I. H., & Pace, G. W. (1982). Recovery of microbial polysaccharides. *Journal of Chemical Technology and Biotechnology*, 32(1), 119-129.
- Soenen, S., & Westerterp-Plantenga, M. S. (2008). Proteins and satiety: implications for weight management. *Current Opinion in Clinical Nutrition & Metabolic Care*, 11(6), 747-751.
- Sousa, A. M. M., Rocha, C. M. R., & Gonçalves, M. P. (2021). Agar. In G. O. Phillips & P. A. Williams (Eds.), *Handbook of Hydrocolloids (Third Edition)* (pp. 731-765). Woodhead Publishing.
- Sow, L. C., Chong, J. M. N., Liao, Q. X., & Yang, H. (2018). Effects of κ -carrageenan on the structure and rheological properties of fish gelatin. *Journal of Food Engineering*, 239, 92-103.
- Stone, A. K., Teymurova, A., Chang, C., Cheung, L., & Nickerson, M. T. (2015). Formation and functionality of canola protein isolate with both high- and low-methoxyl pectin under associative conditions. *Food Science and Biotechnology*, 24(4), 1209-1218.

- Stone, A. K., Teymurova, A., & Nickerson, M. T. (2014). Formation and Functional Attributes of Canola Protein Isolate—Gum Arabic Electrostatic Complexes. *Food Biophysics*, 9(3), 203-212.
- Stowell, L. (2019). Behind the Taihape farm producing 70 tonnes of quinoa a year. *Whanganui Chronicle*
- Sun, X. D., & Arntfield, S. D. (2010). Gelation properties of salt-extracted pea protein induced by heat treatment. *Food Research International*, 43(2), 509-515.
- Sun, X. D., & Arntfield, S. D. (2011). Dynamic oscillatory rheological measurement and thermal properties of pea protein extracted by salt method: Effect of pH and NaCl. *Journal of Food Engineering*, 105(3), 577-582.
- Sun, X. D., & Arntfield, S. D. (2012). Molecular forces involved in heat-induced pea protein gelation: effects of various reagents on the rheological properties of salt-extracted pea protein gels. *Food Hydrocolloids*, 28(2), 325-332.
- Swaisgood, H. E. (1982). Chemistry of milk protein. *Developments in dairy chemistry*, 1, 1-59.
- Sworn, G. (2021). Xanthan gum. In G. O. Phillips & P. A. Williams (Eds.), *Handbook of Hydrocolloids (Third Edition)* (pp. 833-853). Woodhead Publishing.
- Syafiq, A., Amir, I., & Sharon, W. (2014). Mixture experiment on rheological properties of dark chocolate as influenced by cocoa butter substitution with xanthan gum/corn starch/glycerin blends. *International Food Research Journal*, 21(5), 1887.
- Tabilo-Munizaga, G., & Barbosa-Cánovas, G. V. (2005). Rheology for the food industry. *Journal of Food Engineering*, 67(1), 147-156.
- Tan, M., Nawaz, M. A., & Buckow, R. (2021). Functional and food application of plant proteins—a review. *Food Reviews International*, 1-29.
- TAN, Y. L., Ye, A., Singh, H., & Hemar, Y. (2007). Effects of biopolymer addition on the dynamic rheology and microstructure of renneted skim milk systems. *Journal of Texture Studies*, 38(3), 404-422.
- Tang, Q., MaCarthy, O. J., & Munro, P. A. (1995). Effects of pH on whey protein concentrate gel properties: comparisons between small deformation (dynamic) and large deformation (failure) testing. *Journal of Texture Studies*, 26(3), 255-272.
- Tanger, C., Andlinger, D. J., Brümmer-Rolf, A., Engel, J., & Kulozik, U. (2021). Quantification of protein-protein interactions in highly denatured whey and potato protein gels. *MethodsX*, 8, 101243.

- Tanger, C., Müller, M., Andlinger, D., & Kulozik, U. (2022). Influence of pH and ionic strength on the thermal gelation behaviour of pea protein. *Food Hydrocolloids*, *123*, 106903.
- Tapia, M. (2012). La quinua: historia, distribución geográfica, actual producción y usos. *Ambienta: La Revista del Ministerio de Medio Ambiente*(99), 104-119.
- Tarone, A. G., Fasolin, L. H., de Assis Perrechil, F., Hubinger, M. D., & da Cunha, R. L. (2013). Influence of drying conditions on the gelling properties of the 7S and 11S soy protein fractions. *Food and Bioproducts Processing*, *91*(2), 111-120.
- Teixeira, J. (1988). Small-angle scattering by fractal systems. *Journal of Applied Crystallography*, *21*(6), 781-785.
- Thanapornpoonpong, S.-n., Vearasilp, S., Pawelzik, E., & Gorinstein, S. (2008). Influence of various nitrogen applications on protein and amino acid profiles of amaranth and quinoa. *Journal of Agricultural and Food Chemistry*, *56*(23), 11464-11470.
- Thomar, P., & Nicolai, T. (2016). Heat-induced gelation of casein micelles in aqueous suspensions at different pH. *Colloids and Surfaces B: Biointerfaces*, *146*, 801-807.
- Thombare, N., Jha, U., Mishra, S., & Siddiqui, M. (2016). Guar gum as a promising starting material for diverse applications: A review. *International Journal of Biological Macromolecules*, *88*, 361-372.
- To, B., Helbig, N., Nakai, S., & Ma, C. (1985). Modification of whey protein concentrate to simulate whippability and gelation of egg white. *Canadian Institute of Food Science and Technology Journal*, *18*(2), 150-157.
- Tobitani, A., & Ross-Murphy, S. B. (1997). Heat-Induced Gelation of Globular Proteins. 1. Model for the Effects of Time and Temperature on the Gelation Time of BSA Gels. *Macromolecules*, *30*(17), 4845-4854.
- Totosaus, A., Montejano, J. G., Salazar, J. A., & Guerrero, I. (2002). A review of physical and chemical protein-gel induction. *International Journal of Food Science & Technology*, *37*(6), 589-601.
- Tripathy, J., Mishra, D. K., Srivastava, A., Mishra, M. M., & Behari, K. (2008). Synthesis of partially carboxymethylated guar gum-g-4-vinyl pyridine and study of its water swelling, metal ion sorption and flocculation behaviour. *Carbohydrate polymers*, *72*(3), 462-472.
- Trumbo, P. R. (2005). The level of evidence for permitting a qualified health claim: FDA's review of the evidence for selenium and cancer and vitamin E and heart disease. *The Journal of nutrition*, *135*(2), 354-356.

- Tseng, Y.-C., & Xiong, Y. L. (2009). Effect of inulin on the rheological properties of silken tofu coagulated with glucono- δ -lactone. *Journal of Food Engineering*, 90(4), 511-516.
- Tunick, M. H. (2008). Whey protein production and utilization: a brief history. *Whey processing, functionality and health benefits*, 1-13.
- Tunick, M. H. (2011). Small-Strain Dynamic Rheology of Food Protein Networks. *Journal of Agricultural and Food Chemistry*, 59(5), 1481-1486.
- Turgeon, S., Schmitt, C., & Sanchez, C. (2007). Protein-polysaccharide complexes and coacervates. *Current Opinion in Colloid & Interface Science*, 12(4-5), 166-178.
- Turkut, G. M., Cakmak, H., Kumcuoglu, S., & Tavman, S. (2016). Effect of quinoa flour on gluten-free bread batter rheology and bread quality. *Journal of Cereal Science*, 69, 174-181.
- Tuvikene, R. (2021). Carrageenan. In G. O. Phillips & P. A. Williams (Eds.), *Handbook of Hydrocolloids (Third Edition)* (pp. 767-804). Woodhead Publishing.
- Ünal, B., Metin, S., & Işıklı, N. D. (2003). Use of response surface methodology to describe the combined effect of storage time, locust bean gum and dry matter of milk on the physical properties of low-fat set yoghurt. *International Dairy Journal*, 13(11), 909-916.
- Uruakpa, F. O., & Arntfield, S. D. (2006). Network formation of canola protein- κ -carrageenan mixtures as affected by salts, urea and dithiothreitol. *LWT - Food Science and Technology*, 39(8), 939-946.
- USDA. (2015). National Nutrient Database for Standard Reference. www.ndb.nal.usda.gov/ndb
- Valcárcel-Yamani, B., & Lannes, S. d. S. (2012). Applications of quinoa (*Chenopodium quinoa* Willd.) and amaranth (*Amaranthus* spp.) and their influence in the nutritional value of cereal based foods. *Food and Public health*, 2(6), 265-275.
- Vandenbossche, G. M., Van Oostveldt, P., & Remon, J. P. (1991). A fluorescence method for the determination of the molecular weight cut-off of alginate-polylysine microcapsules. *Journal of pharmacy and pharmacology*, 43(4), 275-277.
- Vega-Gálvez, A., Miranda, M., Vergara, J., Uribe, E., Puente, L., & Martínez, E. A. (2010). Nutrition facts and functional potential of quinoa (*Chenopodium quinoa* willd.), an ancient Andean grain: a review. *Journal of the Science of Food and Agriculture*, 90(15), 2541-2547.

- Venkateswara Rao, M., CK, S., Rawson, A., & DV, C. (2021). Modifying the plant proteins techno-functionalities by novel physical processing technologies: a review. *Critical reviews in food science and nutrition*, 1-22.
- Verma, A. K., Rajkumar, V., & Kumar, S. (2019). Effect of amaranth and quinoa seed flour on rheological and physicochemical properties of goat meat nuggets. *Journal of food science and technology*, 56(11), 5027-5035.
- Vilcacundo, R., & Hernández-Ledesma, B. (2017). Nutritional and biological value of quinoa (*Chenopodium quinoa* Willd.). *Current Opinion in Food Science*, 14, 1-6.
- Voragen, A. C. J., Rolin, C., Marr, B. U., Challen, I., Riad, A., Lebbar, R., & Knutsen, S. H. (2003). Polysaccharides. In *Ullmann's Encyclopedia of Industrial Chemistry*.
- Wagner, J., Biliaderis, C. G., & Moschakis, T. (2020). Whey proteins: Musings on denaturation, aggregate formation and gelation. *Critical reviews in food science and nutrition*, 60(22), 3793-3806.
- Wagoner, T. B., & Foegeding, E. A. (2017). Whey protein–pectin soluble complexes for beverage applications. *Food Hydrocolloids*, 63, 130-138.
- Walsh, H., Ross, J., Hendricks, G., & Guo, M. (2010). Physico-chemical properties, probiotic survivability, microstructure, and acceptability of a yogurt-like symbiotic oats-based product using pre-polymerized whey protein as a gelation agent. *Journal of Food Science*, 75(5), M327-M337.
- Wanasundara, J. P., McIntosh, T. C., Perera, S. P., Withana-Gamage, T. S., & Mitra, P. (2016). Canola/rapeseed protein-functionality and nutrition. *OCl*, 23(4), D407.
- Wang, C., Gao, F., Zhang, T., Wang, Y., & Guo, M. (2015). Physicochemical, textural, sensory properties and probiotic survivability of Chinese Laosuan Nai (protein-fortified set yoghurt) using polymerised whey protein as a co-thickening agent. *International Journal of Dairy Technology*, 68(2), 261-269.
- Wang, C., Zheng, H., Liu, T., Wang, D., & Guo, M. (2017). Physicochemical Properties and Probiotic Survivability of Symbiotic Corn-Based Yogurt-Like Product. *Journal of Food Science*, 82(9), 2142-2150.
- Wang, D., Sun, X., Yang, G., & Wang, Y. (2009). Improved water resistance of soy protein adhesive at isoelectric point. *Transactions of the ASABE*, 52(1), 173-177.
- Wang, M., Hettiarachchy, N., Qi, M., Burks, W., & Siebenmorgen, T. (1999). Preparation and functional properties of rice bran protein isolate. *Journal of Agricultural and Food Chemistry*, 47(2), 411-416.

- Wang, X., Zeng, M., Qin, F., Adhikari, B., He, Z., & Chen, J. (2018). Enhanced CaSO₄-induced gelation properties of soy protein isolate emulsion by pre-aggregation. *Food chemistry*, 242, 459-465.
- Wang, Y., Eastwood, B., Yang, Z., de Campo, L., Knott, R., Prosser, C., Carpenter, E., & Hemar, Y. (2019). Rheological and structural characterization of acidified skim milks and infant formulae made from cow and goat milk. *Food Hydrocolloids*, 96, 161-170.
- Wang, Z., Zhang, N., Chen, C., He, R., & Ju, X. (2020). Rapeseed protein nanogels as novel pickering stabilizers for oil-in-water emulsions. *Journal of Agricultural and Food Chemistry*, 68(11), 3607-3614.
- Warnakulasuriya, S. N., & Nickerson, M. T. (2018). Review on plant protein–polysaccharide complex coacervation, and the functionality and applicability of formed complexes. *Journal of the Science of Food and Agriculture*, 98(15), 5559-5571.
- Watanabe, K., & Klostermeyer, H. (1976). Heat-induced changes in sulphhydryl and disulphide levels of β -lactoglobulin A and the formation of polymers. *Journal of Dairy Research*, 43(3), 411-418.
- Watanabe, K., Peng, N. L., Tang, H., & Mitsunaga, T. (2007). Molecular structural characteristics of quinoa starch. *Food Science and Technology Research*, 13(1), 73-78.
- Weder, J., & Belitz, H. (2003). Protein| Functional Properties.
- Whistler, R. L. (1954). Guar gum, locust bean gum, and others. In. ACS Publications.
- Wijayanti, H. B., Bansal, N., & Deeth, H. C. (2014). Stability of Whey Proteins during Thermal Processing: A Review. *Comprehensive Reviews in Food Science and Food Safety*, 13(6), 1235-1251.
- Windhab, E. (1995). Rheology in food processing. In *Physico-chemical aspects of food processing* (pp. 80-116). Springer.
- Wong, D., Vasanthan, T., & Ozimek, L. (2013). Synergistic enhancement in the co-gelation of salt-soluble pea proteins and whey proteins. *Food chemistry*, 141(4), 3913-3919.
- Wood, K., Mata, J. P., Garvey, C. J., Wu, C.-M., Hamilton, W. A., Abbeywick, P., Bartlett, D., Bartsch, F., Baxter, P., & Booth, N. (2018). QUOKKA, the pinhole small-angle neutron scattering instrument at the OPAL Research Reactor, Australia: design, performance, operation and scientific highlights. *Journal of Applied Crystallography*, 51(2), 294-314.
- Wright, K., Pike, O., Fairbanks, D., & Huber, C. (2002). Composition of *Atriplex hortensis*, sweet and bitter *Chenopodium quinoa* seeds. *Journal of Food Science*, 67(4), 1383-1385.

- Wu, C., Hua, Y., Chen, Y., Kong, X., & Zhang, C. (2017). Effect of temperature, ionic strength and IIS ratio on the rheological properties of heat-induced soy protein gels in relation to network proteins content and aggregates size. *Food Hydrocolloids*, *66*, 389-395.
- Wu, G. (2015). Nutritional properties of quinoa. *Quinoa: Improvement and sustainable production*, 193-210.
- Wüstenberg, T. (2015). General overview of food hydrocolloids. *Cellulose and Cellulose Derivatives in the Food industry Fundamentals and Applications; Wüstenberg, T., Ed*, 1-68.
- Xiao, Y., Kang, S., Liu, Y., Guo, X., Li, M., & Xu, H. (2021). Effect and mechanism of calcium ions on the gelation properties of cellulose nanocrystals-whey protein isolate composite gels. *Food Hydrocolloids*, *111*, 106401.
- Xiao, Y., Liu, Y., Wang, Y., Jin, Y., Guo, X., Liu, Y., Qi, X., Lei, H., & Xu, H. (2020). Heat-induced whey protein isolate gels improved by cellulose nanocrystals: Gelling properties and microstructure. *Carbohydrate polymers*, *231*, 115749.
- Xie, F., Li, Z., Li, Z., Li, D., Gao, Y., & Wang, B. (2018). Absolute intensity calibration and application at BSRF SAXS station. *Nuclear Instruments and Methods in Physics Research Section A: Accelerators, Spectrometers, Detectors and Associated Equipment*, *900*, 64-68.
- Xiong, N., Mannicke, D., Lam, T., & Hauser, N. (2017). Gumtree Application for Neutron Scattering. Version 1.13. *Zenodo: Geneve, Switzerland*.
- Yalçın, E., & Çelik, S. (2007). Solubility properties of barley flour, protein isolates and hydrolysates. *Food chemistry*, *104*(4), 1641-1647.
- Yang, C. (2017). Plant protein gel formation mechanisms and their applications as delivery systems of bioactive compounds.
- Yang, C., Wang, Y., & Chen, L. (2017). Fabrication, characterization and controlled release properties of oat protein gels with percolating structure induced by cold gelation. *Food Hydrocolloids*, *62*, 21-34.
- Yang, C., Wang, Y., Vasanthan, T., & Chen, L. (2014). Impacts of pH and heating temperature on formation mechanisms and properties of thermally induced canola protein gels. *Food Hydrocolloids*, *40*, 225-236.
- Yang, D., Gao, S., & Yang, H. (2020). Effects of sucrose addition on the rheology and structure of iota-carrageenan. *Food Hydrocolloids*, *99*, 105317.

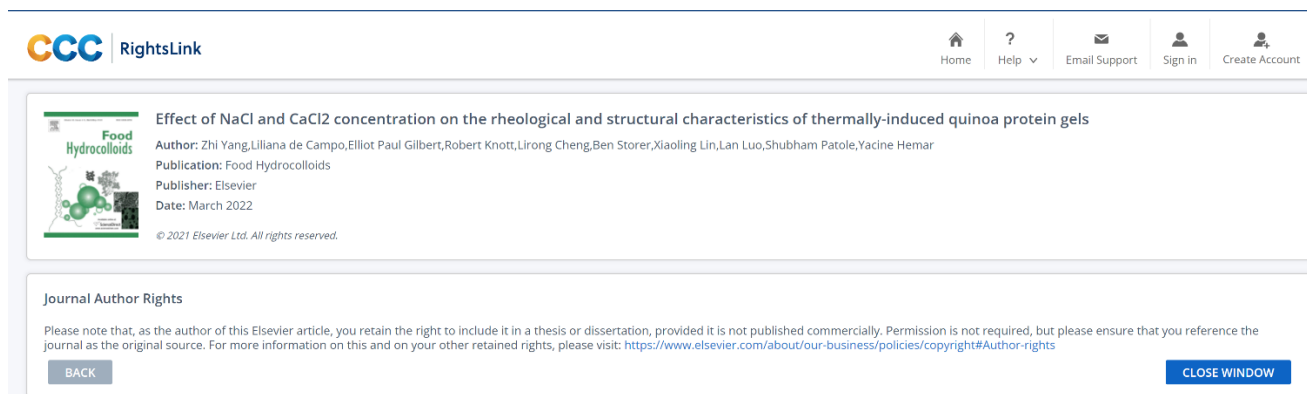
- Yang, X., Li, A., Li, D., Guo, Y., & Sun, L. (2021a). Applications of mixed polysaccharide-protein systems in fabricating multi-structures of binary food gels—A review. *Trends in Food Science & Technology*.
- Yang, X., Li, A., Li, D., Guo, Y., & Sun, L. (2021b). Applications of mixed polysaccharide-protein systems in fabricating multi-structures of binary food gels—A review. *Trends in Food Science & Technology*, *109*, 197-210.
- Yang, X., Li, A., Li, X., Sun, L., & Guo, Y. (2020). An overview of classifications, properties of food polysaccharides and their links to applications in improving food textures. *Trends in Food Science & Technology*, *102*, 1-15.
- Yang, Z., Chaieb, S., Hemar, Y., de Campo, L., Rehm, C., & McGillivray, D. J. (2015). Investigating linear and nonlinear viscoelastic behaviour and microstructures of gelatin-multiwalled carbon nanotube composites. *RSC advances*, *5*(130), 107916-107926.
- Yang, Z., de Campo, L., Gilbert, E. P., Knott, R., Cheng, L., Storer, B., Lin, X., Luo, L., Patole, S., & Hemar, Y. (2022). Effect of NaCl and CaCl₂ concentration on the rheological and structural characteristics of thermally-induced quinoa protein gels. *Food Hydrocolloids*, *124*, 107350.
- Yang, Z., Hemar, Y., Hilliou, L., Gilbert, E. P., McGillivray, D. J., Williams, M. A., & Chaieb, S. (2016). Nonlinear behavior of gelatin networks reveals a hierarchical structure. *Biomacromolecules*, *17*(2), 590-600.
- Yang, Z., Xu, X., Hemar, Y., Mo, G., de Campo, L., & Gilbert, E. P. (2020). Effect of porous waxy rice starch addition on acid milk gels: Structural and physicochemical functionality. *Food Hydrocolloids*, *109*, 106092.
- Yang, Z., Yang, H., & Yang, H. (2018). Effects of sucrose addition on the rheology and microstructure of κ -carrageenan gel. *Food Hydrocolloids*, *75*, 164-173.
- Ye, A. (2008). Complexation between milk proteins and polysaccharides via electrostatic interaction: principles and applications—a review. *International Journal of Food Science & Technology*, *43*(3), 406-415.
- Yin, M., Yang, D., Lai, S., & Yang, H. (2021). Rheological properties of xanthan-modified fish gelatin and its potential to replace mammalian gelatin in low-fat stirred yogurt. *LWT*, *147*, 111643.
- Zárate-Ramírez, L. S., Bengoechea, C., Cordobés, F., & Guerrero, A. (2010). Linear viscoelasticity of carob protein isolate/locust bean gum blends. *Journal of Food Engineering*, *100*(3), 435-445.

- Zhang, R., Cheng, L., Luo, L., Hemar, Y., & Yang, Z. (2021). Formation and characterisation of high-internal-phase emulsions stabilised by high-pressure homogenised quinoa protein isolate. *Colloids and Surfaces A: Physicochemical and Engineering Aspects*, *631*, 127688.
- Zhang, Y.-H., Tang, C.-H., Wen, Q.-B., Yang, X.-Q., Li, L., & Deng, W.-L. (2010). Thermal aggregation and gelation of kidney bean (*Phaseolus vulgaris* L.) protein isolate at pH 2.0: Influence of ionic strength. *Food Hydrocolloids*, *24*(4), 266-274.
- Zhang, Z., Yang, Y., Zhou, P., Zhang, X., & Wang, J. (2017). Effects of high pressure modification on conformation and gelation properties of myofibrillar protein. *Food chemistry*, *217*, 678-686.
- Zhao, H., Chen, J., Hemar, Y., & Cui, B. (2020). Improvement of the rheological and textural properties of calcium sulfate-induced soy protein isolate gels by the incorporation of different polysaccharides. *Food chemistry*, *310*, 125983.
- Zhao, M., Xiong, W., Chen, B., Zhu, J., & Wang, L. (2020). Enhancing the solubility and foam ability of rice glutelin by heat treatment at pH12: Insight into protein structure. *Food Hydrocolloids*, *103*, 105626.
- Zheng, L., Regenstein, J. M., Zhou, L., & Wang, Z. (2022). Soy protein isolates: A review of their composition, aggregation, and gelation. *Comprehensive Reviews in Food Science and Food Safety*, *21*(2), 1940-1957.
- Zhou, Y., & Yang, H. (2019). Effects of calcium ion on gel properties and gelation of tilapia (*Oreochromis niloticus*) protein isolates processed with pH shift method. *Food chemistry*, *277*, 327-335.
- Zhuang, X., Cheng, B., Kang, W., & Xu, X. (2010). Electrospun chitosan/gelatin nanofibers containing silver nanoparticles. *Carbohydrate polymers*, *82*(2), 524-527.
- Zhuang, X., Jiang, X., Zhou, H., Chen, Y., Zhao, Y., Yang, H., & Zhou, G. (2020). Insight into the mechanism of physicochemical influence by three polysaccharides on myofibrillar protein gelation. *Carbohydrate polymers*, *229*, 115449.
- Zittle, C., DellaMonica, E., Rudd, R., & Custer, J. (1957). The binding of calcium ions by β -lactoglobulin both before and after aggregation by heating in the presence of calcium ions. *Journal of the American Chemical society*, *79*(17), 4661-4666.

8. Appendices

Journal author rights:

Chapter 3- Effect of NaCl and CaCl₂ concentration on the rheological and structural characteristics of thermally induced quinoa protein gels



The screenshot displays the Elsevier RightsLink interface. At the top left is the 'CCC RightsLink' logo. On the top right, there are navigation links: Home, Help, Email Support, Sign in, and Create Account. The main content area shows the article title 'Effect of NaCl and CaCl₂ concentration on the rheological and structural characteristics of thermally-induced quinoa protein gels' from the journal 'Food Hydrocolloids'. The author list includes Zhi Yang, Lilliana de Campo, Elliot Paul Gilbert, Robert Knott, Lirong Cheng, Ben Storer, Xiaoling Lin, Lan Luo, Shubham Patole, and Yacine Hemar. The publication date is March 2022. Below this, a 'Journal Author Rights' section contains a disclaimer: 'Please note that, as the author of this Elsevier article, you retain the right to include it in a thesis or dissertation, provided it is not published commercially. Permission is not required, but please ensure that you reference the journal as the original source. For more information on this and on your other retained rights, please visit: <https://www.elsevier.com/about/our-business/policies/copyright#Author-rights>'. There are 'BACK' and 'CLOSE WINDOW' buttons at the bottom of the rights notice.

Supporting data for Chapter 3:

Table S1 X-ray and neutron scattering length density (SLD) of the different solvents

Solvents	X-ray scattering length density (10^{-6}\AA^{-2})	Neutron scattering length density (10^{-6}\AA^{-2})
D ₂ O	9.429	6.375
D ₂ O+20 mM NaCl	9.434	6.373
D ₂ O+50 mM NaCl	9.440	6.370
D ₂ O+100 mM NaCl	9.452	6.366
D ₂ O+200 mM NaCl	9.474	6.357
D ₂ O+20 mM CaCl ₂	9.438	6.371
D ₂ O+50 mM CaCl ₂	9.451	6.366

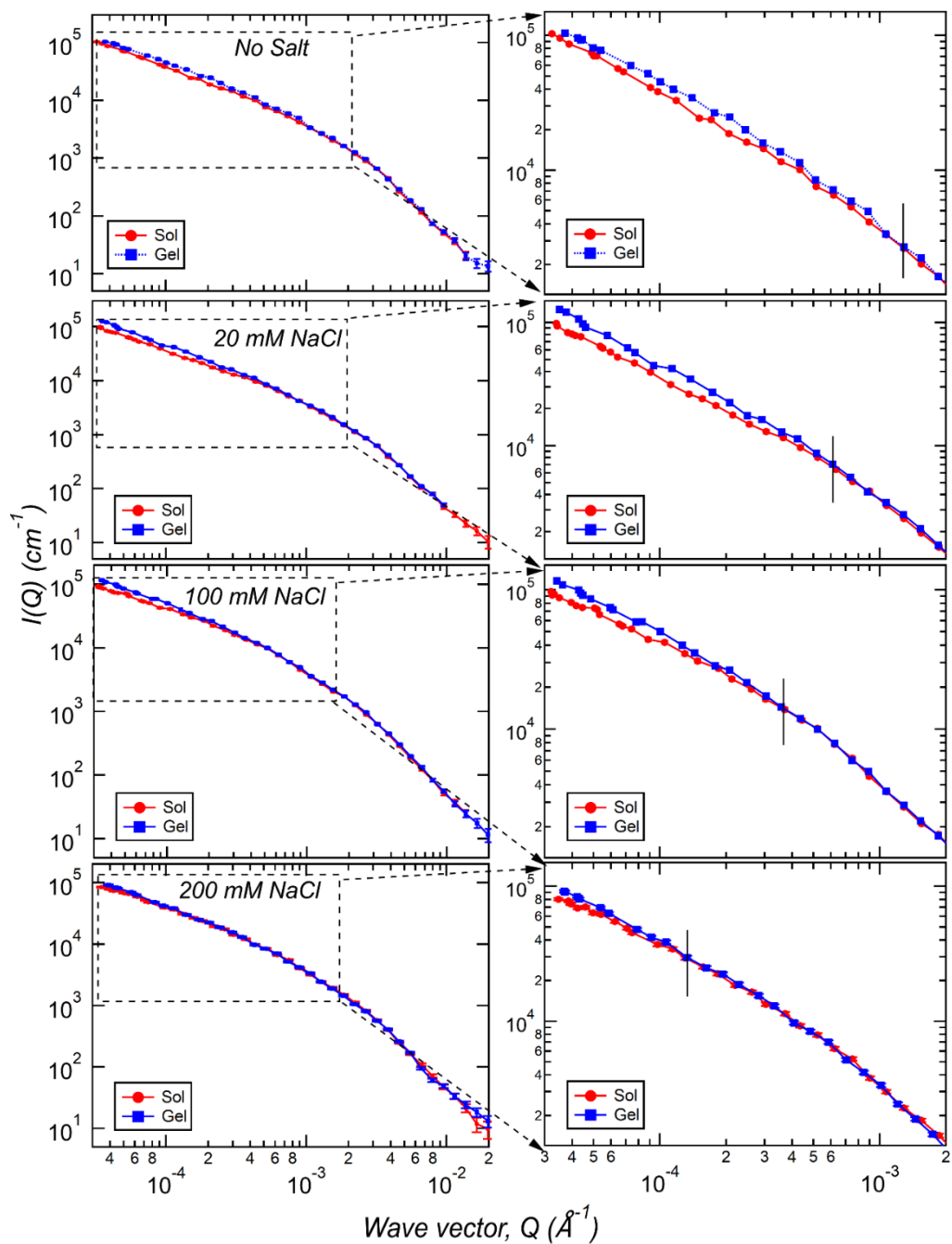


Fig. S1. USANS profiles of QPI samples (10 wt% in D₂O) with various concentrations of NaCl addition before and after heat treatment. The low to mid- Q regions were enlarged in the corresponding right panels to better indicate the differences of the QPI before and after heat treatment. The cross-over point between the scattering profiles of solution and gel is indicated by black vertical lines.

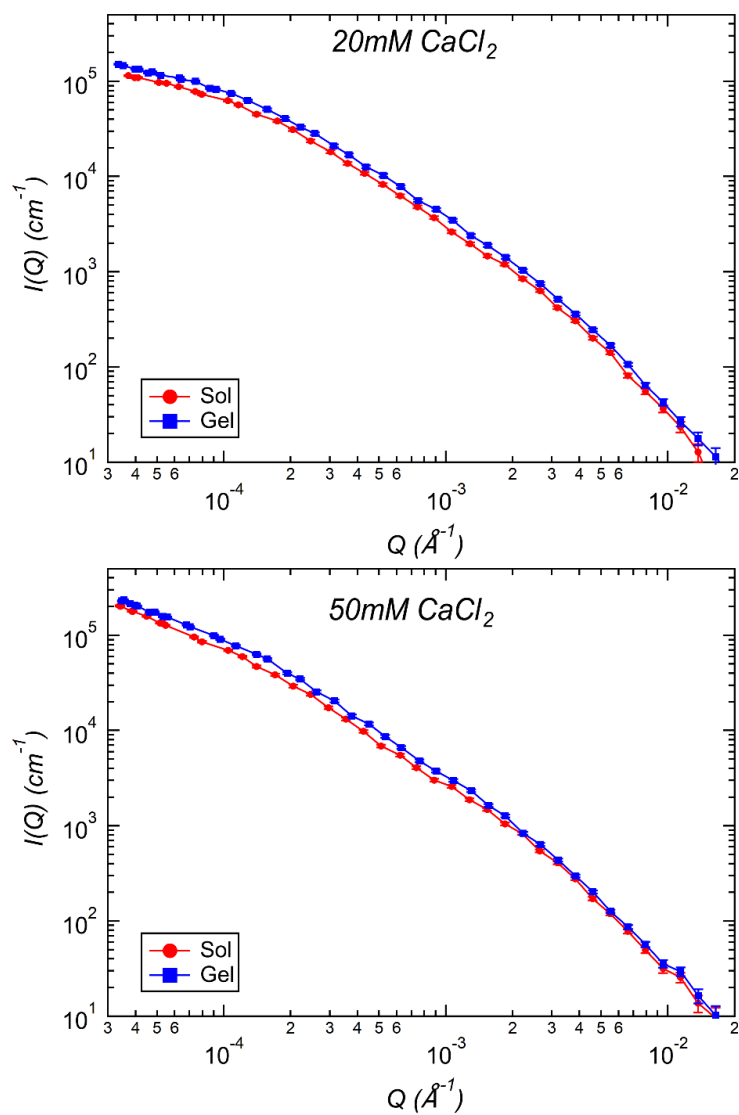


Fig. S2 USANS profiles of QPI samples before and after heat treatment at 10 wt% in D₂O with various 20 mM and 50 mM of CaCl₂ addition. The USANS data are not desmeared.

Chapter 4- Impact of incorporation of various polysaccharides on the rheological and microstructural characteristics of heat-induced quinoa protein isolate gels

Impact of incorporations of various polysaccharides on rheological and microstructural characteristics of heat-induced quinoa protein isolate gels
Author: Shubham Patole et al
Publication: Food Biophysics
Publisher: Springer Nature
Date: Feb 22, 2022
Copyright © 2022, The Author(s)

SPRINGER NATURE

Creative Commons
This is an open access article distributed under the terms of the [Creative Commons CC BY](#) license, which permits unrestricted use, distribution, and reproduction in any medium, provided the original work is properly cited.
You are not required to obtain permission to reuse this article.
To request permission for a type of use not listed, please contact [Springer Nature](#)

Supporting images for Chapter 4

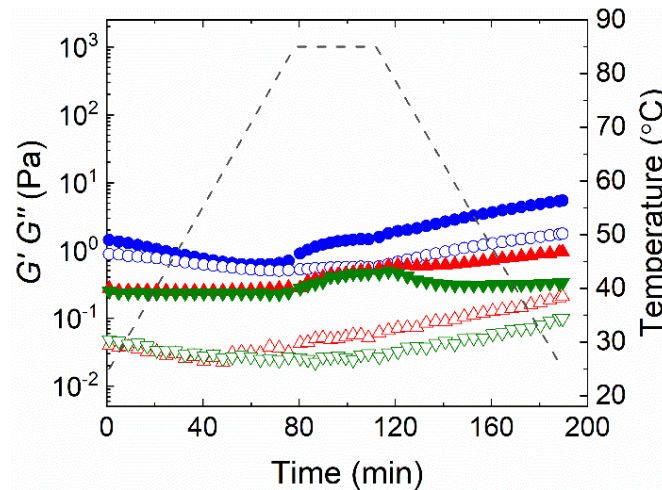


Fig. S1 The evolution of G' (solid symbols) and G'' (open symbols) with temperature for 0.2 wt% of guar gum (\blacktriangledown), locust bean gum (\blacktriangle), and xanthan gum (\bullet).